GRID-CONNECTED ENERGY STORAGE SYSTEMS — BENEFITS, PLANNING AND OPERATION

By

Yuting Tian

A DISSERTATION

Submitted to
Michigan State University
in partial fulfillment of the requirements
for the degree of

Electrical Engineering - Doctor of Philosophy

2018

ABSTRACT

GRID-CONNECTED ENERGY STORAGE SYSTEMS — BENEFITS, PLANNING AND OPERATION

By

Yuting Tian

Deployment of energy storage systems (ESSs) is gaining significant momentum due to economic incentives, power system regulation requirements, and integration of renewable energy resources. This dissertation covers three aspects of grid-connected ESSs: benefits, planning, and operation. First, the benefits and use cases of ESSs are reviewed and a comprehensive evaluation method for estimating stacked revenue of ESSs is proposed. The stacked revenue from an ESS cannot be calculated by merely aggregating the benefits from various applications (e.g., energy arbitrage, frequency regulation, and outage mitigation) as the ESS may not be available for all types of applications during the same time interval. A model incorporating component reliability, power system operation constraints, and storage system operation constraints is developed to evaluate the composite revenue generated from the applications. Second, for planning purposes, a model to estimate the capacity value of ESSs is developed and a sensitivity guided approach to ESS siting is proposed. In contrast to conventional generators with the capability to provide energy upon demand, ESSs are energy-limited resources. In addition, it is possible that the availability of an ESS is low when it is needed to provide its capacity to maintain system reliability due to low state of charge. Thus, the work presented here proposes a method to evaluate the actual capacity contribution of ESSs, considering the energy-limited characteristic and the availability uncertainty. Also, it is necessary to determine suitable locations so as to maximize the benefit of ESSs. This dissertation proposes a sensitivity guided approach which aims at finding the optimal location of ESSs to reduce the peak hour generation cost. The last part of this dissertation proposes a model to determine the operation strategy of battery ESSs. This algorithm not only attempts to maximize the financial benefits but also considers the cycling behavior and its impact on the longevity of battery energy storage systems.

This dissertation is dedicated to my family.

ACKNOWLEDGMENTS

First of all, I would like to express my sincere and deepest gratitude to my advisor Dr. Joydeep Mitra. It is my honor and fortune to be his student and I am really grateful for his encouragement, patience, suggestion, and inspiration. He is the one who taught me the first steps in my research when I started my graduate study. Without his support and guidance, I would not have made progress in my research and finish my Ph.D. program. I truly appreciate and value everything I have learned from him. It will forever remain a major contributor behind my achievements.

I am also thankful to Dr. Bingsen Wang, Dr. Guoming Zhu, Dr. Lixin Dong, and Dr. Fang Z. Peng, for their helpful classes, insightful comments and time serving in my Ph.D. dissertation committee.

I would also like to thank my colleagues in the ERISE lab, for their kind support and priceless friendship, Dr. Niannian Cai, Dr. Mohammed Benidris, Dr. Salem Elsaiah, Dr. Samer Sulaeman, Dr. Nga Nguyen, Mr. Valdama Johnson, Mr. Khaleel O. Khadedah, Mr. Saleh Almasabi, Mr. Atri Bera, and Mr. Fares Theyab Alharbi.

My sincere thanks also go to Dr. Junyong Liu, Dr. Youbo Liu, and Dr. Yue Xiang from Sichuan University in China, for their suggestions, discussions, and host during my stay.

I would like to thank my supervisors at Argonne National Laboratory, Vladimir Koritarov and Dr. Dongbo Zhao for providing me the opportunities to work as a Research Aide in a notable research institute and the chance to learn from all the excellent researchers in the CESSSA group.

Thanks to my entire family and close friends for giving me encouragement, suggestions and love. Most of all, I would like to thank my parents, Dr. Lifeng Tian and Jing Huang, and my husband Chi Xin, for their unconditional love, support, knowledge, patience, and understanding. Thank you for helping me through all the difficulties and cheering me up when I am down. Thank you for sharing all the joys, happiness and achievements in my life.

TABLE OF CONTENTS

LIST OF TABLES

LIST OF FIGURES

Chapter 1

Introduction

1.1 Motivation

Deployment of energy storage systems (ESSs) is gaining significant momentum due to economic incentives, power system regulation requirements, and integration of renewable energy resources. An energy storage device can be considered as a device that mediates between energy generation and energy consumption [1]. The power balance constraint imposes the condition that generation must always equal consumption (including losses). This is challenging, especially after the integration of renewable energy sources. Hence, the deployment of an ESS provides a reserve of electric power which can be used judiciously when the need arises.

Large storage facilities, including pumped hydro storage (PHS) and compressed air energy storage (CAES) have been developed for decades. Battery energy storage systems (BESSs) are also available for grid-scale applications. Sodium-sulfur batteries, vanadium-redox flow batteries, lithium-ion batteries, and lead-acid batteries have been used in grid level applications. For instance, a 200 MW, 800 MWh vanadium redox flow battery storage project is under construction in Dalian, China which will become the world's largest battery storage facility when completed [2]. Also, according to the DOE Energy Storage Database [2], lithium-ion batteries are widely used and applied in most of the grid-scale battery storage projects.

ESSs can provide several services, such as bulk energy services (electric energy time-shift and electric supply capacity), ancillary services (regulation, voltage support, etc.), transmission and distribution (T&D) infrastructure services (T&D upgrade deferral, transmission congestion relief, etc.) and customer energy management services (power quality, demand charge management, etc.) [1, 3, 4]. Despite steadily decreasing costs, the capital cost of an ESS is still considerable, and very few applications of ESSs are directly related to economic incentives. Hence, a comprehensive study is needed to estimate the potential benefits, to guide the planning and to investigate the optimal operating strategy of ESSs.

1.2 Objectives and Challenges

The objectives and challenges of this research work are,

1. Benefits: The first objective is to estimate the maximum revenue that an energy storage system can generate. The stacked revenue from an ESS cannot be calculated by simply aggregating the benefits from individual applications. This is because a quantity committed to one market may not be committed to another during the same time interval. Thus it is necessary to build a comprehensive model which is able to estimate the stacked revenue and the results can be utilized by industries including utilities and manufacturers to build business cases when they want to install an ESS for their facilities.
2. Planning: The second objective is to develop an approach which helps the system planners to better understand and estimate the actual capacity contribution of an ESS, especially when the ESS is expected to provide multiple services. When performing system capacity expansion studies, the reliability target should be first met. The capacity value of a generating unit can reflect the contribution of a unit to meet the desired reliability level. However, the ESS availability uncertainty and the energy-limited characteristic make the estimating process complicated. This part also proposes a sensitivity guided approach to determine the optimal location of ESSs which aims at minimizing the peak hour generation cost.

3. Operation: The task for operation is to build a model which provides optimal operating strategy in electricity markets. This strategy should consider not only the operating policies and system constraints, but also the cycling behavior of the ESS and its impact on longevity. This is because participating in certain markets can result in significant cyclings of the ESSs and deep cycles can have large negative impact on the longevity for some types of battery ESSs, such as Lithium-ion batteries.

1.3 Contributions

The contributions of this dissertation are as follows,

- Developing a mathematical model to evaluate the stacked revenue of ESSs.
- Co-optimizing the ESSs applications, including energy arbitrage, frequency regulation and outage mitigation.
- Developing a mathematical model to evaluate the system reliability improvement with ESSs.
- Proposing the model to estimate the capacity value of ESSs considering the availability uncertainty of ESSs when providing multiple services.
- Proposing a sensitivity-guided approach to determine the optimal location of ESSs.
- Modeling the effect of battery degradation in determining the optimal operating strategies.
- Investigating the impacts of battery operating policies on the longevity of the battery ESSs.

1.4 Organization of the Thesis

This thesis presents the proposed approaches, case studies and results, which are organized as follows.

Chapter 2 introduces several types of grid-scale energy storage systems and briefly discussed the application and benefits of ESSs in the power grid.

Chapter 3 describes the proposed model to evaluate the stacked revenue of grid-connected energy storage systems.

Chapter 4 presents the model and procedure to estimate the capacity value of an ESS when it is expected to provide multiple services.

Chapter 5 proposes a sensitivity guided approach to determine the optimal location of ESSs which aims at reducing the peak generation cost.

Chapter 6 provides the method to determine optimal operating strategies of Lithium-ion battery ESSs considering the battery degradation.

Chapter 7 describes concluding remarks of this dissertation.

Chapter 2

Background and Literature Review

The first chapter of the dissertation includes a literature review of existing and near-term energy storage technologies, engineering and materials. This chapter also introduced the potential applications of the energy storage on the power systems, such as peak shaving, frequency regulation, outage mitigation, transmission & distribution upgrade deferral, etc.

2.1 Types of Energy Storage Systems

The energy storage systems introduced in this section are: pumped storage hydro, compressed air energy storage systems, and battery energy storage systems (BESS). Several types of BESSs are also discussed, such as Lithium-ion batteries, Sodium-sulfur batteries, Lead-acid batteries, Vanadium Redox Flow batteries, etc.

2.1.1 Pumped Storage Hydro

Pumped Storage Hydro (PSH) is one of the largest energy storage technologies currently applied around the world. This technology is mature and has been applied since 1880s. The first PSH plant in the U.S was the Rocky River pumped storage plant, which is constructed in the late 1920s in Connecticut. PSH is one of the most cost-effective ESSs and currently accounts for 95% of all

utility-scale energy storage in the US. The total rated power of PSH is more than 185 GW world wide [2].

A typical conventional PSH project consists of two interconnected reservoirs with different elevations [5]. The PSH store and generate power by moving water between two reservoirs through tunnels. For example, PSH can employs off-peak energy to pump water from the lower reservoir up to the upper reservoir. Also, it can release water from the upper reservoir into the lower reservoir to generate electricity when the electricity demand is high.

2.1.2 Compressed Air Energy Storage

Compressed Air Energy Storage (CAES) typically has underground cavern or aboveground pipes or vessels. It is another type of ESSs which has large capacity other than PSH. The CAES systems can compress air and store it in a reservoir during periods of excess power. When the electricity is required, the stored high-pressure air is heated, expanded and returned to the surface and applied to generate electricity.

There are two operating large CAES systems. One is a 290 MW, 4 hours in-ground natural gas combustion compressed air project in Germany built in 1978 and another one is the 110 MW, 26 hours project in Alabama, US, built in 1991 [2]. Another noteworthy project is the Bethel Energy Center which is a planned 317 MW CAES facility that will be located in Anderson County, within Texas ERCOT power market. This facility can provide power for over 300,000 homes and has the energy capacity of 30,000 MWh when completed (anticipated commercial operation date is Summer 2020) [6].

2.1.3 Vanadium Redox Flow Battery

Vanadium redox flow battery (VRFB) is a relatively mature type of flow battery. The power of flow batteries is defined by the size and design of the electrochemical cell while the energy depends on the size of the tanks [7]. Like other redox-flow batteries, vanadium redox flow batteries have high energy efficiency, short response time, long cycle life (more than 10,000 cycles), independently

tunable power rating and energy capacity, and consistently stable performance [8]. VRFB uses ions of the same metal on both sides and this attribute prevents cross contamination and resulting in electrolytes with a potentially unlimited life. These batteries are also inherently safe, with no thermal runaway, since the electrolyte is aqueous and non-flammable.

VRFB has already been used in various stationary applications and the number of VRFB projects is increasing. Vanadium redox flow batteries are mostly used for applications such as renewable capacity firming, renewable energy time shift, onsite renewable generation shifting, frequency regulation, electric energy time shift and voltage support. The size of the VRFB can be expanded to more than 100 MW. For instance, a 200 MW, 800 MWh vanadium redox flow battery storage project is under construction in Dalian, China which will become the world's largest flow battery storage facility when completed [2].

2.1.4 Lithium-ion batteries

Lithium-ion (Li-ion) batteries were first commercialized in the early 1990s and now have become one of the most preferred storage technologies in many applications, due to their high energy density, high voltage ratings, high efficiency, low self-discharge, and fast response. In addition, the Li-ion battery market is expanding and a lot of manufactures are available, for example, Tesla, A123, LG Chem, BYD, SAFT, etc. However, Li-ion batteries have some disadvantages, such as high cost, heat management issues and narrow operating temperatures [7] and the biggest issue for Li-ion batteries is safety due to flammability.

Li-ion batteries have several subtypes based on cathode material, including Lithium Manganese Oxide (LMO), Lithium Iron Phosphate (LFP), Lithium Nickel Cobalt Aluminum (NCA), Lithium Titanate (LTO) , Lithium Nickel Manganese Cobalt (NMC), etc. In general, LFP is the most popular type for power grid in terms of the number of projects installed.

The largest Li-ion battery available today is the one installed by Tesla in the Hornsdale Wind Farm in South Australia [9]. This 100 MW, 129 MWh battery is used to store renewable energy and provide back-up power. The number of Li-ion batteries is increasing rapidly. Among the projects

that are under-construction, announced and contracted, more than half of the projects are Li-ion batteries. Li-ion batteries are mostly applied for renewable capacity firming, frequency regulation, electric energy time shift, and so on.

2.1.5 Sodium-Sulfur Battery

Sodium-sulfur (NaS) battery technology was first invented in the 1960s by Ford Motor Company. After decades of development and support, nowadays there are many operational NaS projects worldwide and it has been applied to many applications such as, electric utility distribution grid support, wind power integration, and high-value grid services [1]. The advantages of NaS batteries are long discharge period, relatively high energy densities, fast response and commercial maturity. Moreover, the NaS battery uses inexpensive, non-toxic materials leading to high recyclability [10]. NaS battery normally requires a temperature of 300°C to 350°C to ensure the electrodes in liquid states, so each unit has a build-in heating element. Therefore, one of the drawbacks of NaS battery is that the internal heating unit uses the batterys own stored energy and thus reduces the battery performance. Another downside is the risk of fire, since it uses materials such as metallic sodium which is combustible if exposed to water.

2.1.6 Lead-Acid Battery

Lead-acid (LA) batteries have been commonly used in many industry application including stationary and mobile applications [7]. There are two main types of lead acid batteries which are carbon lead acid technologies and advanced lead-acid technologies. Lead-acid batteries have advantages such as fast recharge rates, simple charging technology, long cycle lives in deep discharge applications, favorable cost/performance ratio [7, 11]. Lead-acid batteries have high commercial maturity and relatively low disposal cost, total installed cost and relocation cost [11]. However, the Lead-acid batteries have a hazardous material prohibited or restricted in various jurisdictions, could cause harmful impacts on the environment and may need high maintenance cost [7].

2.1.7 Other Types of Battery Sotrage

Nickel-Based Batteries

Nickel cadmium (NiCd) and nickel metal hybrid (NiMH) batteries are the two main members in the nickel-based family. All nickel-based batteries utilize nickel hydroxide as the cathode. NiCd uses a metallic anodecadmium, while NiMH has anode that store hydrogen.

a. Nickel Cadmium Battery

Nickel cadmium (NiCd) has been in the commercial market since 1915, which is a relatively mature technology, but few grid-scale deployments exist. This type of battery is capable of performing well even at low temperatures. Vented Ni-Cd batteries can operate on a scale similar to lead-acid batteries, and compared to lead acid batteries, nickel-based batteries have a higher power density, a slightly greater energy density, and the number of cycles is higher [7]. Despite the many advantages, NiCd batteries also pose several disadvantages. The material cadmium is prohibited for customer use, since it is very toxic and dangerous to the environment.

b. Nickel Metal Hydride Battery

Nickel metal hydride (NiMH) Battery was developed as an alternative for NiCd because of the toxicity of cadmium and became available around 1995. Although NiMH batteries share almost all the advantages of NiCd batteries, the maximal nominal capacity is still ten times less when compared to NiCd and lead acid [7]. Furthermore, it charges slower than NiCd and does not withstand very low operating temperatures.

Sodium-Nickel-Chloride Battery

Sodium nickel chloride (NaNiCl) batteries are also known as ZEBRA (Zero Emission Battery Research Activities). They are high-temperature batteries like sodium-sulfur batteries, but they use nickel chloride for the positive electrode instead of sulfur. NaNiCl batteries has several advantages, such as low environmental impact, fast response, long cycle life, tolerance of short circuits, constant performance and cycle life in harsh operating environments, and high energy density [1]. It has proven to present relatively low intrinsic risks during normal operation.

Zinc-Bromine Battery

The Zinc-bromine battery (ZBB) is a type of hybrid flow batteries (HFB) which is developed in the early 1970s. This battery is still in an early stage of field deployment and demonstration trials for utility applications. ZBB is a promising and emerging technology. It combines the features of a conventional battery and flow battery, and thus allows higher power and energy densities than other types of flow batteries. It also has long estimated lifetimes as 20 years, since the active materials themselves do not degrade and the lifetime is not strongly dependent on the number of cycles or the depth of discharge [1].

Zinc-Air Battery

Zinc-air is one type of metal-air batteries. Metal-air batteries consist of the anode made from pure metal and the cathode connected to an inexhaustible supply of air [7]. This type of batteries should be able to offer low material cost and high specific energy. However, it is still in early stage for utility application.

Iron-Chromium Battery

Iron-chromium (Fe-Cr) battery is the first developed technology of flow batteries in 1970s by NASA. The Fe-Cr type batteries has safety advantage as other redox flow batteries due to the separation of power and energy. They also have design flexibility, since the power capacity (stack size) can be specifically tailored to the applications load or generation profile [12]. Moreover, they use abundant and low-cost materials and have no volume change during cycling, results in a less-complex design and simpler control compared to Li-ion, lead-acid, NaS, Zinc-bromine and others [1]. They are also environmental benign, since the utilized iron and chromium species are low toxic. However, this technology is still in R&D phase for grid services markets. Once it becomes commercially mature, it would be an advancing option for time shift on either the utility or customer side of the meters and also frequency regulation services.

2.2 Applications of Energy Storage System

ESSs can provide several services, such as bulk energy services (electric energy time-shift and electric supply capacity), ancillary services (regulation, voltage support, etc.), transmission and distribution (T&D) infrastructure services (T&D upgrade deferral, transmission congestion relief, etc.) and customer energy management services (power quality, demand charge management, etc.) [1, 3, 4]. This section focuses on describing outage mitigation, energy arbitrage, frequency regulation, and other technical benefits of ESSs.

2.2.1 Mitigation of Outages

Numerous factors may affect system reliability, such as failures of generating units, system faults and equipment failures. All these factors may lead to loss of load. In such situations, an ESS can effectively support customer loads when partial or complete loss of power from the source utility takes place. Sometimes, due to the capacity constraint, it might not be possible for the ESS to completely mitigate the outage. However, for such an event, it can shorten the interruption duration or reduce the number of interrupted customers.

The ESS can be installed at the transmission level, distribution level, or close to a customer site. The closer the location of the ESS to a customer, the more helpful it is. If the ESS is owned by a utility with a large capacity, it can be treated as a dispatchable resource (subject to its energy limit) in improving the reliability in the interconnected area. It can also serve the customer needs at an outage event, especially in some critical locations such as hospitals and correctional facilities, which can significantly benefit from using an ESS. This support may require the ESS and customer loads to island during the outage and re-synchronize with the utility when power is restored.

2.2.2 Energy Arbitrage

An energy storage system can be utilized to store energy during off-peak hours and then discharge at peak demand period for peak shaving or load following. This helps to reduce the generation cost

and postpone the need for peaking units. It is also profitable for the ESS owners as they can take advantage of the energy price difference. The Locational Marginal Price (LMP) is usually used for wholesale electricity price, which indicates the value of energy at a particular location at any given point of time. To gain maximum benefit from this application, the ESS should be charged with less expensive energy at off-peak hours and discharged during the peak hours when LMPs are high. Therefore, locations with large variability in LMPs can be considered as ideal locations.

2.2.3 Frequency Regulation

Frequency regulation is another service for which energy storage is well suited. Frequency regulation helps to maintain the grid frequency within specified limits and to comply with the Real Power Balancing Control Performance (BAL001) and Disturbance Control Performance (BAL002) Standards of the North American Electric Reliability Council (NERC) [13].

The frequency of any system may deviate from the specified value if there is an unforeseen imbalance between the generation and the load. Several generator actions are needed at this moment to restore the frequency back to the normal operating range. These include primary, secondary, and tertiary frequency control and may range from a few seconds to several minutes. A fast-acting ESS can help in such a situation, which helps to restore the frequency very quickly. The response of an ESS can be twice as effective compared to conventional fossil fuels generators, which includes coal units and combustion turbines (CTs) [14]. This property of the storage devices has been utilized by several utilities.

2.2.4 Other Technical Benefits

ESSs can also be used in a variety of other technical applications (not directly related to monetary benefits) that are crucial to the power grid operation and equipment lifetime. These applications can be classified according to the customers that are being served, e.g., residential, commercial, or industrial customers. Some of these applications are described in this section.

Voltage Flicker Mitigation

In power distribution systems, voltage flicker is often a problem that needs to be addressed. It is harmful for all types of customers. Voltage flicker may damage electrical devices ranging from the most common appliances used in a household to large equipment used in the industry. It may also lead to spoilage from semi-finished products in an industry. However, if an ESS is installed in the system, it helps to stabilize the voltage by ramping up or down within a very short period of time, thus protecting the customer equipment.

Power Factor Improvement

The requirements of power factor improvement can be seen mostly among industrial customers who use a significant amount of reactive power for their daily operation. In most of the cases, they are charged with a penalty from the utility serving them if the power factor drops below a pre-specified limit. Those customers will be greatly benefited if they already have an ESS installed at their facilities.

Upgrade Deferral

An ESS can also be used for the deferral of transmission/distribution system upgrades. It can help in delaying investments that would otherwise be necessary to maintain the transmission and distribution capacity in accordance with the load demand. For example, purchase of a new transformer with a high capacity may be avoided by using an ESS instead.

Voltage-regulator Lifetime Extension

The deployment of distributed generators, such as photo-voltaic (PV) and wind power at the distribution system level, may decrease the lifetime of voltage regulators due to the increase in voltage fluctuations (e.g., the number of tap-changes increases). If ESSs are used at the distribution system level, (e.g., at a feeder) to reduce voltage fluctuations, the number of tap-changes of the regulator can be reduced, thus extending its lifetime.

Emission Reduction

Climate change and global warming are matters of concern nowadays and they are mostly related to emissions from fossil-fueled power plants. Thermal power plants across the world are among the largest consumers of fossil fuels. Since the peak power generated from renewable energy sources may not coincide with the system peak, integration of ESSs with these sources will reduce the peak time and level and therefore significantly reduce emissions from fossil-fueled power plants [15]. In other words, ESSs can store clean energy at off-peak hours (e.g., when wind power generation is high at night while load demand is low) and then discharge it at peak hours [16].

Black Start

Black Start service is needed to energize transmission and distribution lines and provide station power to bring power plants on-line following blackout events. NERC defines a Black Start Resource as, "A generating unit(s) and its associated set of equipment which has the ability to be started without support from the System or is designed to remain energized without connection to the remainder of the System, with the ability to energize a bus, meeting the Transmission Operators restoration plan needs for Real and Reactive Power capability, frequency and voltage control, and that has been included in the Transmission Operators restoration plan." Storage systems can provide an active reserve of power and energy within the grid and can be applied for providing black start service. For example, Golden Valley Electric Association uses the battery system in Fairbanks for this service when there is an outage of the transmission intertie with Anchorage.

Chapter 3

Evaluation of Stacked Revenue

This chapter proposes a comprehensive evaluation of stacked revenue generated from grid-connected energy storage systems (ESSs). The stacked revenue from an ESS cannot be calculated by merely aggregating the benefits from various applications (e.g., energy arbitrage, frequency regulation, and outage mitigation) as the ESS may not be available for all types of applications during the same time intervals. This is because a quantity committed to one market may not be committed to another. In this study, different types of applications for grid-connected ESSs are identified, and a model incorporating component reliability, power system operation constraints, and storage system operation constraints is developed to evaluate the composite revenue generated from these applications. In this model, the types of applications of ESSs are prioritized according to their intended contributions and system operating conditions. Sequential Monte Carlo simulation is used for evaluating the reliability improvement and a quadratically constrained linear programming model is built for estimating the maximum revenue from arbitrage and regulation markets. The proposed method is demonstrated on the IEEE reliability test system (IEEE-RTS) using historical PJM price data.

3.1 Introduction

Deployment of energy storage systems (ESSs) is gaining significant momentum due to economic incentives, power system regulation requirements, and integration of renewable energy sources. The ESSs have several applications in power systems including peak load shaving, power outage mitigation, and frequency regulation. Despite steadily decreasing costs, the capital cost of an ESS is still considerable, and a few applications of ESSs are directly related to economic incentives. Hence, a cost-benefit analysis is necessary to evaluate the profit and justify the investment. This study investigates the economics of the system when several applications of the ESS are stacked together to generate a cumulative revenue. Benefits from reliability improvement, energy arbitrage, and regulation are considered in estimating the stacked revenue from ESSs.

An energy storage device can be considered as a device that mediates between energy generation and energy consumption [1]. The power balance constraint imposes the condition that generation must always equal consumption (including losses). This is not always feasible, especially after the integration of renewable energy sources. Hence, the deployment of an ESS provides a reserve of electric power which can be used judiciously when the need arises. Utilities and research organizations have performed comprehensive research on the applications of ESSs in power systems [1, 3]. A number of studies have been dedicated to identifying individual use cases and generating revenues from ESSs [17, 18]. A co-operation scheme for wind power and battery storage to bid into electricity market in providing frequency regulation, in terms of monetary income, has been described in [19]. Also, estimation of maximum potential revenue of grid connected ESSs based on the arbitrage and regulation markets has been presented in [20–22]. However, in these studies, the benefits of outage mitigation are not considered. A quantitative method to determine the size of ESSs to meet specified reliability targets was proposed by one of the authors in [23, 24]. The method presented in [23, 24] was extended in [25] to quantify the size of the required energy storage to firm up wind power and improve system reliability to a specific target. Although the prior work presented in [23–25] shows the benefits of an energy storage system from the point view of improving system reliability and firming up wind generation, the cost-benefit

from improving reliability and other merits is not presented.

Different types of ESSs are being used nowadays. Large storage facilities, including pumped hydro storage (PHS) and compressed air energy storage (CAES) have been developed for decades. Battery energy storage systems (BESSs) are also available for grid-scale applications. Sodium-sulfur batteries, vanadium-redox flow batteries, lithium-ion batteries, and lead-acid batteries have been used in grid level applications. For instance, a 200 MW, 800 MWh vanadium redox flow battery storage project is under construction in Dalian, China which will become the world's largest battery storage facility when completed [2]. Also, according to the Energy Storage Database of the Department of Energy [2], lithium-ion batteries are widely used and applied in a significant majority of grid-scale battery storage projects. The work presented in this chapter considers the potential benefits for different types of applications from fast-acting ESSs, such as batteries, flywheels, etc; determination of the type of storage to be used is beyond the scope of this work.

The stacked revenue from an ESS cannot be calculated by simply aggregating the benefits from individual applications because a quantity committed to one market may not be committed to another during the same time interval. Hence, they have to be prioritized based on several factors such as customer satisfaction and economic viability. In this chapter, improving system reliability is prioritized along with generating revenues from energy arbitrage and frequency regulation. Also, the cost-benefit analysis for each individual application of ESSs is studied and stacked with other applications for estimating the possible maximum revenue. In this study, service continuity is considered with the highest priority. This means that in the event of an outage, the ESS should discharge in an attempt to minimize the downtime at the load, even though participating in the energy or regulation market may bring higher profit.

Sequential Monte Carlo simulation (MCS) is used to track the state of charge (SOC) of the ESS and the outage events in the system while evaluating the reliability indices and interruption cost. Also, the same sequence of failures is used for the tested cases to provide a common base for the comparisons. The variable behavior of load and the forced outages of generators are also captured by the sequential simulation. For estimating the revenue from electricity market, a quadratically

constrained linear programming optimization problem is developed. In this model, the control strategy for the ESS not only considers the energy storage capacity and charging/discharging power limits, but also includes the market mechanism constraints and application priority.

The remainder of this chapter is organized as follows. Section 3.2 explains the mathematical models that are developed to calculate the revenue generated from each use case. Section 3.3 describes the ESS operation strategy and managing concerns. Section 3.4 presents case studies on evaluating the contribution of ESSs. Section 3.5 provides concluding remarks.

3.2 Mathematical Modeling

In this section, the mathematical models for evaluating revenue from mitigating outages, participating in energy arbitrage, and regulation market are presented.

3.2.1 Value from Mitigating Outages

When a contingency occurs, such as a generation loss or a transmission line tripping, the load demand may not be satisfied. In the sequential MCS, random component failures are simulated. For each hour, the system state is defined by the component states and capacities. The sufficiency of power supply to each load is the combined effect of operation and generation and transmission adequacy. Then, a feasible dispatch is sought by solving an optimization problem, subject to the equality and inequality constraints of the power system operation limits and the availability of system components [26, 27].

Customer damage functions (CDFs) are usually applied to display customer interruption costs, which can be determined for a given customer type and aggregated to produce section customer damage function for the various classes of customers [28]. The value of CDF depends on the type of customer served (e.g., the interruption cost for an industrial user is higher than a residential or an agricultural user). Composite customer damage function (CCDF) at each load point can be calculated by aggregating the weighted individual sector CDF at that load point. The CCDF can

be converted into another index, i.e., the interrupted energy assessment rate (IEAR) in \$/kWh to evaluate the monetary loss as a function of the energy not supplied. The equations below show how to evaluate the system reliability indices and interruption cost.

$$\text{Minimize} \quad Cost^{\text{int}} = \left(\sum_{i=1}^{N_b} C_i \times IEAR_i \right) \tag{3.1}$$

subject to

$$\begin{gathered} P(V,\delta) - P_D + C = 0 \\ Q(V,\delta) - Q_D + C_Q = 0 \\ P_G^{\min} \leq P_G \leq P_G^{\max} \\ Q_G^{\min} \leq Q_G \leq Q_G^{\max} \\ V^{\min} \leq V \leq V^{\max} \\ |F(V,\delta)| \leq F^{\max} \\ -\pi \leq \delta \leq \pi \end{gathered} \tag{3.2}$$

where C_i is the load curtailment at bus i, $IEAR_i$ is the Interrupted Energy Assessment Rate at bus i, C is the vector of load curtailments $(N_b \times 1)$, C_Q is the vector of reactive load curtailments $(N_b \times 1)$, V is the vector of bus voltage magnitudes $(N_b \times 1)$, δ is the vector of bus voltage angles $(N_b \times 1)$, P_D and Q_D are the vectors of real and reactive power loads $(N_b \times 1)$, P_G and Q_G are the vectors of real and reactive power outputs of the generators $(N_g \times 1)$, $P_G^{\min}$, $P_G^{\max}$, $Q_G^{\min}$ and $Q_G^{\max}$ are the vectors of real and reactive power limits of the generators $(N_g \times 1)$, $V^{\max}$ and $V^{\min}$ are the vectors of maximum and minimum allowed voltage magnitudes $(N_b \times 1)$, $F(V,\delta)$ is the vector of power flows in the lines $(N_\ell \times 1)$, and $F^{\max}$ is the vector of power rating limits of the transmission lines $(N_\ell \times 1)$. In the foregoing description, N_b is the number of buses, N_ℓ is the number of transmission lines, and N_g is the number of generators.

The above model implies that for any encountered scenario (generation and transmission avail-

ability and load state) power will be routed through the network in such a manner so as to minimize the system interruption cost.

(a) Loss of load probability (LOLP): The LOLP is a widely used reliability index and it can be estimated as follows [27].

$$LOLP = E[\hat{\theta}] \tag{3.3}$$

where

$$\hat{\theta} = \frac{1}{T}\sum_{i=1}^{N_c} T_i^{\text{down}} \tag{3.4}$$

and T_i^{down} is the duration of an interruption encountered during the sequential MCS. N_c is the total number of simulated cycles and T is the total period of simulation.

(b) Expected demand not supplied (EDNS): The EDNS is the sum of the products of probabilities of failure states and the corresponding load curtailments, which can be estimated as follows.

$$EDNS = E[\hat{d}] \tag{3.5}$$

where

$$\hat{d} = \frac{1}{T}\sum_{i=1}^{N_c}(T_i^{\text{down}}\sum_{j=1}^{N_b} C_j) \tag{3.6}$$

(3) Interruption Cost: The interruption cost in this study is defined as the annual interrupted energy cost and can be calculated as follows.

$$\text{Interruption Cost} = E[\hat{\phi}] \tag{3.7}$$

where

$$\hat{\phi} = \frac{1}{T}\sum_{i=1}^{N_c}(T_i^{\text{down}}\sum_{j=1}^{N_b} C_j \times \text{IEAR}_j) \tag{3.8}$$

(4) Value From Outage Mitigation: The value of reliability provided by the ESS is calculated by comparing the interruption cost with and without an ESS. The ESS is operated with the objective

of maximizing the revenue from the arbitrage and regulation market at normal operating states where the SOC varies with time. The integration of an ESS can be modeled by a multistate model to capture the varying behavior. For each state, if the SOC value and its corresponding probability is provided, then the value from this use case can be expressed as follows:

$$\text{Value}_{\text{rel}} = E[\hat{\phi}_{\text{base}}] - \sum_{n=1}^{N_{\text{soc}}} E[\hat{\phi}_n] p_n^{\text{soc}} \tag{3.9}$$

where N_{soc} is the total number of SOC states and p_n^{soc} is the corresponding probability. $E[\hat{\phi}n]$ is the interruption cost when the initial SOC of an outage event is at the nth state and $E[\hat{\phi}_{\text{base}}]$ is the interruption cost for the base case without an ESS.

3.2.2 Revenue from Arbitrage Market

In this section, a model for calculating the revenue from energy arbitrage is defined. If the ESS is operated for a period of time T_m, the total revenue from the arbitrage market can be calculated as:

$$\text{Income}_{\text{arb}} = \sum_{t=1}^{T_m} (R_t^{\text{lmp}} E_t^{\text{arb}_{\text{d}}} - R_t^{\text{lmp}} E_t^{\text{arb}_{\text{c}}}) \tag{3.10}$$

where R_t^{lmp} is the locational marginal price ($/MWh) of the system at time t; $E_t^{\text{arb}_{\text{d}}}$ and $E_t^{\text{arb}_{\text{c}}}$ are the quantities of energy sold (discharged) and purchased (charged) at time t, respectively.

3.2.3 Revenue from Regulation Market

Independent System Operators (ISOs) and utilities purchase frequency regulation service from ESSs to compensate area control error (ACE) and to maintain frequency stability. According to the Federal Energy Regulatory Commission (FERC) order 755, market operators are required to apply pay-for-performance mechanism which should reflect the speed and accuracy of the device. ESSs are able to respond rapidly while following the regulation signal and therefore are motivated

to participate in the regulation market. In PJM market, two different regulation signals are applied, i.e., RegA and RegD. RegA is mostly designed for traditional regulating resources, which is a low-pass filtered ACE signal [29]. On the other hand, RegD is generally used for faster responding resources like energy storage, which is a high pass filtered ACE signal.

Different ISOs implement pay-for-performance using different models. In this study, the estimation method is developed based on a method used by PJM Interconnection. PJM implements frequency regulation by using a payment method that consists of two parts; a capability payment based on regulation market capability clearing price (RMCCP) and a performance payment using regulation market performance clearing price (RMPCP). These two parts are added up to obtain the total revenue from regulation market. Both the capacity and performance payments employ an actual performance score. Also, the performance credit includes a mileage ratio. The calculations are shown in the following equations [29]. The capability credit for a particular hour can be calculated as follows.

$$\text{Capability Credit} = P_t^{\text{reg}} \times S_t \times R_t^{\text{rmccp}} \tag{3.11}$$

where P_t^{reg} is the hourly-integrated regulation capacity (MW), S_t is the actual performance score, and R_t^{rmccp} is the RMCCP at time t. Similarly, the performance credit is calculated as follows.

$$\text{Performance Credit} = P_t^{\text{reg}} \times S_t \times \beta_t \times R_t^{\text{rmpcp}} \tag{3.12}$$

where β_t is the mileage ratio for that hour and R_t^{rmpcp} is the RMPCP at time t. Here mileage represents the absolute sum of the movement of the regulation signal in a given period and is the proxy metric for the amount of work performed. In this case, the mileage ratio is the ratio between the requested mileages of RegD signal and the referenced traditional regulation signal (RegA), which is defined as follows.

$$\text{Mileage Ratio} = \frac{\text{Mileage RegD}}{\text{Mileage RegA}} \tag{3.13}$$

The total income from the regulation market is the total of capability credit and performance credit and is expressed as follows.

$$\text{Income}_{\text{reg}} = \sum_{t=1}^{T_m} [S_t(R_t^{\text{rmccp}} + \beta_t R_t^{\text{rmpcp}}) P_t^{\text{reg}}] \tag{3.14}$$

3.3 Energy Storage System Operation Strategy

In this section, the optimization model to estimate the maximum stacked revenue from improving system reliability and participating in energy and regulation markets is presented.

3.3.1 Objective

The objective of this problem is to estimate the maximum benefit from an ESS in the grid which is equal to the summation of value from outage mitigation ($\text{Value}_{\text{rel}}$), income from the arbitrage and regulation markets ($\text{Income}_{\text{arb}}$ and $\text{Income}_{\text{reg}}$) as stated in (3.15).

$$\text{Benefit} = \text{Value}_{\text{rel}} + \text{Income}_{\text{arb}} + \text{Income}_{\text{reg}} \tag{3.15}$$

In this study, the reliability is given a higher priority than monetary benefits, which implies that in the event of an outage, the ESS should discharge to minimize the downtime of service to the load, no matter which use case brings more monetary benefits. During the periods when there is no outage event, the storage system is operated to maximize the revenue from the arbitrage or the regulation market. The value from outage mitigation can be evaluated by calculating the reduction in the interruption cost, which is presented in section III.

To estimate the income from the arbitrage and regulation, a quadratically constrained linear programming model is developed. In this optimization model, the variables are $P_t^{\text{arb}_\text{d}}, P_t^{\text{arb}_\text{c}}$ and P_t^{reg}, where $P_t^{\text{arb}_\text{d}}, P_t^{\text{arb}_\text{c}}$ are the capacities sold and purchased in the arbitrage market at time t; P_t^{reg} is the committed regulation capacity at time t, which can be utilized for regulation up

or down based on the regulation signal. The objective is to maximize the income from the energy and regulation markets as follows.

$$\text{Maximize} \quad \sum_{t=1}^{T_m} \Big[R_t^{\text{lmp}} P_t^{\text{arb}_\text{d}} \tau / \gamma_d - R_t^{\text{lmp}} P_t^{\text{arb}_\text{c}} \tau \gamma_c + S_t (R_t^{\text{rmccp}} + \beta_t R_t^{\text{rmpcp}}) P_t^{\text{reg}} \Big] \tag{3.16}$$

where τ is the duration of the energy market dispatch time interval and it is considered to be one hour in this study, γ_c and γ_d are the charging and discharging efficiencies (%). $R_t^{\text{lmp}} P_t^{\text{arb}_\text{d}} \tau / \gamma_d$ represents the revenue by selling the energy and $R_t^{\text{lmp}} P_t^{\text{arb}_\text{c}} \tau \gamma_c$ is the cost of purchasing energy from arbitrage market; $S_t (R_t^{\text{rmccp}} + \beta_t R_t^{\text{rmpcp}}) P_t^{\text{reg}}$ represents the revenue from the regulation market.

3.3.2 Constraints

The operation of an ESS can be modeled by its energy storage capacity, charging and discharging power limits, charging and discharging efficiencies. The state of charge of an ESS reflects the ratio of the current capacity to the rated capacity, which depends on the SOC of the previous period and the current charging/discharging operation. The state of charge at time t is represented as follows.

$$SOC_t = SOC_{t-1} + \frac{\triangle E_t}{E^{\text{r}}} \tag{3.17}$$

where E^r is the rated energy capacity, and $\triangle E_t$ is calculated as below.

$$\triangle E_t = E_t^{\text{arb}_\text{c}} - E_t^{\text{arb}_\text{d}} + E_t^{\text{reg}_\text{c}} - E_t^{\text{reg}_\text{d}} \tag{3.18}$$

where $E_t^{\text{arb}_\text{c}}$ and $E_t^{\text{arb}_\text{d}}$ are the charged and discharged energy in the arbitrage market; $E_t^{\text{reg}_\text{c}}$ and $E_t^{\text{reg}_\text{d}}$ are the charged and discharged energy in the regulation market, respectively. They are

calculated as follows.

$$E_t^{\text{arbc}} = P_t^{\text{arbc}} \tau \gamma_c$$

$$E_t^{\text{arbd}} = P_t^{\text{arbd}} \tau / \gamma_d$$

$$E_t^{\text{regc}} = \begin{cases} -P_t^{\text{reg}} \eta_t^{\text{reg}} \tau \gamma_c, & \text{if } \eta_t^{\text{reg}} < 0 \\ 0, & \text{otherwise} \end{cases} \tag{3.19}$$

$$E_t^{\text{regd}} = \begin{cases} P_t^{\text{reg}} \eta_t^{\text{reg}} \tau / \gamma_d, & \text{if } \eta_t^{\text{reg}} > 0 \\ 0, & \text{otherwise} \end{cases}$$

where η_t^{reg} is the RegD signal at time t. The positive/negative sign of the RegD signal implies that the power system needs regulation up/down service and the ESS is required to discharge/charge accordingly.

The operation is subject to the following constraints.

$$SOC^{\min} \leq SOC_t \leq SOC^{\max}, \ \forall t \in T_m \tag{3.20}$$

$$0 \leq P_t^{\text{arbd}}, P_t^{\text{arbc}}, P_t^{\text{reg}} \leq P^{\max}, \forall t \in T_m \tag{3.21}$$

$$(P_t^{\text{arbd}} + P_t^{\text{arbc}}) \times P_t^{\text{reg}} = 0, \ \forall t \in T_m \tag{3.22}$$

$$P_t^{\text{arbd}} \times P_t^{\text{arbc}} = 0, \ \forall t \in T_m \tag{3.23}$$

$$P_t^{\text{arbd}}, P_t^{\text{arbc}}, P_t^{\text{reg}} = 0, \forall t \in T^{\text{down}} \tag{3.24}$$

$$SOC_t = SOC_t^{\text{down}}, \forall t \in T^{\text{down}} \tag{3.25}$$

$$\sum_{t=1}^{T_m} (E_t^{\text{arbd}} + E_t^{\text{regd}}) \leq \eta_{\text{cyc}} (SOC^{\max} - SOC^{\min}) \tag{3.26}$$

where T^{down} is the set of all intervals when the system has an outage event and the system is in a down state. SOC_t^{down} is the state of charge at the time when the system is in the down

state. T^{down} and SOC_t^{down} are obtained from the sequential MCS. SOC is constrained with lower and upper bounds by $SOC^{\min}$ and $SOC^{\max}$ as shown in (3.20). Charging and discharging power limits are represented by (3.21). The quadratic constraint in (3.22) indicates that during each period, the ESS is assumed to participate in one market at most. Besides, it is assumed that the ESS cannot sell and buy energy in the arbitrage market simultaneously as stated in (3.23). Equation (3.24) shows that when an outage event occurs, the ESS should discharge to mitigate the outage and (3.25) implies the SOC should be equal to the SOC value at the down states.

The life of ESSs is a vital concern for the operators and utilities, which is determined by its calendar life and cycle life. Calendar life of an ESS captures its aging and degradation over time and is affected by several factors such as temperature and humidity. This implies that the battery degrades even though it is stored and unused. On the other hand, cycle life depends on cycle aging, which not only includes the number of cycles, but may also depend on the depth of discharge and the mean SOC of cycles. For example, deep cycles can reduce the life span of lithium-ion batteries significantly, but the cycle life of vanadium redox flow battery is not dependent on the depth of discharge [1]. To extend the lifetime of the ESS, (3.26) is included to limit the number of discharge cycles (η_{cyc}) [30].

3.4 Case Studies and Results

In this study, the IEEE Reliability Test System (IEEE-RTS), which has been extensively used for power system reliability studies, is utilized for estimating the profit from mitigating outages by an ESS. This system consists of 24 buses, 33 transmission lines, 5 transformers, and 32 generating units. The system data, including generation capacities, transmission limits, load profile and reliability parameters, are provided in [31] and the single line diagram of this test system is shown in Fig. 3.1. Also, the IEAR values for this test system is presented in table 3.1 [32].

PJM historical data is utilized for evaluating the revenue from participating in energy and regulation markets [33–35]. The historical data, including the LMP, RMPCP, RMCCP, mileage ratio,

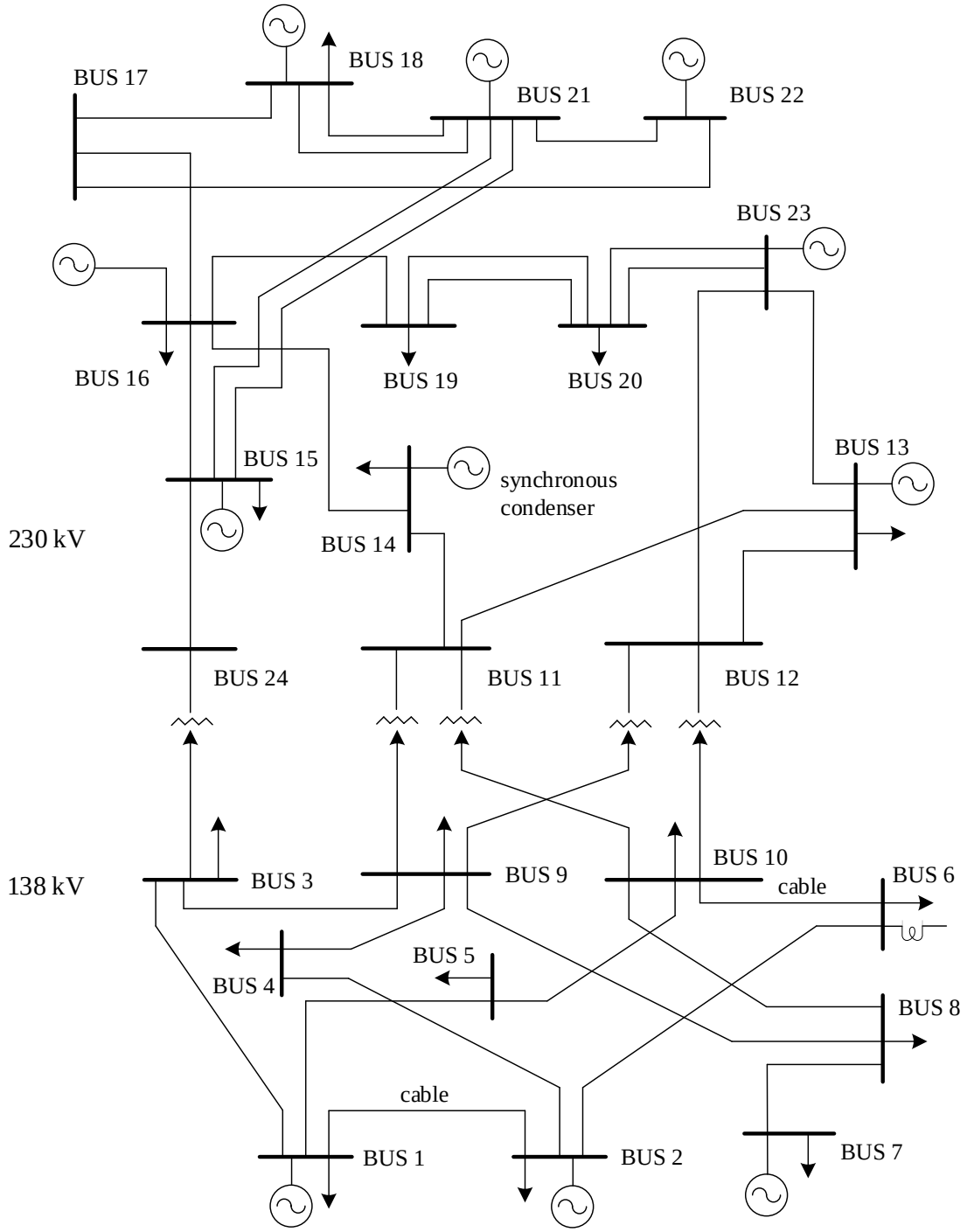

Figure 3.1: Single line diagram for IEEE RTS

and RegD signal are available on the PJM website. Data from June, 2016 to May, 2017 are used in this study. In the PJM regulation market, the regulation up and down signals are considered as one

Table 3.1: IEEE RTS-24 IEAR Values

Bus No.	IEAR ($/kWh)	Bus No.	IEAR ($/kWh)	Bus No.	IEAR ($/kWh)
1	6.20	9	2.30	17	–
2	4.89	10	4.14	18	3.75
3	5.30	11	–	19	2.29
4	5.62	12	–	20	3.64
5	6.11	13	5.39	21	–
6	5.50	14	3.41	22	–
7	5.41	15	3.01	23	–
8	5.40	16	3.54	24	–

signal. The RegD regulation signal is normalized so that the values lie between -1 and 1, where the negative and positive signs represent for regulation down and up, respectively. All data used here are converted to hourly data.

3.4.1 ESS Size and Location

While determining the location and size of an ESS, several aspects need to be considered. First, the land availability needs to be given importance. The utility or the investor needs to make sure that there is enough space for an ESS. An alternative is to use a mobile trailer which provides a flexible solution for smaller ESSs. Other concerns, such as noise regulations, customer types and existing system performance should also be taken into consideration. Locations which require system upgrades, have larger LMP fluctuations or inferior reliability may be better candidate locations than others. In this study, the candidate locations are evaluated based on the amount of reliability improvement it can bring to the system, i.e., the extent to which an ESS at a candidate location can improve the system EDNS and reduce the interruption cost. The power and energy capacity of the ESS are set as 20 MW and 20 MWh, and it is assumed that this chosen size is not sufficiently large to impact the market price.

The SOC is constrained between 15% and 95% to avoid very low or very high values. The

charging and discharging efficiencies are both 85%. Redox flow batteries are considered for the demonstration, since they are suitable for grid-scale applications and have large cycle life [36, 37]. The ESS parameters are shown in table 3.2.

Table 3.2: ESS Parameters

Parameter	Value
Power Capacity	20 MW
Energy Capacity	20 MWh
$SOC^{\min}$	15%
$SOC^{\max}$	95%
γ_c	85%
γ_d	85%

3.4.2 Solution Procedure

The results are obtained by following the three steps as shown in figure 3.2.

Step I

Estimate the distribution of the SOC and develop the multi-state model for the reliability analysis. The annual hourly SOC can be obtained by solving the optimization problem with the objective function (3.16) and subject to constraints (3.20)–(3.23) and (3.26).

Step II

Calculate the reliability indices and value from outage mitigation by solving the model represented by (3.1)–(3.9). Also, track the time interval when system is in down state (T^{down}) and the SOC at that time (SOC^{down}) for the next step, since the same sequence of failures is used to provide a common base for the comparisons.

Step III

Solve the optimization problem given in (3.16)–(3.26). The revenue from arbitrage and regulation market with market mechanism constraints and application priority is obtained.

The optimization problems in step I and III are solved by General Algebraic Modeling System

(GAMS).

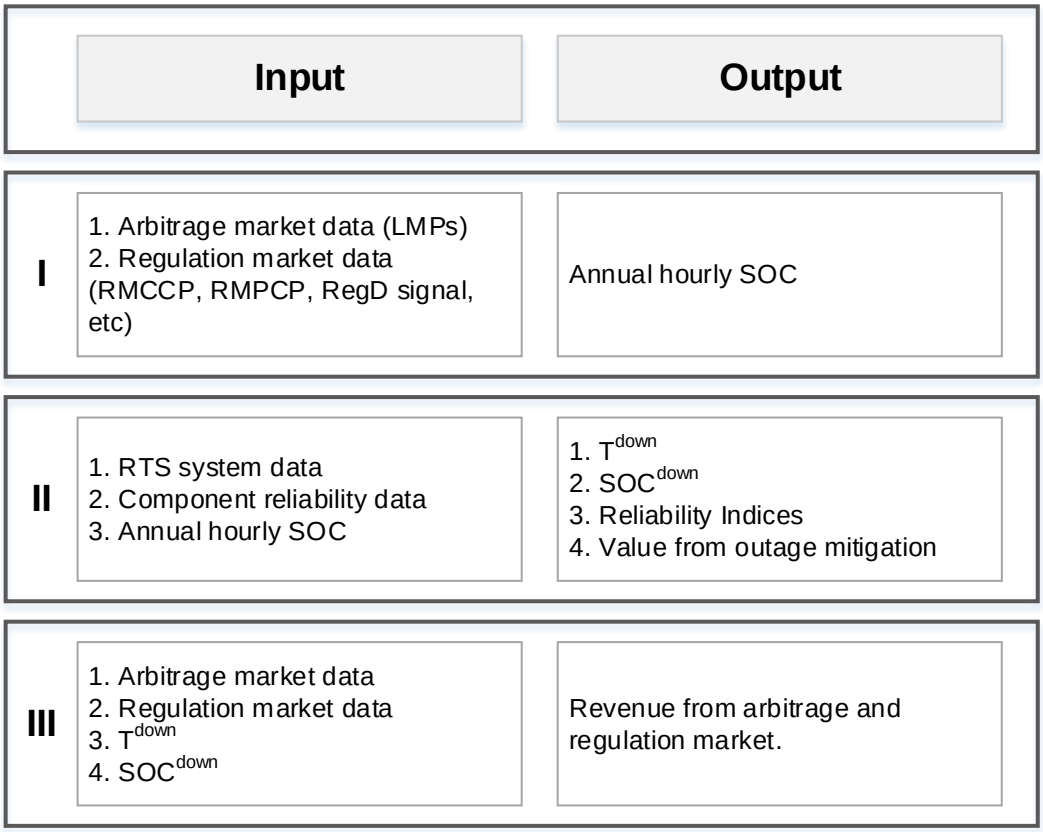

Figure 3.2: Proposed solution procedure

3.4.3 Results

3.4.3.1 Histogram of Annual SOC

In this section, the histogram of hourly SOC for a year is presented. The histogram is shown in figure 3.3. The average value of each bin and the corresponding probability is given in table 3.3.

3.4.3.2 Reliability Improvement

First, the sequential MCS is performed on the base case (without ESS) to estimate the reliability indices and the interruption cost. The results are shown in table 3.4.

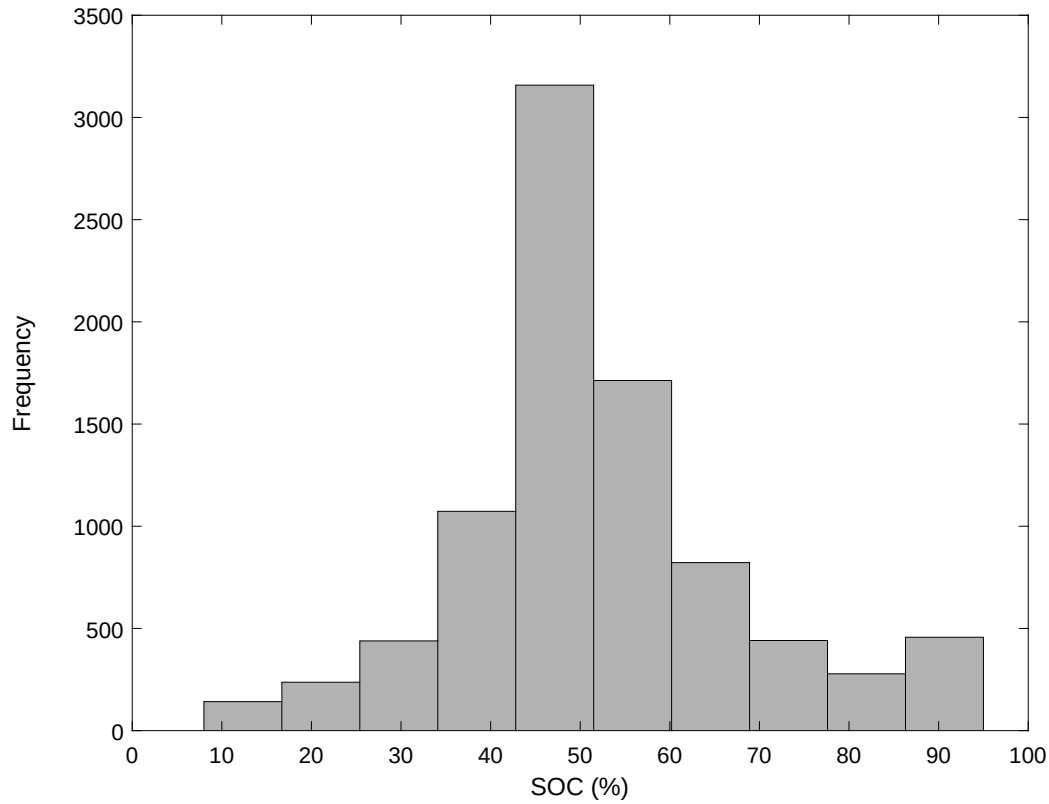

Figure 3.3: Histogram of SOC for a year

Table 3.3: ESS SOC Value and State Probability

State No.	1	2	3	4	5
Average SOC (%)	19	27	35	43	51
Probability	0.0337	0.0381	0.0783	0.1572	0.3692
State No.	6	7	8	9	10
Average SOC (%)	59	67	75	83	91
Probability	0.1332	0.0715	0.0402	0.0296	0.0491

Table 3.4: Reliability Indices of the Base case

Base Case	LOLP	EDNS (MW/year)	Interruption cost ($/year)
Value	0.0026	0.23504	4,719,762

The evaluation of a 20 MW, 20 MWh ESS at five selected load buses (bus 6, 9, 10, 13 and 18) are performed; the system reliability improves more when the ESS is installed on these buses [25].

Table 3.5: Reliability Improvement with the ESS

Bus No.	LOLP	EDNS (MW/year)	Interruption cost ($/year)
6	0.0026	0.22895	4,597,234
9	0.0026	0.22905	4,599,175
10	0.0026	0.22904	4,599,133
13	0.0026	0.22915	4,601,397
18	0.0026	0.22907	4,599,724

The SOC value at the beginning of the outage event is represented by the multi-state model as given in table 3.3. The results for these five cases are shown in table 3.5. The improvement on the other buses are very small. The reliability indices and interruption costs are almost the same as in the base case, therefore, they are not displayed here. From the results, we can see that the LOLP is not improved and the EDNS and interruption costs are reduced. This happens as the ESS does not have enough capacity to compensate the loss of load. Thus, the ESS cannot reduce the number of outage events. However, it is still significant in improving system reliability, since it can reduce the number of interrupted customers and the interruption cost.

3.4.3.3 Revenue from Arbitrage and Regulation Markets

The simulation runs on a daily base ($T_m = 24$), and an additional constraint: $SOC_{24} - SOC_0 = 0$ is considered to ensure that the initial and the final states are consistent [38], i.e., SOC at the beginning of a day is the same as the SOC at the end of the previous day. The SOC_0 is assumed to be 50% for the case studies.

Figure 3.4 illustrates the optimal amount of capacity participated in the arbitrage and regulation markets and the variation of SOC for one day with no outage event.

The outage events and durations are tracked in the sequential MCS. For these hours, the ESS is unavailable to generate revenue from the arbitrage or the regulation market. The results for each day are obtained by solving the quadratically constrained linear programming. The revenue for each month and the whole year are calculated and listed in table 3.6.

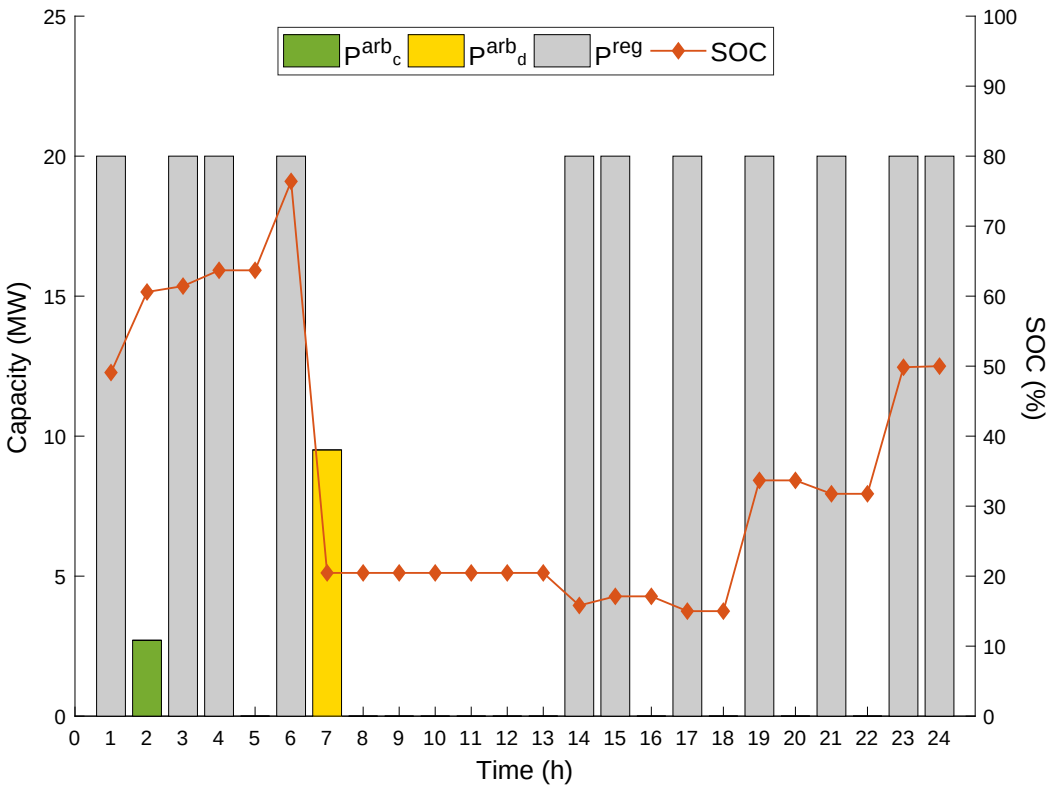

Figure 3.4: Capacity and SOC for an example day

Table 3.6: Revenue from Arbitrage and Regulation Market

Month	Arbitrage Market ($)	Regulation Market ($)
January	5,423	178,075
February	2,790	134,877
March	11,242	132,593
April	4,466	132,593
May	5,771	204,478
June	8,461	183,584
July	8,460	250,559
August	10,189	232,081
September	5,010	246,339
October	4,967	231,261
November	3,826	197,093
December	6,970	160,945
Annual	77,575	2,300,486

3.4.3.4 Stacked Revenue

Table 3.7 presents the stacked revenue for a year. From the results, it can be concluded that the regulation market generates more revenue than the arbitrage market since the ESS purchases energy from the arbitrage market but sells most of the energy to the regulation market, where the revenue is higher.

Table 3.7: Stacked Revenue for a Year

Bus No.	Outage Mitigation ($)	Arbitrage Market ($)	Regulation Market ($)	Stacked Revenue ($)
6	122,528	77,575	2,300,486	2,500,589
9	120,587	77,575	2,300,486	2,498,648
10	120,629	77,575	2,300,486	2,498,690
13	118,365	77,575	2,300,486	2,496,426
18	120,038	77,575	2,300,486	2,498,099

3.4.4 Estimated Income

This part discusses the total estimated income an ESS can generate. The total expenditure for an ESS can be broken down into capital and operation and maintenance (O&M) costs. Typically, the capital cost and O&M costs for a Redox flow BESS can be assumed to be $900/kWh and $5.7/kWh per year [36], respectively. The cost for O&M has been considered as an average value since it changes over the years. The cost increases as the battery ages, since more maintenance is required to keep the performance of the degrading battery at a constant level. Hence, for the BESS considered in this study, the installation cost is estimated to be $18 M with an additional $0.114 M (average) per year for operation and maintenance. Table 3.8 below summarizes the cycle life, capital cost and O&M cost of redox flow batteries [1, 36].

In this study, the number of discharge cycles (η_{cyc}) is restricted to 3.5 cycles per day, thus it can be used for 10 years. Then the approximate stacked income can be calculated by subtracting the installation and O&M cost from the total stacked revenue of the 10 years. Table 3.9 tabulates

Table 3.8: Parameters of Redox Flow Battery

Parameter	Calendar Life [1]	Cycle Life [36]	Capital Cost ($/kWh) [36]	O&M Cost ($/kWh/yr) [1]
Value	10 years	13,000	900	5.7

the estimated income when an ESS is installed at bus 6.

Table 3.9: Estimated Income

Parameter	Value
Annual Stacked Revenue (M$)	2.5
Lifespan (year)	10
Total Revenue (M$)	25
Total Installation and O&M (M$)	19.14
Total Income (M$)	5.86

3.4.5 Discussion

From the results of the case studies, it can be observed that the ESS generates the majority of its profit from the regulation market. However, participating in the regulation market also leads to frequent cycling. Operators need to consider the cycling constraint when they make decisions for bidding. In addition, the prices for the regulation markets have declined over the years and as the trend continues, the utilities should keep in mind this factor while estimating their revenue from the applications of an ESS.

Although the value derived from the mitigation of outages is smaller than revenues from the markets, it bears an intangible but significant value in terms of customer satisfaction. It helps the utility to build positive reputation among its customers by providing a reliable power supply. The value of improving reliability can be higher if the ESS is able to serve some critical loads, such as schools and hospitals. Also, the results presented in the previous section applied only one year as the example. The reliability value of an ESS may vary with time, as in some years the number of outage events can be much higher than the others, due to weather conditions or natural disasters.

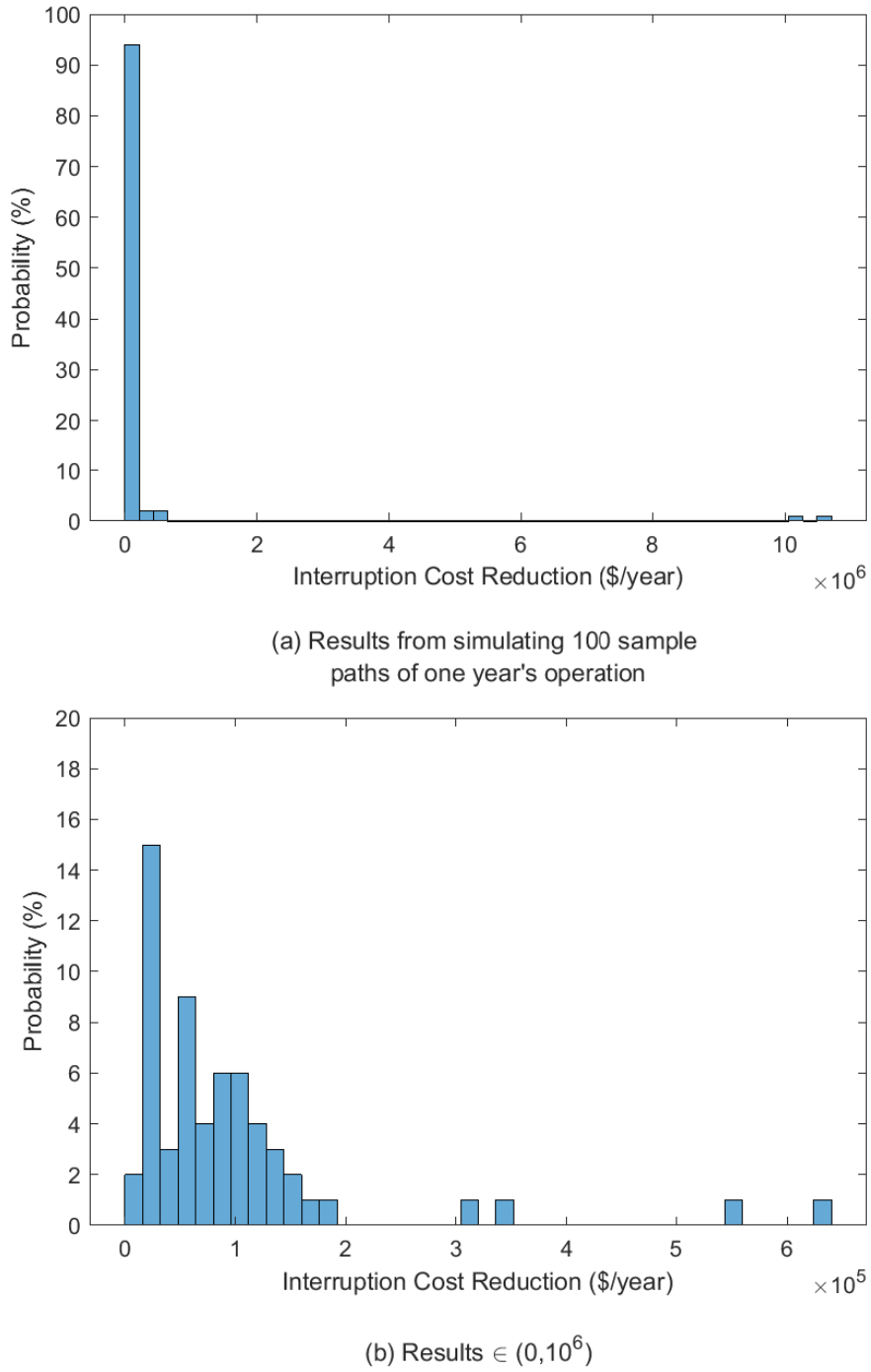

Figure 3.5: Histogram of simulation results

Here, the impact of simulating 100 sample paths of one year's operation of the ESS has been studied. The maximum and average value of outage mitigation are $10,760,504 and $266,118 in

this simulation. Figure 3.5 (a) presents the histogram of the result. As is evident from the figure, only a small number of years have the interruption cost reduction larger than $1,000,000. Figure 3.5 (b) shows the histogram of the results where the value is between zero and one million dollars.

3.5 Conclusion

This chapter has presented a method for quantifying the benefits of stacking up the applications of an ESS. Three applications (outage mitigation, energy arbitrage, and frequency regulation) were considered. Several case studies were performed to evaluate the reliability indices and the cost benefits. Sequential MCS was used to track the charging and discharging performance of the ESS and also the outage events in the system while evaluating the reliability indices and interruption cost. The variable behavior of load demand and the forced outages of generators are also captured by the sequential MCS. A quadratically constrained linear programming model was established to estimate the potential revenue from arbitrage and regulation markets. The study presents several benefits from installing an ESS and utilizing it for the applications stated above. The approach described in this study can be utilized by industries including utilities and manufacturers to build business cases when they want to install an ESS for their facilities. Future work includes the development of a more comprehensive framework and converting the benefits from other applications to monetary profits and stacking them up to estimate the maximum revenue. Also, a detailed and comprehensive methodology on the revenue generated over a longer period of time, e.g., ten years, considering the improvement of the ESS technology, the variability of market price and the trade-off between cycle life and profit, is under development.

Chapter 4

Estimating the Capacity Value of ESSs

4.1 Introduction

Since the energy demand may increase and some power supply resources may retire over time, it is necessary for utilities and ISO/RTOs to make plans to ensure long-term grid reliability by procuring the appropriate amount of generation capacity needed to meet predicted energy demand in the future. Although energy storage systems do not produce energy by themselves, the abilities to discharge and shift energy make them one solution to meet the demand and thus can be considered as a generation capacity resource. However, unlike the conventional generators with the capability to provide energy upon demand, almost all the energy storage systems are energy-limited resources. In addition, as aforementioned, ESSs can provide multiple services to the grid. It is possible that the available energy of an ESS reaches its lower bound when needed due to low state of charge. Participating in different markets or providing different services place an uncertainty on the availability of the ESSs. Therefore, due to the energy-limited characteristic and the availability uncertainty, it is essential to conduct the research to evaluate the actual capacity contribution of ESSs.

Reliability methods for power system adequacy assessment play a significant role in assessing the contribution of intermittent resources such as wind and PV systems to the power grids. The

term capacity value is usually used to measure the capacity contribution of variables resources to power system capacity planning. The evaluation process in this manner is carried out to make sure that the system reliability will be maintained when the intermittent resources are introduced to the power grid. In this chapter, a methodology to estimate the capacity value of energy storage systems is presented. The ESS is assumed to participate in the energy market at normal operating conditions and to mitigate outage when contingencies occur. The capacity value of different sizes of the ESS is evaluated. The proposed framework and results can be applied to conduct the capacity planning.

Capacity value is a commonly used metric to evaluate the contribution of renewable generation, such as PV and wind power. It measures the capacity of conventional generation units that can be replaced or the amount of extra load demand that can be supplied while maintaining the same reliability level. The methods to evaluate the capacity value have been investigated in many studies. For instance, Monte Carlo simulation technique has been used in [39] for reliability assessment of a hybrid system of wind and PV systems. A combination of deterministic and probabilistic techniques has been used in the reliability evaluation of these systems. In [40], the hourly mean solar radiation data has been used as the primary input, and Monte Carlo simulation technique was implemented to evaluate the system reliability. In [41], the reliability of a wind and solar system has been evaluated using the Monte Carlo simulation technique. In [42], the work introduces an analytical method to calculate the capacity credit of PV system in a manner that considers both the effect of input uncertainty and system components availability. The IEEE Power and Energy Society Task Force on the capacity value of wind power has described a preferred method for calculation of the capacity value of wind [43]. It also discussed some approximate methods for the calculation with their limitations highlighted. In [44], authors identified the capacity value and capacity factor of wind power with the historical data in Ireland. In [45], authors applied the composite system reliability analysis to evaluate the capacity value of wind power, which is able to capture the effects of transmission constraints. However, a few studies have been applied to estimate the effect of ESS, especially considering the ESSs providing multiple services. Reference

[46] proposed a method to estimate the capacity value of storage and it used a dynamic program to model the effect of power system outages on the operation and state of charge of storage in subsequent periods. In [47], a framework was proposed to assess the capacity credit of electrical energy storage and demand response.

The remainder of this chapter is organized as follows. Section 4.2 discusses the different approaches to evaluate the capacity value. Section 4.3 explains the evaluation of power system reliability using Monte Carlo Simulations. Section 4.4 explains the mathematical models that are applied to evaluate the reliability indices. Section 4.5 describes the ESS operation strategy and developed the model to estimate the capacity value of the ESSs. Section 4.6 presents case studies on evaluating the capacity contribution of ESSs. Section 4.7 provides concluding remarks of this chapter.

4.2 Capacity Value Evaluation Approaches

In this section, the normally applied capacity value evaluation approaches are briefly discussed. The approaches are effective load carrying capability (ELCC), equivalent firm power (EFP), and equivalent conventional power (ECP).

4.2.1 Equivalent Load Carrying Capability

The Equivalent Load Carrying Capability of a generator is defined as the amount of load can be increased when a new generator is added, while keeping the same reliability level. The reliability level can be represented by the Loss of Load Probability (LOLP), Loss of Load Expectation (LOLE), Expected Demand Not Supplied (EDNS) or the Expected Energy Not Supplied (EENS).

4.2.2 Equivalent Firm Capability

The equivalent firm capability of a generating resource is the capacity of a 100% reliable generator that can be replaced. ELCC defines the capacity contribution a resource from the load perspective,

while EFC is described from the point of view of the generation side.

4.2.3 Equivalent Conventional Capability

Similar to EFC, the equivalent conventional capability determines the capacity value of a generator by comparing the generator under investigation and a benchmark generator. The difference is that the selected benchmark unit is not assumed to be perfectly reliable, the failure rate of this unit is considered when evaluating ECC.

4.3 Monte Carlo Simulation

In power system, the reliability indices can be estimated by collecting data on the occurrence of failures and the time to repair. The Monte Carlo Simulation (MCS) can be applied to mimic the failure and repair history of the components and the system. In MCS, a complex system can be decomposed into several components and the behavior of each component can be represented by deterministic or probability distributions. The MCS can be effectively used to assess the reliability of composite power systems and it is a more practical approach than the analytical methods. MCS methods that are used for power system reliability studies can be classified into two categories: sequential or non-sequential.

4.3.1 Sequential Monte Carlo Simulation

When time-dependent issues are considered, the sequential MCS is more suitable to imitate the component or system behavior over time. The mathematical model of the system is allowed to generate an artificial chronological history, and appropriate statistical inferences are drawn from this information. In this study, the sequential MCS has been applied, since the time-varying behavior of energy storage SOC should be considered in the estimation. There are two kinds of method to represent time in the simulation process: the fixed time interval method and the next event method [27]. A brief introduction on these two types MCS is presented here for completeness.

4.3.1.1 Fixed Time Interval Method

The fixed time interval method, also known as synchronous timing method, is a two-step method. When applying the fixed time interval method, the basic time interval Δt will first be chosen depending upon the operating characteristics of the system. Starting in the initial state, time is advanced by Δt and the program then checks if an event has occurred. The system is then updated by determining the resulting state of the system. If no event has occurred then the system stays in the same state. These two steps may be repeated as many times as desired.

4.3.1.2 Next event method

The next event method is also called the asynchronous timing method. Unlike the fixed time interval method, in this method, the simulated time is advanced by a variable amount rather than a fixed amount each time. The computer proceeds by keeping a record of the next few simulated events scheduled to occur. The most imminent event is assumed to occur and the simulated time is advanced to the point of occurrence of the event. The cycle is repeated as many times as desired. The general procedure of the algorithm is described as follows:

Step 1: Read failure rate and duration data for all components;

Step 2: Assume that all the component are available at the beginning, that is to set the initial states of all component as UP;

Step 3: For each component, draw a random number and compute the time to the next event;

Step 4: Find the minimum time and change the state of the corresponding component; and update the total time;

Step 5: Check if there is a change in system status. If yes, update reliability indices; otherwise, go to step 3;

Step 6: Check if the simulation converges. If yes, terminate the calculation, otherwise; go to step 3.

The distributions assumed for up and down times are exponential in this work, then the time to the next transition can be calculated as follows [48],

$$T_i^{ttc} = -\frac{1}{\rho_i}\ln(r_i) \tag{4.1}$$

where T_i^{ttc} is the time to the next transition for component i. ρ_i is the failure rate when the component is at the up state, and is the repair rate at the down state of the ith component; r_i is the generated random number for component i.

4.3.2 Non-sequential Monte Carlo Simulation

In the non-sequential simulation, the states are sampled from the state space proportional to their probabilities. This technique is suitable when component failures and repairs are independent. This can be achieved simply by sampling states of individual components to construct system states and repeat until an adequate number of system state samples are generated [49]. This approach does not memorize sampling component up and down cycles and store chronological history on the system state.

4.4 Reliability Evaluation

Similar to the reliability model presented in Section 3.3, a composite system reliability model with the objective to minimize the loss of load is applied. The mathematical modeling and the definition of the reliability indices are presented here for completeness.

4.4.1 System Modeling

For each hour, the system state is defined by the component states and capacities. The output of wind power is determined by the corresponding wind turbine states and hourly output power. Then, a feasible dispatch is sought by solving the following minimization problem [26].

$$\text{Loss of Load} = \min \left(\sum_{i=1}^{N_b} C_i \right) \tag{4.2}$$

subject to

$$\begin{aligned}
P(V,\delta) - P_D + C &= 0 \\
Q(V,\delta) - Q_D + C_Q &= 0 \\
P_G^{\min} \leq P_G &\leq P_G^{\max} \\
Q_G^{\min} \leq Q_G &\leq Q_G^{\max} \\
V^{\min} \leq V &\leq V^{\max} \\
|F(V,\delta)| &\leq F^{\max} \\
-\pi \leq \delta &\leq \pi
\end{aligned} \tag{4.3}$$

where C_i is the load curtailment at bus i, C is the vector of load curtailments $\big(N_b \times 1\big)$, C_Q is the vector of reactive load curtailments $\big(N_b \times 1\big)$, V is the vector of bus voltage magnitudes $\big(N_b \times 1\big)$, δ is the vector of bus voltage angles $\big(N_b \times 1\big)$, P_D and Q_D are the vectors of real and reactive power loads $\big(N_b \times 1\big)$, P_G and Q_G are the vectors of real and reactive power outputs of the generators $\big(N_g \times 1\big)$, $P_G^{\min}$, $P_G^{\max}$, $Q_G^{\min}$ and $Q_G^{\max}$ are the vectors of real and reactive power limits of the generators $\big(N_g \times 1\big)$, $V^{\max}$ and $V^{\min}$ are the vectors of maximum and minimum allowed voltage magnitudes $\big(N_b \times 1\big)$, $F(V,\delta)$ is the vector of power flows in the lines $\big(N_\ell \times 1\big)$, and $F^{\max}$ is the vector of power rating limits of the transmission lines $\big(N_\ell \times 1\big)$. In the foregoing description, N_b is the number of buses, N_ℓ is the number of transmission lines, and N_g is the number of generators.

The above model implies that for any encountered scenario (generation and transmission availability and load state) power will be routed through the network in such a manner so as to minimize the system load curtailment.

4.4.2 Calculation of Reliability Indices

In order to capture interruption times and temporal relationships such as state of charge of the storage system, all indices are determined from sequential Monte Carlo simulation [27, 50].

1) Loss of load probability (LOLP): The LOLP is a widely used reliability index and it can be estimated as follows,

$$LOLP = E[\hat{\theta}] \tag{4.4}$$

where

$$\hat{\theta} = \frac{1}{T}\sum_{i=1}^{N_C} T_i^{\text{down}} \tag{4.5}$$

and T_i^{down} is the duration of an interruption encountered during the sequential MCS. N_C is the total number of simulated cycles and T is the total period of simulation.

2) Expected demand not supplied (EDNS): The EDNS is the sum of the products of probabilities of failure states and the corresponding load curtailments, which can be estimated as follows.

$$EDNS = E[\hat{d}] \tag{4.6}$$

where

$$\hat{d} = \frac{1}{T}\sum_{i=1}^{N_C}(T_i^{\text{down}}\sum_{j=1}^{N_b} C_j) \tag{4.7}$$

3) Expected energy not supplied (EENS): The EENS is also known as Expected Unserved Energy (EUE) or Loss of Energy Expectation (LOEE), which measure the amount of energy expected to be lost when demand exceeds the available generation. This metric can be calculated as ENDS$\times$8760.

4.4.3 Stopping Criterion

In using Monte Carlo simulation to estimate power system reliability indices, a convergence criterion should be applied to stop the algorithm if there is not much change in the reliability indices.

In this study, the stopping criterion is applied on the reliability indices as follows:

$$COV = \frac{\sqrt{\text{Var}(\rho_{N_C})}}{E[\rho_{N_C}]} \leq \epsilon_m \tag{4.8}$$

where COV is the coefficient of variation, Var($\cdot$) is the variance function, ρ_{N_C} is the value of the estimate of the reliability index of interest (such as LOLP or EDNS) at the end of N_C cycles, and ϵ is a predefined tolerance. At intervals of several cycles, the COV is calculated. If this amount is less than or equal to the specified tolerance ϵ_m, the algorithm is terminated; otherwise, the simulation continues.

4.5 Proposed Solution

The models utilized here include a) an optimization model for determining the optimal operation strategies of the ESS, b) k-means clustering to build the multi-state model of the ESSs, and c) a reliability evaluation model solved by the sequential Monte Carlo Simulation.

4.5.1 Operating Strategy for the ESS

In this section, the optimization model to estimate the maximum revenue from the energy market is presented. This model is similar to the model presented in the previous chapter, but only the energy arbitrage benefit is considered her for simplicity to illustrate the framework. Other use cases can be easily included in this model when needed.

4.5.1.1 Revenue from the Energy Market

An ESS can be used to accumulate energy by charging the battery when the electricity prices are low, i.e., during the off-peak hours, and then by discharging during the peak hours, when the demand and energy prices are higher. This application also contributes to the reduction of generation costs and defers the installation of peaking units. The energy price difference can be

used as an advantage by the ESS owners in earning profits. The locational marginal price (LMP) is a metric used for representing wholesale electricity price, and it indicates the value of energy at a particular location at a given point of time. Hence, locations with a high variation in their LMPs can be considered as ideal for this application.

The total income from the energy market can be calculated as follows.

$$\text{Income}_{\text{arb}} = \sum_{t=1}^{T} (R_t^{\text{lmp}} E_t^{\text{arb}_\text{d}} - R_t^{\text{lmp}} E_t^{\text{arb}_\text{c}}) \tag{4.9}$$

where R_t^{lmp} is the LMP (\$/MWh) of the system at time t; $E_t^{\text{arb}_\text{d}}$ and $E_t^{\text{arb}_\text{c}}$ are the quantities of energy sold (discharged) and purchased (charged) at time t, respectively. The ESS is operated for a period of time T.

4.5.1.2 Objective

To maximize the revenue from the energy market, a quadratically constrained linear programming model has been developed. In this model, the variables are $P_t^{\text{arb}_\text{d}}$ and $P_t^{\text{arb}_\text{c}}$, which are the power levels sold and purchased in the arbitrage market at time t. The objective function is represented as follows [51].

$$\text{Max} \quad \sum_{t=1}^{T} \left(R_t^{\text{lmp}} P_t^{\text{arb}_\text{d}} \tau - R_t^{\text{lmp}} P_t^{\text{arb}_\text{c}} \tau \right) \tag{4.10}$$

where τ is the duration of the energy market dispatch time interval and it is considered to be one hour in this study. $R_t^{\text{lmp}} P_t^{\text{arb}_\text{d}} \tau$ represents the revenue by selling the energy and $R_t^{\text{lmp}} P_t^{\text{arb}_\text{c}} \tau$ is the cost of purchasing energy from arbitrage market.

4.5.1.3 Constraints

The operation of an ESS can be modeled by its energy storage capacity, charging and discharging power limits and efficiencies. The SOC of an ESS represents the ratio of the current to the rated

capacity. It depends on the SOC of the previous period and the current operating state of the ESS, i.e., whether it is charging or discharging. The SOC at time t is represented as follows.

$$SOC_t = SOC_{t-1} + \frac{\triangle E_t}{E^{\mathrm{r}}}, \forall t \in T \tag{4.11}$$

where E^{r} is the rated energy capacity, and $\triangle E_t$ is calculated as below.

$$\triangle E_t = E_t^{\mathrm{arbc}} - E_t^{\mathrm{arbd}} \tag{4.12}$$

where E_t^{arbc} and E_t^{arbd} are the charged and discharged energy in the arbitrage market and are calculated as follows.

$$E_t^{\mathrm{arbc}} = P_t^{\mathrm{arbc}} \tau \gamma_c, \;\; E_t^{\mathrm{arbd}} = P_t^{\mathrm{arbd}} \tau / \gamma_d \tag{4.13}$$

where γ_c and γ_d are the charging and discharging efficiencies (%).

The operation is subject to the following constraints.

$$SOC^{\min} \leq SOC_t \leq SOC^{\max}, \; \forall t \in T \tag{4.14}$$

$$0 \leq P_t^{\mathrm{arbd}}, P_t^{\mathrm{arbc}} \leq P^{\max}, \forall t \in T \tag{4.15}$$

$$P_t^{\mathrm{arbd}} \times P_t^{\mathrm{arbc}} = 0, \; \forall t \in T \tag{4.16}$$

SOC is constrained with lower and upper bounds by $SOC^{\min}$ and $SOC^{\max}$ as shown in (4.14). Different operating strategies mainly depend on this constraint. Charging and discharging power limits are represented by (4.15). The quadratic constraint in (4.16) indicates that during each period, the ESS cannot buy and sell energy in the arbitrage market simultaneously.

4.5.2 K-means Clustering

K-means clustering is a well-known and popular partitioning clustering method, which aims to segment several observations into k groups defined by centroids [52]. The result of the clustering analysis brings insight into the observations by dividing and grouping the data into several clusters of similar data. The goal is that the data in the same group be similar to each other and be different from the objects in other groups. In a standard K-means clustering, the similarity can be represented with the sum of squared Euclidean distance. Then the objective is to minimize the total sum of squared errors, which can be represented as below.

$$\text{Minimize} \qquad ||d||^2 = \sum_{i=1}^{N} \sum_{j=1}^{K} r_{ij} ||x_i - c_j||^2 \tag{4.17}$$

where N is the number of data points, c_1, ..., c_j are the centroids of k clusters, r_{ij} is the indicator denoting whether point x_i belongs to cluster j, $r_{ij} = 0$ or 1.

4.5.2.1 General Procedures

The overall procedures to perform k-means clustering is as follows:

Step 1: Randomly assign k initial cluster centers (centroids).

Step 2: Compute point-to-cluster-centroid distances of all observations to each centroid.

Step 3: Assign each observation to the cluster with the closest centroid

Step 4: Compute the average of the observations in each cluster and update the new center for each cluster.

Step 5: Repeat steps 2 through 4 until the cluster centroids do not change, or the maximum number of iterations is reached. The final cluster assignments constitute the clustering solution.

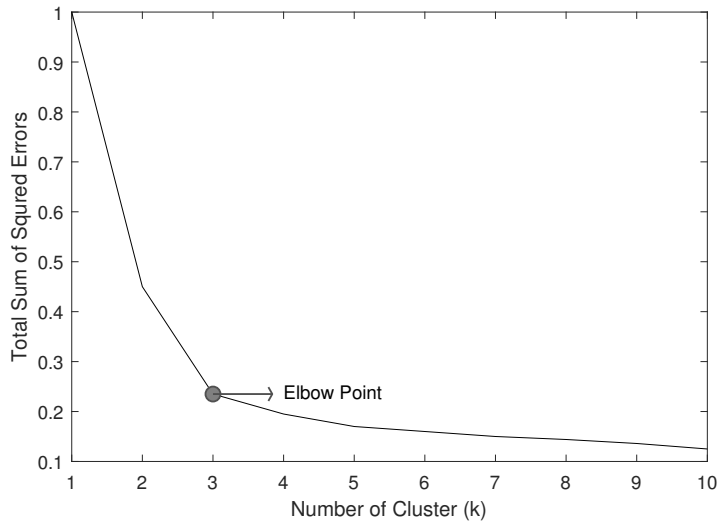

Figure 4.1: Identification of elbow point

4.5.2.2 Optimal Number of Clusters

K-means method is a useful and simple unsupervised machine learning method to divide data into several clusters. However, since the number of clusters k is determined by the user and this number may not be the correct one. For instance, the user may set a relatively small k, but k clusters cannot represent the dataset closely enough, and it may also be not necessary to assign a large k to a dataset with only a very limited number of unique values. Therefore, finding the appropriate number of clusters in a dataset is essential.

The Elbow method is a commonly used method to determine the optimal number of cluster, which uses the turning point in the curve of within-cluster sums of point-to-centroid distance as the optimal point for k. Figure 4.1 illustrates the elbow point in the curve. The turning point is chosen because increasing the number of k does not lead to a much better representation of the data. In this method, the clustering method is firstly applied for different value of k, for example, from one to ten. Then within-cluster sum of point-to-centroid distance is evaluated for each clustering result with different k. After all the ks are examined, the algorithm can determine the elbow point.

4.5.3 Capacity Value Evaluation

The work proposed here applied the EDNS as the reliability index. Since the ESS may not in a large size in power or energy, the effect on improving LOLP or LOLE is not significant. Therefore, to avoid underestimating the contribution of ESSs, EDNS is applied to estimate the capacity value of the ESSs. The ELCC method is applied here for the capacity value evaluation. For each iteration, the added virtual load (VL) (P^{vl}) is updated as shown in equation (4.18).

$$P_i^{\mathrm{vl}} = P_{i-1}^{\mathrm{vl}} + \Delta P^{\mathrm{vl}} \tag{4.18}$$

This process stops when the difference between the reliability indices of the original system and the system with the ESS and added virtual load is smaller than a specified tolerance ϵ_C. The stopping criteria is as follows,

$$|EDNS^{\mathrm{base}} - EDNS^{\mathrm{vl}}| \leq \epsilon \tag{4.19}$$

where $EDNS^{\mathrm{base}}$ is the EDNS of the base case and $EDNS^{\mathrm{vl}}$ is EDNS of the system with ESS and VL.

Then the capacity value of the ESS can be determined by the following equation,

$$\text{Capacity Value} = \frac{P^{\mathrm{vl}}}{P^{\mathrm{ess}}} \times 100\% \tag{4.20}$$

where P^{ess} is the power capacity of the ESS.

4.6 Case Studies and Results

In this study, the IEEE Reliability Test System (IEEE-RTS) is utilized for estimating the capacity value of ESSs. PJM historical data is utilized for evaluating the revenue from participating in the

Table 4.1: Description of Six Cases

Case No.	Power Capacity	Energy Capacity	SOC Uncertainty
Case 1	10	10	Y
Case 2	10	40	Y
Case 3	10	80	Y
Case 4	10	10	N
Case 5	10	40	N
Case 6	10	80	N

energy market [34]. The historical data, including the LMPs and the load profile, is available on the PJM website. Data from July 1st, 2017 to June 30th, 2018 at the Dominion Energy area is used in this study. The load data at this location is also applied to modify the load profile provided by the test system. The correlation between the LMPs and the load profile is 0.5614.

In this study, six different cases are studied for capacity value estimation as shown in Table 4.1. Three ESS sizes are considered, the power capacity is set as 10 MW for all the cases, but the energy capacity is different. The capacity value is also investigated with and without considering the SOC uncertainty. When the ESS availability is considered, the SOC can be represented by the multi-state model obtained by the k-means clustering method. While the SOC uncertainty is not considered, the ESS is assumed to serve as a backup resource only and it is not participating in any market. In this case, only the energy-limited characteristic is considered, and the SOC of the ESS is assumed to be 100% when an outage event occurs.

4.6.1 SOC Multi-state Model

When the SOC uncertainty is considered, the multi-state model for ESSs with different energy capacities is built for each hour, i.e., for each case, the SOC is represented by $\sum_{h=1}^{24} N_h^k$ states, where N_h^k is the number of SOC clusters at hour h. The SOCs are clustered for each hour separately, because the SOC of ESSs has different patterns for each period. The SOC is normally high at the beginning of each day as it gets charged at night, and is commonly low after the peak hours

Table 4.2: Number of Clusters in Case 1 – 3

Hour	Case 1		Case 2		Case 3	
	N_h^k	$\|\|d\|\|^2$	N_h^k	$\|\|d\|\|^2$	N_h^k	$\|\|d\|\|^2$
1	3	0	3	345.77	3	573.28
2	3	0	4	510.55	5	1223.26
3	3	0	4	541.04	6	1982.51
4	3	0	4	364.88	5	1644.36
5	3	0	4	142.53	5	1919.99
6	3	0	3	642.01	5	1147.12
7	2	0	3	515.04	4	1667.90
8	2	0	3	807.38	4	2806.40
9	2	0	3	3326.90	4	4576.65
10	2	0	4	317.49	4	6986.90
11	2	0	3	2236.77	4	7096.23
12	2	0	4	534.11	4	5514.97
13	2	0	4	567.98	4	6571.82
14	2	0	4	699.84	5	3501.99
15	2	0	4	685.55	5	5338.08
16	2	0	4	714.24	5	3214.65
17	2	0	4	719.01	5	3790.92
18	2	0	4	617.78	5	5711.13
19	2	0	4	668.71	5	6129.84
20	2	0	4	839.63	5	2285.72
21	3	0	4	764.51	5	2878.24
22	3	0	4	426.87	4	1339.16
23	3	0	3	227.49	3	54.70
24	1	0	1	0	1	0

as it discharges when the LMPs are high at peak hours. Also, the probability that a power outage event occurs at the time when the demand is high is larger than the other hours. Therefore, it is necessary to perform clustering for the SOC at each hour, as ignoring the time-dependent fact may lead to inaccurate results.

Table 4.2 lists the number of clusters at each hour for cases 1, 2 and 3. The table also presents the total sum of squared errors for each case.Table 4.3 gives an example of the SOC multi-state of Case 1 at each hour.

Table 4.3: Case 1: SOC States

(%)	State			(%)	State		
Hour	1	2	3	Hour	1	2	3
1	34.8	42.5	22.7	13	51.8	0.0	48.2
2	55.6	22.7	21.6	14	52.6	0.0	47.4
3	53.7	15.6	30.7	15	49.0	0.0	51.0
4	27.1	5.2	67.7	16	39.2	0.0	60.8
5	14.2	1.4	84.4	17	37.0	0.0	63.0
6	15.1	0.3	84.7	18	46.6	0.0	53.4
7	20.0	0.0	80.0	19	57.0	0.0	43.0
8	28.2	0.0	71.8	20	67.9	0.0	32.1
9	33.4	0.0	66.6	21	77.8	0.3	21.9
10	36.4	0.0	63.6	22	91.0	1.1	7.9
11	41.1	0.0	58.9	23	86.0	10.1	3.8
12	43.0	0.0	57.0	24	0.0	100.0	0.0

4.6.2 Reliability Evaluation

First, the reliability indices are evaluated for the base case. The ENDS and EENS of the base case are 0.04574 MW/yr and 408.12 MWh/yr, respectively. Then the reliability is evaluated for different sizes of ESSs with and without the SOC uncertainty considered.

When the SOC uncertainty is included, the time when a contingency occurs is first determined and then the corresponding clusters of SOC for that hour are applied to represent the availability of ESSs. For instance, if a power shortage event occurs at 6 pm, then the SOC model for hour 18 will be applied. While the SOC is assumed as 100% if the uncertainty is not counted.

The results are shown in tables 4.4. Considering the SOC uncertainty, the system reliability can be improved by 1.83%, 3.79%, and 5.01% for case 1, 2 and 3, respectively. Results also show that the system reliability can be improved by 2.33%, 4.93%, and 5.90% in Case 1, 2, and 3, if the ESS serves as a backup resource only.

4.6.3 Capacity Value

At last, the capacity value of the ESS in each case is estimated by the ELCC method. While maintaining the same reliability level, the load can be increased by 2.14 MW, 4.65 MW, and 5.75

Table 4.4: Reliability Improvement with ESSs

	EDNS (MW/yr)	EENS (MWh/yr)	Reduction
Base	0.04659	408.12	-
Case 1	0.04574	400.66	1.83%
Case 2	0.04483	392.66	3.79%
Case 3	0.04426	387.68	5.01%
Case 4	0.04550	398.60	2.33%
Case 5	0.04429	388.00	4.93%
Case 6	0.04384	384.05	5.90%

MW with the ESSs in cases 1 to 3, respectively, when the ESS is also participating in the energy market. When the SOC serves as a backup resource only, the ESS can carry 2.64 MW, 5.75 MW, and 6.96 MW additional load in cases 4 to 6. Table 4.5 summarizes the capacity value of ESSs for all the cases with and without considering the SOC variation.

Table 4.5: Capacity Value of ESSs

	EDNS (MW/yr)	EENS (MWh/yr)	CV
Case 1	0.04667	408.82	21.4%
Case 2	0.04659	408.10	46.5%
Case 3	0.04659	408.14	57.5%
Case 4	0.04659	408.13	26.4%
Case 5	0.04663	408.50	57.5%
Case 6	0.04659	408.11	69.6%

Figures 4.2 – 4.4 present the results for the three cases with and without taken the SOC uncertainty into consideration. In these figures, the EDNS of the base case is represented by the red horizontal line and the orange horizontal line represents the EDNS of the system when an ESS is connected to the system. The blue line shows the change of EDNS when an additional load is added to the system with the ESS connected.

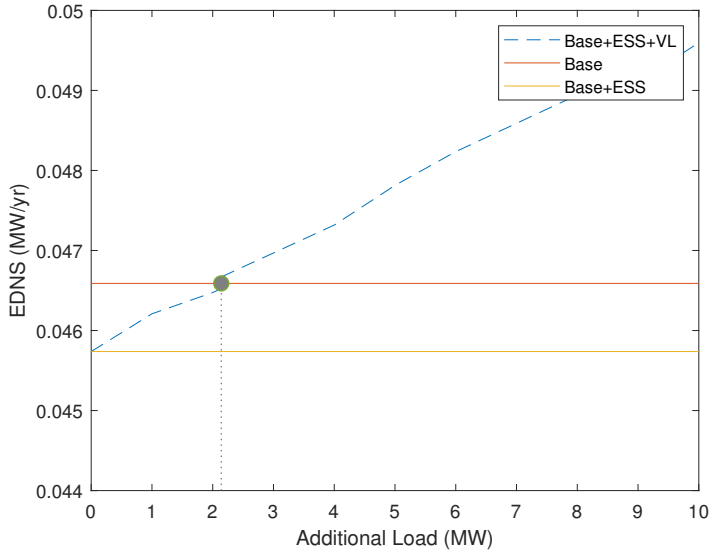

Figure 4.2: Capacity value of an ESS: Case 1

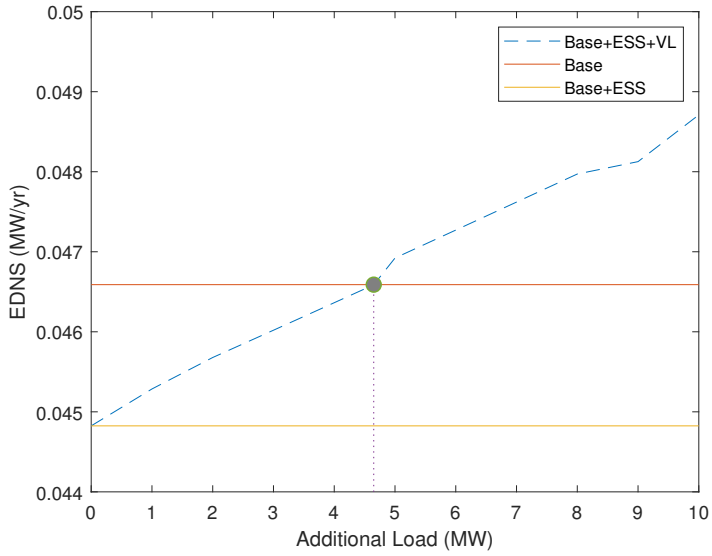

Figure 4.3: Capacity value of an ESS: Case 2

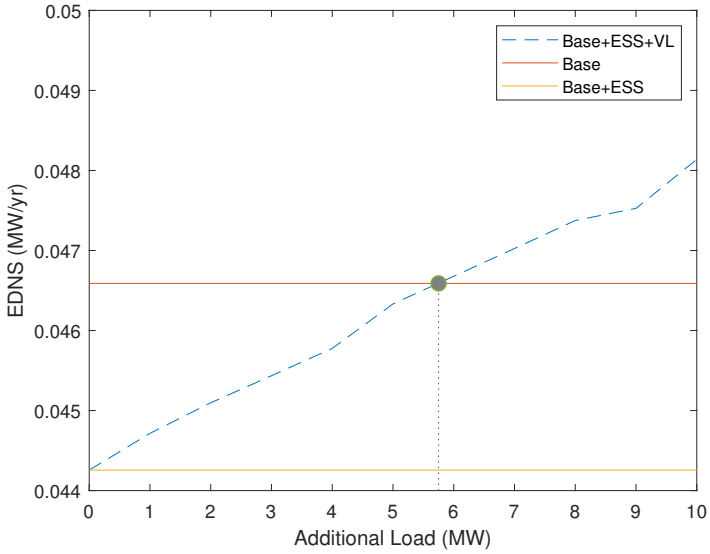

Figure 4.4: Capacity value of an ESS: Case 3

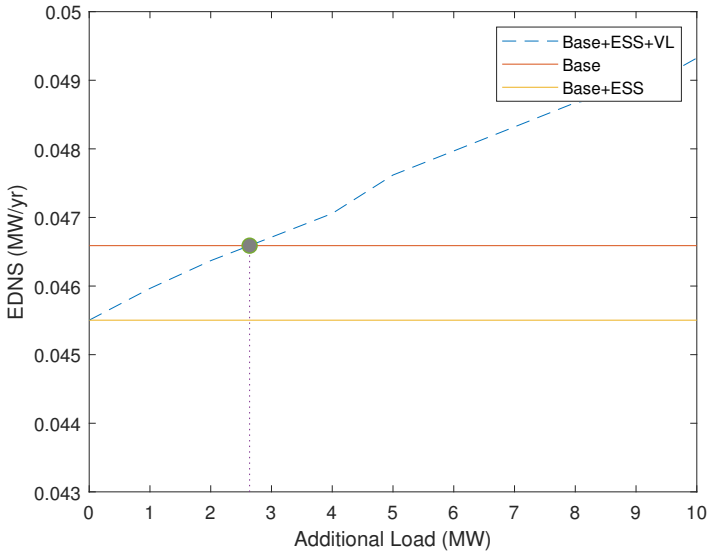

Figure 4.5: Capacity value of an ESS: Case 4

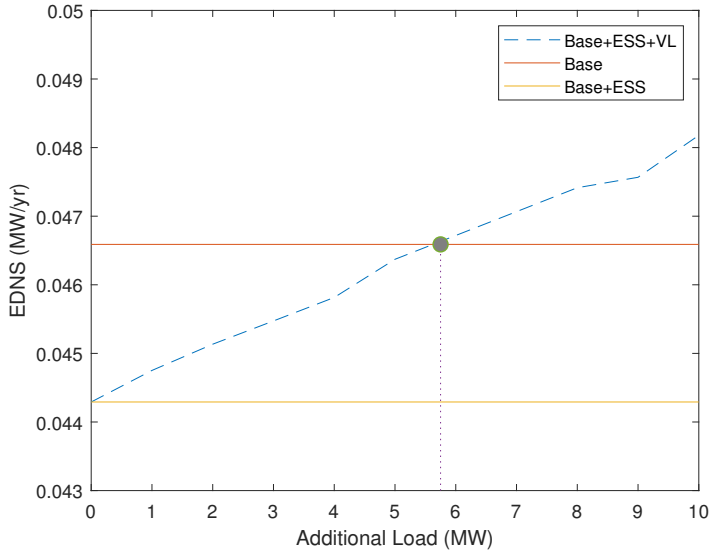

Figure 4.6: Capacity value of an ESS: Case 5

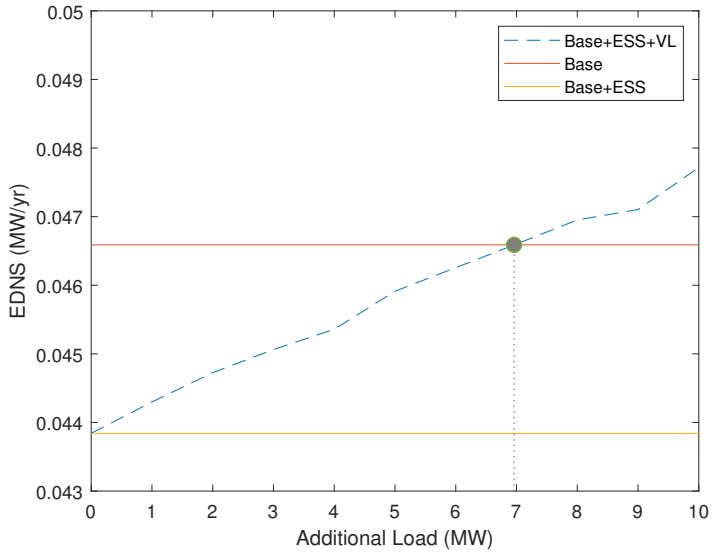

Figure 4.7: Capacity value of an ESS: Case 6

Figure 4.8 shows the comparison of capacity value of the ESS with and without the SOC uncertainty considered. It can been seen that, if the SOC uncertainty is considered, the CVs of cases 1 to 3 are lower than the CVs when the SOC variation is not considered. In the real world, if power system planners do not consider the ESS availability in the planning stage, while the ESS

actually performs other functions, then the power system may face unforeseen power shortage events. This is because the ESSs may not be able to release enough energy as the planners expected. Therefore, to avoid overestimating the ESS capacity contribution, it is essential to consider the ESS availability when evaluating the capacity value of the ESS as the SOC can be fluctuating.

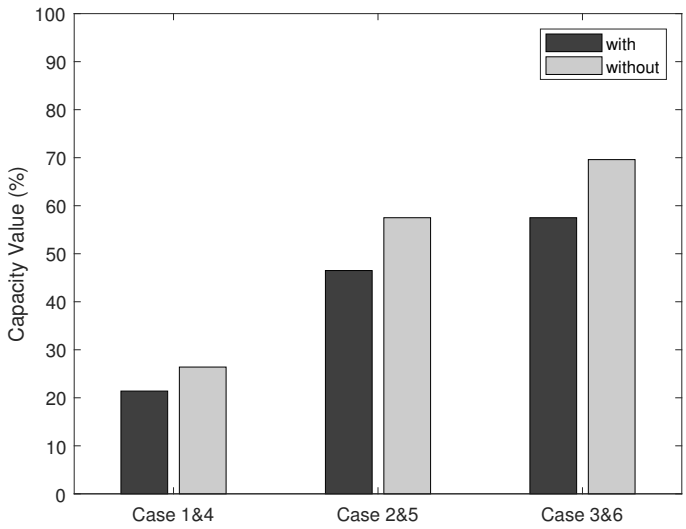

Figure 4.8: Comparison of CV with and without the SOC uncertainty considered

4.7 Conclusion

This chapter proposed a methodology to evaluate the capacity value of the energy storage system considering the SOC uncertainty. The SOC is fluctuating when the ESS participants in the energy market seeking for arbitrage opportunities or provides multiple services to the grid. The capacity value of ESSs with different energy capacity sizes are estimated. It is important to consider the SOC uncertainty, since it is unlikely that the ESS remains unused all the time and is scheduled to perform as a backup resource only in the real world. This is because the capital cost of the ESS is still relatively high and it is not cost-effective to utilize the ESS only as a backup resource. Thus, the work presented here suggested to use a multi-state model to represent the SOC with the k-means clustering method to capture the variation. In this work, the number of states for each

hour is determined by the elbow method. The results indicate that the longer the duration that an ESS can be used, the larger capacity contribution can be made. The results can provide the system planners an estimation of the ESSs capacity value with and without considering the SOC fluctuation. More importantly, the framework and method proposed here can be applied in the capacity planning process to evaluate the actual capacity contribution of energy storage systems considering the uncertainty of the storage available capacity.

Chapter 5

Sensitivity Guided Approach to ESS Siting

This chapter introduces an enhanced Genetic Algorithm (GA) which can be applied to determine the optimal location of an ESS. The proposed method uses sensitivity analysis concepts to develop an encoding strategy for improving the computational efficiency of the search process. The objective is to determine the optimal placement of ESSs for generation cost reduction and transmission congestion relief. Locational Marginal Price (LMP) is employed as an indicator to quantify the need for additional units at candidate locations. LMP at each node is determined from Lagrange multipliers associated with the power balance equation at that node. By renumbering and encoding the locations based on their LMP ranks, desired candidate locations are gathered and encoded to share more common genes. Then the genetic algorithm is utilized jointly with the AC optimal power flow model to search for the optimal locations for ESSs with varied sizes. The method is demonstrated on several test systems, including IEEE 14, 30, 57 and 118 bus test systems. The placement of ESSs with minimum generation costs of these systems are found and the results also validate the improvement in convergence speed.

5.1 Introduction

The global movements toward the deployment of energy storage facilities and renewable energy resources are notable because of the need to reduce dependence on fossil fuels, environmental

concerns, avoidance of the time and cost of transmission and distribution (T&D) expansion, and government subsidies. Planned expansion through optimization of location and size of ESSs further increases their benefits, such as reducing the overall generating cost.

One straightforward way to search for the optimal placement with the objective of minimizing the generation cost is exclusively evaluating the combinatorial possibilities; calculate the generation cost for all the possible solutions and then determine the best solution. However, this approach is quite time-consuming and computationally expensive even for an off-line planning problem. Although brute-force methods have been applied in smaller systems, there has been considerable research on systematic means of optimizing location, or sizes, or both. Reference [53] uses dynamic programming, while others use intelligent methods such as simulated annealing [54, 55], particle swarm optimization [56], and genetic algorithm [57–62]. Although these methods have improved the computational efficiency, the need remains to develop methods that can be applied to larger and more complex systems.

A factor which is often overlooked is that an appropriate encoding strategy of variables may enhance the efficiency of intelligent methods. In this work, sensitivity analysis is used to develop an encoding strategy to increase the convergence speed for determining the optimal placement of the ESSs. Sensitivity analysis has been amply used in several disciplines to determine the change in an objective function with respect to problem constraints. It has been used in [63] to forecast the short-term transmission congestion. It has also been used in the evaluation of some construction projects and management [64]. Lagrange multipliers have been used in enhancing power system reliability in [65, 66].

In this work, a sensitivity guided genetic algorithm (SGGA) is proposed. The locational marginal price (LMP) which is given by the Lagrange multipliers that is associated with power balance equations is used as an indicator to help determine the optimal placement problem [67]. First, the sensitivity analysis is applied to determine the potential candidate locations. The locations which have high LMPs are considered as good candidates for ESSs. Since these locations are supplied by relatively more expensive generators or these areas are more congested than other

locations. This implies that installation of ESSs on these locations would benefit the system by reducing the congestion and generation cost. An optimal power flow with an objective function of minimizing the generation cost is solved for the base case (no ESSs). From the dual solution of the optimization problem, the LMPs are determined for all the locations. The LMPs are ranked in a descending order and the locations are numbered by their ranks instead of their original bus numbers. After renumbering the buses, the genetic algorithm is utilized and combined with optimal power flow model to find the optimal placement for the ESSs with respect to the minimum generation cost. There is nothing sacrosanct about the use of GA; the sensitivity analysis based approach can be combined with any intelligent search method.

This chapter is organized as follows. Section 5.2 describes the importance of encoding strategy of the genetic algorithm and analyzes the benefit of the desired search space regarding to the convergence performance. Section 5.3 presents the mathematical model of the optimization problem, describes the sensitivity analysis, and provides definition for the local marginal cost. Section 5.4 describes the problem and solving process. Section 5.5 demonstrates the effectiveness of the proposed method on several test cases. Finally, a conclusion of the whole contribution is given in Section 5.6.

5.2 Encoding Strategy in Genetic Algorithm

Genetic algorithm is an effective and widely used population based method for solving optimization problems, which mimics the process of natural selection and reproduction [68]. In Genetic Algorithm, the variables are represented as chromosomes which are composed of genes. The evolution leads to the survival of chromosomes with higher fitness value and eliminates the worse chromosomes. At the end, all the chromosomes will be evolved to share the same genes with highest fitness value, which is the optimal solution of the problem. The steps of a typical genetic algorithm is as follows [68, 69].

Step 1: Choose a coding to represent problem parameters, a selection operator a crossover oper-

ator, and a mutation operator. Choose population size n, crossover probability p_C , and mutation probability p_m . Initialize a random population of strings of size ℓ. Choose a maximum allowable generation number $t_{\max}$. Set $t = 0$.

Step 2: Evaluate each string in the population.

Step 3: If $t > t_{\max}$ or other termination criteria is satisfied, Terminate.

Step 4: Perform reproduction on the population.

Step 5: perform crossover on random pairs of strings.

Step 6: Perform mutation on every string.

Step 7: Evaluate strings in the new population. Set $t = t + 1$ and go to Step 3.

5.2.1 Coding Strategy

There are two aspects of intrinsic characteristics of the evolution: (1) the initial chromosomes evolve to the optimal chromosomes iteratively and gradually. During several generations of evolution, some randomly generated chromosomes alter to sub-optimal chromosomes and then to the optimal. The probability of evolution from the initial population directly to the best solution is extremely low. (2) The sub-optimal chromosomes and the optimal chromosome usually share some common genes. After the selection operation, the good genes are kept and meanwhile the bad ones are abandoned; by doing so, the population is able to evolve to contain the optimal chromosome [70].

Fig. 5.1 exhibits three examples of search spaces with different coding strategies [71]. In Fig. 5.1 (a) and (b), the search space is not in a desirable form, while (c) is a preferred search space which is the scenario we endeavor to approach by our coding strategy. In this figure, the optimal solution is represented by a black triangle, the gray dots stand for the sub-optimal solutions and the white area shows the rest of solutions in the search space. In Fig. 5.1 (a), sub-optimal solutions and the optimal solution are spread out randomly in the solution space. In this case, the sub-optimal solutions and optimal solution only share limited common genes. It is troublesome for GA to converge to the optimal solution. Hence, it is inefficient, time-consuming and undesired. In Fig.

5.1 (b), the optimal solution is outside the region of good solutions. It is highly likely that the final population will be trapped into the sub-optimal region and end up with a local optimum instead of the global optimal solution. Fig. 5.1 (c) is a preferred search space. Initially, the population is arbitrarily distributed over the solution space; after several generations, the population will reach to the sub-optimal solutions region and finally evolve to the optimal point inside this area. Therefore, our assumption is that if sub-optimal and optimal solutions are coded to share more common genes, they are more likely to be gathered and thus speed up the convergence.

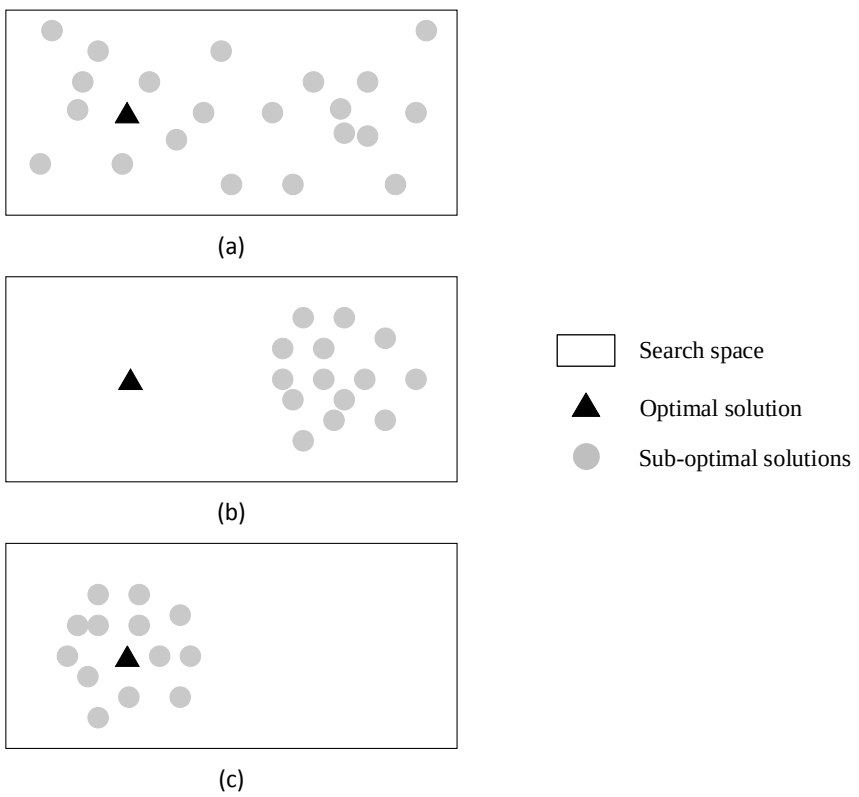

Figure 5.1: Three examples of search space.

In this optimal placement problem, if the variables are represented by their bus numbers, the optimal solution and other solutions are spread out randomly in the search space as shown in Fig. 5.1 (a), since the bus numbers do not have mathematical meaning regarding to the optimization problem. The optimal solution may not share several genes corresponding to sub-optimal solutions. However, after renumbering the locations based on their LMPs, candidate locations with smaller

total generation cost are aggregated and encoded to share more common genes with smaller distance. In this way, the optimal solution should be surrounded by some sub-optimal solutions and the convergence performance can be improved.

5.2.2 Reproduction

Reproduction, also known as selection operator. Reproduction selects good strings in a population and forms a mating pool [23]. Roulette-wheel selection and tournament selection are often used to form mating pool. In this work, tournament selection is applied. First, pick s individuals from the population, then choose the best among them to the mating pool. A binary tournament selection with $s = 2$ is used in this work. After forming the mating pool, stings in mating pool are going to the next step: crossover.

5.2.3 Crossover

In a crossover operator, new strings are created by exchanging information among strings of the mating pool [23]. This step is mainly responsible for the search of new strings. In order to create new strings, two strings are selected randomly from the mating pool, and these two strings are called parent strings, the newly created strings are known as children strings. After randomly selecting the parent strings from the mating pool, a single-point crossover is applied. First, a crossing point is randomly chosen. Then exchange all the bits on the right side of the crossing point. Not all the old strings are used in crossover, a crossover probability p_C is used in order to preserve some of the good strings. Only $100p_C$ percent of old strings are used in crossover operation.

5.2.4 Mutation

Mutation of gene happens with low probability in nature. In GAs, a mutation operation is applied to mimic this change. The mutation operator changes 1 to 0 and vice versa for each bit of every

string with a small mutation probability p_m . This step allows the algorithm to a local search around current solutions.

5.3 Sensitivity Analysis

A typical optimization problem with an objective function, equality constraints and inequality constraints is shown in 5.3.

$$\text{Min:} \quad F(\mathbf{x}, \mathbf{u}) \tag{5.1}$$

$$\text{Subject to:} \quad g_{i=1,2,3...,m}(\mathbf{x}, \mathbf{u}) \leq 0 \tag{5.2}$$

$$h_{j=1,2,3...,n}(\mathbf{x}, \mathbf{u}) = 0 \tag{5.3}$$

where $F(\mathbf{x}, \mathbf{u})$ is the objective function; $g_i(\mathbf{x}, \mathbf{u})$ is the inequality constraint; $h_j(\mathbf{x}, \mathbf{u})$ is the equality constraint.

From the optimization point of view, Lagrange multipliers can be interpreted as the rate of change in the objective function for an infinitesimal change in the right-hand side of the linear/non-linear programming problem. From a geometric perspective, Lagrange multipliers can be understood as the sub-gradients of the objective function along the dimension of resource provisioning changes. The Lagrangian function can be expressed as:

$$L = F(\mathbf{x}, \mathbf{u}) + \sum_{i=1}^{m} \mu_i g_i(\mathbf{x}, \mathbf{u}) + \sum_{j=1}^{n} \lambda_j h_j(\mathbf{x}, \mathbf{u}) \tag{5.4}$$

where μ and λ are Lagrange multipliers for inequality and equality constraints respectively and λ is called marginal cost of the equality constraint. It reflects the change of objective function when changing the constant of equality constraint slightly.

In economic dispatch studies, power flow analysis is usually carried out in solving optimization problems for minimum generation cost. In this work, the AC optimal power flow model is used to solve for minimum generation cost and to determine the value of Lagrange multiplies. The

objective function is subject to equality and inequality constraints of the power system operation limits. The equality constraints include the power balance at each bus and the inequality constraints are the capacity limits of generating units, power carrying capabilities of transmission lines, voltage limits at the nodes and reactive power capability limits. The objective is formulated as follows [26].

$$F = \min \sum_{i=1}^{N_g} F_i \left(P_{Gi}\right) \tag{5.5}$$

where F is the generation cost function, P_{Gi} is the generated power of unit i and and N_g is the number of generators. Locational marginal cost is the marginal cost of the equality constraint of the economic dispatch problem, which can be obtained by solving the dual problem.

5.4 Solution Approach

In this proposed method, the AC optimal power flow model with an objective function of minimizing the generation cost for the base case is first solved by MATPOWER [72]. From the dual solution of the optimization problem, the LMPs are determined for all the locations and are ranked in a descending order. Locations with high LMPs are considered as good candidates for additional generations. Since these locations are supported by higher cost generators or are more congested areas, they should have more significant drops in LMP once the ESSs are installed. Then the locations are numbered by their ranks instead of their original bus numbers and then translated to binary strings. By renumbering and encoding the locations based on their LMPs, the locations with good fitness values are gathered and encoded to share more common genes. For example, in the IEEE 14 test system, the locations for three different sizes ESSs are represented by three binary strings. [0011 1110 1010] represents that bus 3, 14 and 10 are the best locations for the ESSs.

After encoding the locations, the GA is utilized jointly with AC-OPF model to search for the optimal locations and sizes for the ESSs. In this minimization problem, the fitness function is defined in terms of the generation cost function F which can be obtained by the AC power flow

model. The expression of the fitness function is shown below and Fig. 5.2 shows the flowchart of the whole process.

$$Fitness = \frac{1}{1+F} \tag{5.6}$$

5.5 Case Studies and Simulation Results

To validate the effectiveness of the proposed encoding strategy and determine the optimal placement of DERs, the method is applied on several systems including IEEE 14, 30, 57 and 118 bus systems [73]. The system data is presented in table 5.1.

Take the test on IEEE 30 bus system as an example. There are 30 buses, 6 generating units and 41 transmission lines in this test system. Total installed generating capacity is 335 MW and three ESSs are planned to support the system. We assume that all the 30 buses are possible locations for the storage facilities. Then a 5-bit binary string can be used to represent the bus number, since it is capable of representing $2^5 - 1 = 31$ different locations. Suppose there are three ESSs with different capacities (30 MW/ 30 MWh, 20 MW/ 20 MWh and 10 MW/ 10 MWh) under scheduling. A $3 \times 5 = 15$ bits binary string is applied to represent the locations for the three ESSs. The first five bits represent the location of the 30 MW/ 30 MWh ESS and the last five bits represent the location of the 10 MW/ 10 MWh ESS. Then the optimal placement problem is solved as follows.

The discharged power from ESSs are treated as negative loads with zero fuel cost. The stochastic nature is not considered, but it should not be difficult to include this consideration, which can be implemented by applying a multi-state model as described in the previous chapter. The case studies are performed based on peak-load scenario, but hourly load data or clustered load data for a study period can be applied to this framework when necessary, by simply changing the fitness value to an average or weighted value.

First of all, an AC-OPF problem is solved for the base case without any added ESSs. LMPs at buses are determined from the Lagrange multipliers associated with the power balance equation

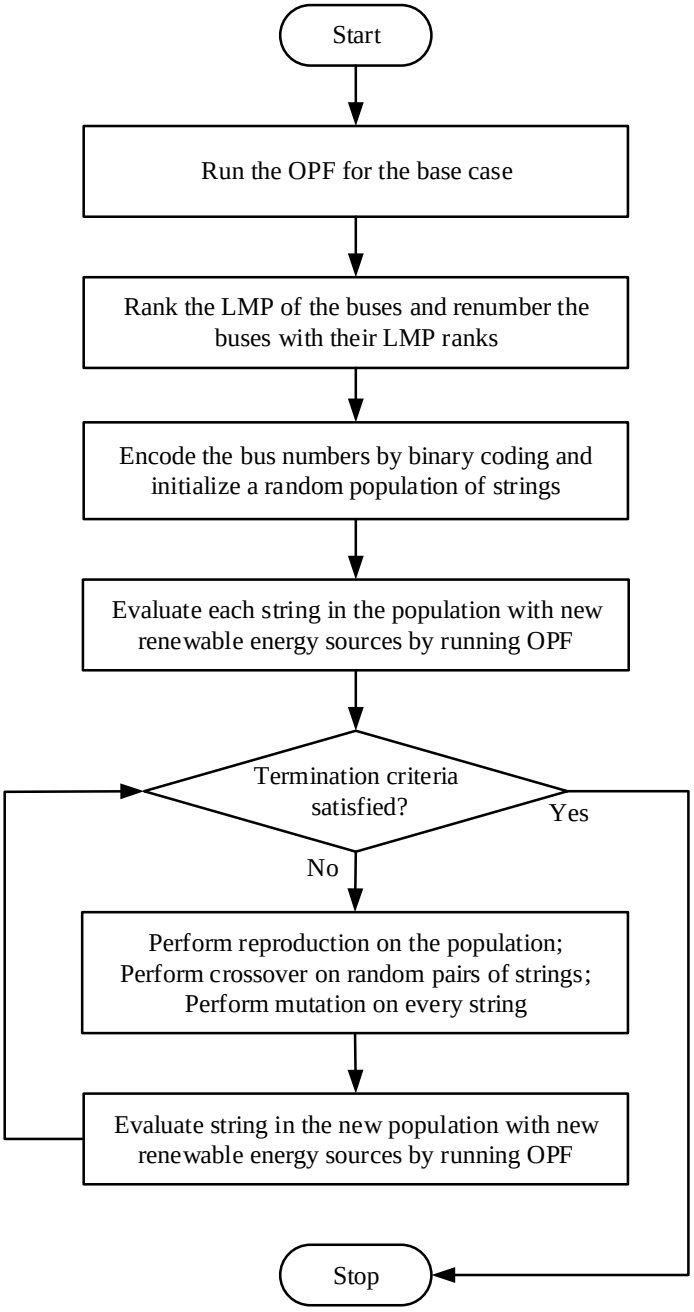

Figure 5.2: Flowchart of the proposed method.

Table 5.1: System Sizes of Test Cases

Test System	Number of Generating Units	Number of Transmission Lines	Total Generation (MW)	Added Energy Storage (MW)
IEEE 14 bus	5	20	772.4	60
IEEE 30 bus	6	41	335	60
IEEE 57 bus	7	80	1975.9	150
IEEE 118 bus	54	186	9966.2	150

at the buses and are obtained from the dual solution. Then, rank the LMPs of all the buses in a descending order and rename the buses by their ranking numbers instead of their original bus numbers and then code the variables by binary stings as shown in table 5.2. Second, genetic algorithm is applied to find the optimal solution. The population size is set as 50 and the maximum iteration number is set as 150. The crossover probability p_C and mutation probability p_m are 0.85 and 0.05, respectively. The proposed method converged after around 30 iterations, but the simple genetic algorithm converges after around 60 iterations. It shows that the proposed encoding strategy is helpful to enhance the convergence performance of the genetic algorithm. Besides, the generation cost at peak hour for the base case is $8,909 at peak hour. After adding the ESSs, the generation cost at peak hour drops to $6,488 with around 27% reduction.

Table 5.5 shows the comparison of convergence speed between the proposed sensitivity guided genetic algorithm (SGGA) method and the simple genetic algorithm without enhanced encoding strategy for all the case studies. The number of iterations needed to converge is used to compare the convergence speed, instead of a actual computational time, since the computational time depends not only on the algorithm, but also on the features of a computer and many other factors. Therefore, the number of generations is considered as an appropriate indicator to show the improvement of computational speed. Fig. 5.3 depicts the convergence performance on IEEE 118 bus system. The red line and the blue line represent the average value of the population for the enhanced genetic algorithm and the simple genetic algorithm, respectively. These results prove that renumbering the locations based on their LMPs is helpful to increase the convergence speed, since candidate

Table 5.2: Renamed Bus Numbers

Original Bus Number	LMP ($/MWh))	Renamed Bus Number	Binary-coded String
1	36.31	30	11110
2	38.11	29	11101
3	38.82	28	11100
4	39.56	27	11011
5	40.58	10	01010
6	40.08	24	11000
7	40.56	11	01011
8	40.25	18	10010
9	40.08	22	10110
10	40.09	21	10101
11	40.08	23	10111
12	39.65	25	11001
13	39.65	26	11010
14	40.31	17	10001
15	40.50	14	01110
16	40.10	20	10100
17	40.24	19	10011
18	40.93	6	00110
19	41.03	5	00101
20	40.82	8	01000
21	40.52	12	01100
22	40.50	13	01101
23	40.87	7	00111
24	41.03	4	00100
25	40.78	9	01001
26	41.54	2	00010
27	40.31	16	10000
28	40.32	15	01111
29	41.45	3	00011
30	42.23	1	00001

Table 5.3: Optimal Locations and Sizes Using the Proposed SGGA and Traditional Sensitivity Analysis Methods

System		Location and Size					
		SGGA			TSA		
IEEE 14 bus	Bus	3	14	10	4	10	12
	Size (MW)	30	20	10	30	20	10
IEEE 30 bus	Bus	5	19	30	4	16	24
	Size (MW)	30	20	10	30	20	10
IEEE 57 bus	Bus	12	38	36	15	35	55
	Size (MW)	60	50	40	60	50	40
IEEE 118 bus	Bus	41	112	53	30	60	90
	Size (MW)	60	50	40	60	50	40

Table 5.4: Comparison of Generation Cost among Different Placements

System	Cost ($/hr)		
	Base Case	TSA	SGGA
IEEE 14 bus	8,171	5,724	5,687
IEEE 30 bus	8,906	6,553	6,488
IEEE 57 bus	41,737	35,379	35,279
IEEE 118 bus	129,660	123,860	123,567

locations with high potential are gathered and encoded to share more common genes. The number of iterations can be reduced by around 35% by applying the proposed coding strategy.

Besides, the results obtained by SGGA and traditional sensitivity analysis (TSA) methods are compared. The traditional sensitivity analysis methods are based on determining the Lagrange multiplier values from the current operating point and do not consider the range of validity of the Lagrange multipliers [74]. The optimal locations and sizes using the proposed SGGA and the traditional sensitivity analysis are presented in Table 5.3 and Table 5.4.

From the case studies, we can see that compared with the traditional sensitivity analysis methods, the proposed SGGA obtained better results in determining the optimal locations and sizes of ESSs for reducing generation cost. Although the simple GA receives the same results as the

Table 5.5: Comparison of Convergence Speed

System	Number of iterations		Reduction
	Simple GA	SGGA	
IEEE 14 bus	45	30	33 %
IEEE 30 bus	60	30	50 %
IEEE 57 bus	150	90	40 %
IEEE 118 bus	90	60	33 %

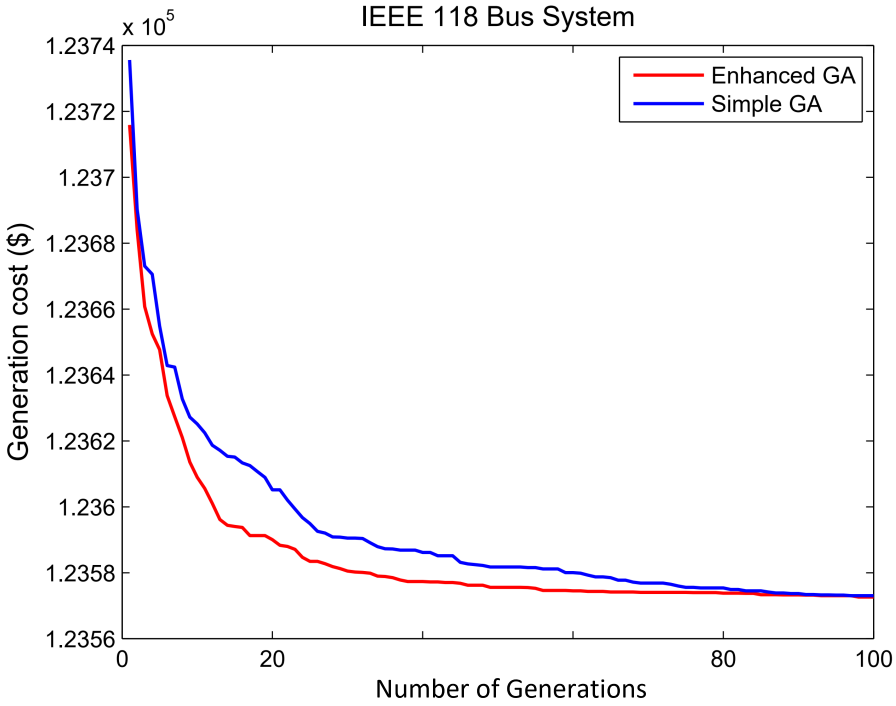

Figure 5.3: Convergence performance on IEEE 118 bus system.

proposed SGGA, the proposed method is less computationally expensive, since it converges faster.

5.6 Conclusion

This work has introduced the use of sensitivity analysis and locational marginal price to enhance the computational efficiency and speed of the genetic algorithm in determining the optimal placement of ESSs. The proposed algorithm is demonstrated on several test systems, including IEEE 14,

30, 57 and 118 bus systems. For each case, economic dispatch and genetic algorithm are applied to search for the optimal solution. The objective function used in the tested systems is the generation cost function. Therefore, the best locations for different size ESSs are deployed according to the saving in generation production cost. Also the convergence performances to find the optimal solution with and without the proposed encoding strategy are compared. The results demonstrated that the computational efficiency and speed are improved by the sensitivity analysis-based encoding approach. The use of sensitivity analysis is not restricted to GA. In the future, we will apply the sensitivity analysis to other intelligent methods and will also test it on problems not only at distribution level, but also in generation or transmission systems.

Chapter 6

Optimal Operating Strategies for ESSs

Batteries are increasingly becoming a more viable form of grid-level energy storage as time progresses. Among the different types of batteries present, Li-ion batteries have particularly gained widespread popularity due to their high energy density, high efficiency and decreasing costs. This chapter presents a detailed study on maximizing the monetary benefits from a Li-ion Battery Energy Storage System (BESS) for a number of applications, considering the BESS degradation process. The BESS is assumed to be participating in the energy market and is also being applied to supply critical loads when outage events occur to improve the resilience and reliability of the power system. Different operating strategies are tested and the results can be summarized into several suggestions on how to optimally operate the battery while performing energy arbitrage, enhancing system resilience and reliability, and also inhibiting the degradation of the battery.

6.1 Introduction

Battery energy storage systems (BESS) are becoming inseparable parts of the modern day power grid due to the increasing penetration of renewable resources. The intermittent behavior of renewable resources like wind and solar encourages the application of BESS which can restore normalcy to the grid by performing a number of applications. In addition to these, BESS can also be used for improving the resilience and reliability of the grid. Grid resilience has drawn a lot of attention

in recent years since the number of outages caused by severe weather and natural disasters have occurred quite frequently. For instance, hurricanes Sandy, Harvey, and Irma, have left millions of people without power. Also, component failures and other issues may affect system reliability. When a power outage event occurs, a BESS can be utilized to support the loads and help enhance the grid resilience and reliability. BESS also has other applications, such as shaving the peak load, providing frequency regulation service, and deferring the distribution system upgrades.

However, the degradation of batteries is an issue that must be taken into account while utilizing a BESS for grid-level applications. This study investigates the decay of life of Lithium ion (Li-ion) batteries under different operating strategies while being used for improving system resilience, reliability and for participating in the energy market. A relationship is then established considering the trade-off between maximizing the revenue from markets, restoring loads, and prolonging the life of the BESS.

A number of battery technologies are in use today for grid-level applications, including lithium-ion, lead-acid, vanadium redox, sodium-nickel-chloride to mention a few [1, 75]. Among these, Li-ion batteries are the most widely used [2] due to their high energy density, high efficiency and decreasing costs [76]. The different types of Li-ion batteries commercially established include lithium-cobalt oxide, lithium-titanate, lithium-iron phosphate, lithium-nickel manganese cobalt and lithium manganese oxide. The type of Li-ion battery to be used depends on the application itself, while the size can vary from a few hundred kilowatts to several megawatts. The largest Li-ion battery available today is the one installed by Tesla in the Hornsdale Wind Farm in South Australia [9]. This 100 MW, 129 MWh battery is used to store renewable energy and provide back-up power. The battery project in Sterling, MA, USA, is another noteworthy Li-ion installation. This 2 MW, 3.9 MWh battery is used as a back-up for the Sterling police station and is designed to support critical infrastructure during grid outages. It can island from the grid during an outage and can provide up to 12 days of back-up power with the help of solar generation [77]. The detailed value proposition for this project can be found in [78].

BESS can be used for several grid level applications as shown by the authors in [1]. They can be

used for participating in the energy and ancillary markets [17,21,79–81]. Reference [82] discusses the operation of a grid-connected Li-ion BESS for primary frequency regulation and also takes into account the battery lifetime, while [83] discusses the optimal sizing of a BESS for primary frequency control. Energy storage can also be used for improving the reliability of the grid [4, 16, 84]. Different operating strategies for operation of energy storage with wind farms for reliability improvement have been discussed in [85]. The authors in [23–25] proposed a quantitative method to determine the size of the energy storage systems to meet specified reliability targets. Reference [86] discusses the improvement in reliability of bulk power system achieved by the utilization of an energy storage integrated with renewable energy generation. However, the degradation of batteries is a pressing issue which must be addressed while planning for long-term energy storage applications. The authors in [87] proposes a semi-empirical model for assessing battery cell life loss from operating profiles. Reference [88] discusses the effects of battery degradation on multi-service portfolios and revenue of distributed energy storage plants providing multiple services. Research has also been performed involving the combination of all the above-mentioned factors to produce an optimal strategy for operating the battery storage [89]. In [90], the authors propose an optimal bidding strategy of battery storage in power markets considering the battery cycle life.

In this work, the lifespan benefits of a Li-ion BESS has been examined. The BESS is assumed to participate in the energy market for peak shaving and be able to gain profit by selling energy at peak hours when the energy prices are high, and purchasing energy at off-peak hours when the prices are low. The price-taker model is applied for evaluating this revenue. The BESS is also assumed to be able to provide energy to the connected consumers when power outage events occur. A multi-state model is used for modeling the availability of battery during outages and the expected avoided interruption cost is evaluated. This study also considers the degradation of the BESS, and the lifespan benefits under different operating strategies.

The remainder of this chapter is organized as follows. Section II discusses the operation strategy of the BESS for maximizing the energy arbitrage revenue. Section III explains how the degradation of Li-ion batteries takes place and is quantitatively measured. Section IV describes the value

from outage mitigation incorporating the stochastic availability of the BESS and the model of interruption cost reduced by using the BESS. Section V presents case studies with different operating polices and provides their results. Section VI provides concluding remarks.

6.2 Operating Strategy for the BESS

In this section, the optimization model for estimating the maximum revenue from the energy market is presented.

6.2.1 Energy Market

A BESS can be used to accumulate energy by charging when the electricity prices are low, i.e., during the off-peak hours, and then by discharging during the peak hours, when the energy prices are higher. This application also contributes to the reduction of generation costs and defers the installation of peaking units.

Two types of energy trading settlements prevalent in the U.S. energy market, viz., the day-ahead and the real-time settlements. Here, the day-ahead market is used for investigation of the optimal operating strategy of the BESS. Day-ahead and real-time settlements are the two types of energy trading settlements prevalent in the US energy market. Here, we use the day-ahead market as an example for investigation of the optimal operating strategy of the BESS. In this market, suppliers can submit supply bids and consumers can submit demand bids. Also, participants can choose to submit only quantity bids, or both quantity and price bids. If the participants submit a quantity bid only, it implies that they will always accept the market clearing price. On the other hand, if the participants submit both quantity and price bids, it implies that the supplier will sell only when the clearing price is higher than the price bids and the buyer will purchase the energy only when the clearing price is lower than the price bids.

The money received by selling energy can be expressed as:

$$\mathbb{1}(R_t^{\mathrm{bd}} \leq R_t^{\mathrm{lmp}}) R_t^{\mathrm{lmp}} E_t^{\mathrm{bd}} \tag{6.1}$$

while, the money spent by buying energy can be expressed as:

$$\mathbb{1}(R_t^{\mathrm{lmp}} \leq R_t^{\mathrm{bc}}) R_t^{\mathrm{lmp}} E_t^{\mathrm{bc}} \tag{6.2}$$

where R_t^{lmp} is the cleared market price at time t; R_t^{bd} and R_t^{bc} are the price bids for selling (discharge) and purchasing (charge); $\mathbb{1}(R_t^{\mathrm{bd}} \leq R_t^{\mathrm{lmp}}) = 1$ when the clearing price is higher than the price bids of sell and $\mathbb{1}(R_t^{\mathrm{lmp}} \leq R_t^{\mathrm{bc}}) = 1$ when the clearing price is lower than the price bid of purchase. $E_t^{\mathrm{bd}} = P_t^{\mathrm{bd}} \tau$ and $E_t^{\mathrm{bc}} = P_t^{\mathrm{bc}} \tau$ are the energy sold and purchased, where P_t^{bd} and P_t^{bc} are the quantity bids of supply and demand at time t, respectively.

6.2.2 Objective

The difference between selling and purchasing prices can be used as an advantage by the BESS owners in earning profits. Thus, a BESS owner needs to determine the supply or demand bids properly to maximize the profit. In this work, we assume that the BESS is not large enough to affect the energy price and thus it is represented as a price-taker. Before submitting the bids, operators will normally forecast the price in advance based on historical data or other factors. Considering the price uncertainty, the operation strategy can be obtained by solving the following stochastic programming problem, which aims at maximizing the expected profit from the day-ahead market.

.

$$\text{Maximize} \quad \sum_{t=1}^{T} \sum_{k=1}^{K} p_k^{\mathrm{lmp}} R_{t,k}^{\mathrm{lmp}} \Big(\mathbb{1}(R_t^{\mathrm{bd}} \leq R_{t,k}^{\mathrm{lmp}}) P_t^{\mathrm{bd}} \tau - \mathbb{1}(R_{t,k}^{\mathrm{lmp}} \leq R_t^{\mathrm{bc}}) P_t^{\mathrm{bc}} \tau \Big) \tag{6.3}$$

where T is the operation time and T has been considered to be 24 in this study as the model is built for determining the operating strategy for the next day; K is the number of price scenarios. p_k^{lmp} is the probability of the scenario k; τ is the duration of the energy market dispatch time interval and it is considered to be one hour in this study.

Battery degradation is an essential factor which affects the total value of the BESS. To avoid overuse of the battery, degradation cost has been included in the objective function as a penalty. The degradation cost is represented by a linear function of the discharged energy. The objective function of (6.3) can now be modified by the following expression. The details of battery degradation are discussed in section 6.3.

$$\begin{aligned} &\text{Maximize} \\ &\sum_{t=1}^{T}\sum_{k=1}^{K} p_k^{\mathrm{lmp}} R_{t,k}^{\mathrm{lmp}} \Big(\mathbb{1}(R_t^{\mathrm{bd}} \leq R_{t,k}^{\mathrm{lmp}}) P_t^{\mathrm{bd}} \tau \\ &\qquad\qquad - \mathbb{1}(R_{t,k}^{\mathrm{lmp}} \leq R_t^{\mathrm{bc}}) P_t^{\mathrm{bc}} \tau \Big) \\ &-\omega \sum_{t=1}^{T} \Big(\beta_1 \mathbb{1}(R_t^{\mathrm{bd}} \leq R_{t,k}^{\mathrm{lmp}}) P_t^{\mathrm{bd}} \tau / E^{\mathrm{r}} \gamma_d + \beta_0 \Big) \end{aligned} \tag{6.4}$$

where ω is the degradation cost weight (DCW) and it varies from 0 to 1. When $\omega = 0$, the degradation cost model is not considered and as ω increases, more importance is given to the degradation cost model. β_1 and β_0 are the coefficients of the linearized degradation cost function, E^{r} is the rated energy capacity, and γ_d is the discharging efficiency.

6.2.3 Constraints

The state of charge (SOC) of a battery represents the ratio of the current to the rated capacity. It depends on the SOC of the previous period and the current operating state of the BESS, i.e., whether it is charging or discharging. The SOC at time t is represented as follows.

$$SOC_t = SOC_{t-1} + \frac{\triangle E_t}{E^{\mathrm{r}}},\ \forall t \in T \tag{6.5}$$

where $\triangle E_t$ is calculated as below.

$$\triangle E_t = E_t^{\mathrm{c}} - E_t^{\mathrm{d}} \tag{6.6}$$

where E_t^{c} and E_t^{d} represent the actual energy charged and discharged from the battery respectively. They are different from the bidding quantities E_t^{bc} and E_t^{bd}, as charging and discharging efficiencies are not 100%. E_t^{c} and E_t^{d} are calculated as follows.

$$E_t^{\mathrm{c}} = \mathbb{1}(R_{t,k}^{\mathrm{lmp}} \leq R_t^{\mathrm{bc}}) P_t^{\mathrm{bc}} \tau \gamma_c \tag{6.7}$$

$$E_t^{\mathrm{d}} = \mathbb{1}(R_t^{\mathrm{bd}} \leq R_{t,k}^{\mathrm{lmp}}) P_t^{\mathrm{bd}} \tau / \gamma_d \tag{6.8}$$

where γ_c and γ_d are the charging and discharging efficiencies (%).

The operation of a BESS is constrained by its energy storage capacity, charging and discharging power limits, etc. The constraints are represented by the following equations.

$$SOC^{\min} \leq SOC_t \leq SOC^{\max},\ \forall t \in T \tag{6.9}$$

$$0 \leq P_t^{\mathrm{d}}, P_t^{\mathrm{c}} \leq P^{\max},\ \forall t \in T \tag{6.10}$$

$$P_t^{\mathrm{d}} \times P_t^{\mathrm{c}} = 0, ,\ \forall t \in T \tag{6.11}$$

$$SOC_t = SOC^{\mathrm{c}},\ \text{for } t = 0 \tag{6.12}$$

$$SOC_t = SOC^{\mathrm{c}},\ \text{for } t = T \tag{6.13}$$

SOC is constrained with lower and upper bounds by $SOC^{\min}$ and $SOC^{\max}$ as shown in (6.9). Different operating strategies mainly depend on this constraint as the $SOC^{\min}$ and the $SOC^{\max}$ are varied for different scenarios. Charging and discharging power limits are represented by (6.10). The quadratic constraint in (6.11) indicates that during each period, the BESS cannot buy and sell

energy in the arbitrage market simultaneously. Equations (6.12) and (6.13) indicate that the SOC at the end of the day is equal to the SOC at the beginning of the day. In this study, SOC^{c} is set as 50%. It is worth-noting that as the capacity loss increases, the $SOC^{\max}$ decreases. Hence, it should be updated based on the remaining capacity of the battery.

6.3 Degradation of Lithium-ion Batteries

The lifetime of a BESS is crucial for utilities and operators. Two quantities, viz., the cycle life and the calendar life are used for determining the lifetime of a BESS. The cycle life is affected by cycle aging, which includes, besides the number of cycles, depth of discharge (DOD), mean SOC of cycles and several other factors. Calendar life, on the other hand, represents the aging and degradation of a BESS over time, and is affected by weather conditions such as temperature and humidity. This implies that the degradation of the battery continues even though it is stored and unused. In this section, the methodologies for counting the cycles and evaluating the life of Li-ion battery are discussed.

6.3.1 Degradation Model of Li-ion Battery

A battery life assessment model with a linearized degradation rate is applied here. According to [87], the linearized degradation rate depends on the number of cycles, the SOC, the depth of discharge (DOD), cell temperature, C-rate and the elapsed time. The state of health (SOH) is normally used to represent the remaining capacity of the battery, which can be estimated from the ratio of its remaining capacity E^{rem} to its rated capacity as represented below.

$$SOH = E^{\mathrm{rem}}/E^{\mathrm{r}} \times 100\% \tag{6.14}$$

The degradation model used here is capable of evaluating the capacity loss (L). The SOH can then be calculated as $1 - L$. For a new battery, $L = 0$ and $SOH = 100\%$. In this study, it is

assumed that the battery reaches its end of life (EOL) when it can provide only 80% of its rated energy capacity at most, i.e, when $L = 0.2$ and $SOH = 80\%$. The degradation assessment model can be represented as follows.

$$L = 1 - \alpha_1 e^{(-\alpha_2 f_d)} - (1 - \alpha_1) e^{(-f_d)} \tag{6.15}$$

where f_d is the linearized degradation rate as expressed in (6.16). It is the sum of f_{cyc} and f_{cal}, which reflect the cycle and calendar aging, respectively. α_1 and α_2 are coefficients of the solid electrolyte interphase (SEI) model [87].

$$f_{\mathrm{d}} = f_{\mathrm{cyc}} + f_{\mathrm{cal}} \tag{6.16}$$

$$f_{\mathrm{cyc}} = \sum_{i=1}^{N^{\mathrm{cyc}}} f_D(DOD_i) \times f_S(SOC_i) \times f_C(C_i) \times f_T(T_i) \tag{6.17}$$

$$f_{\mathrm{cal}} = k_t \times t \times f_S(\overline{SOC}) \times f_T(\overline{T}) \tag{6.18}$$

where $f_D(DOD)$, $f_S(SOC)$, $f_C(C)$ and $f_T(T)$ are the aging models associated with the DOD, SOC, C-rate and temperature stress, respectively. The constant k_t represents the time stress coefficient, t the test time (s), $\overline{SOC}$ the average SOC, $\overline{T}$ the average cell temperature, and N^{cyc} the number of cycles. The aging models are calculated as follows [91].

$$f_D(DOD) = (k_{D1} DOD^{k_{D2}} + k_{D3})^{-1} \tag{6.19}$$

$$f_S(SOC) = e^{k_S(SOC - SOC_{\mathrm{ref}})} \tag{6.20}$$

$$f_C(C) = e^{k_C(C - C_{\mathrm{ref}})} \tag{6.21}$$

$$f_T(T) = e^{k_T(T - T_{\mathrm{ref}})} \frac{T_{\mathrm{ref}}}{T} \tag{6.22}$$

where $K_{D1}, K_{D2}, K_{D3}, K_S, K_C$, and K_T are coefficients, and $SOC_{\mathrm{ref}}, C_{\mathrm{ref}}$, and T_{ref} are

reference values in the stress factor model.

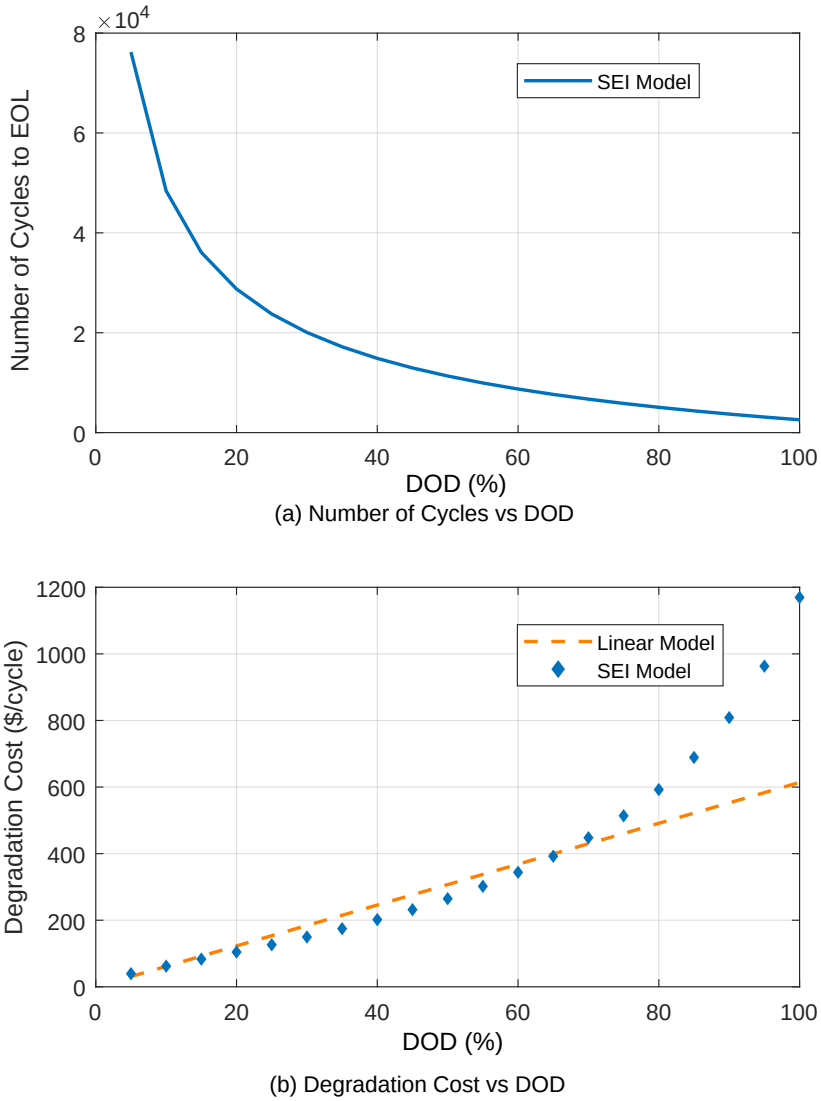

Figure 6.1: BESS degradation performance

6.3.2 Degradation Cost

Based on the aforementioned degradation model (SEI model), the number of cycles at different DODs up to the end of life (EOL), i.e., 80% of its rated capacity, is illustrated in Figure 6.1(a). The degradation cost per cycle is calculated based on the number of cycles and the replacement cost of the BESS, which is assumed to be 300,000 $/MWh [92]. For example, if a 1 MW, 1MWh BESS

can operate 30,000 cycles at 20% DOD, then the degradation cost of a 20% cycle is calculated as

$$\frac{300,000\$/\mathrm{MWh} \times 1\mathrm{MWh}}{30,000 \text{ cycles}} = 10\$/\text{cycle} \tag{6.23}$$

The degradation cost per cycle for different levels of DOD is illustrated in fig. 6.1(b). Since deep cycles degrade the battery faster, the DOD of the BESS is normally restricted above a certain boundary, e.g, 80% of the rated capacity. Thus, the cycle cost can be represented by a linear model when the DOD of the battery is restricted within 0% and 80%. The fitted model obtained by linear regression for this range is also plotted in fig. 6.1(b). Then the degradation cost can be calculated as $(\beta_1 DOD + \beta_0)$, where β_0 and β_1 are the coefficients of the degradation cost linear model.

6.3.3 Rainflow Counting Method

As mentioned in the end of section II, the $SOC^{\max}$ is changing and although the degradation cost has been added to the objective function, the actual SOH remains unknown without a degradation assessment. Therefore, it is necessary to check the SOH and update the $SOC^{\max}$ periodically. The rainflow counting method is applied in this study, which has been extensively used in fatigue analysis [93–95], including the battery technology field [82, 87]. It can be used to determine number of cycles, cycle mean and cycle amplitude of the BESS. In this work, it has been used to count the number of cycles for evaluating the battery degradation. The information regarding the cycling of the BESS, including its SOC profile, is obtained by solving the optimization problem described in section II. Thus, the rainflow counting method is used to count the cycles and assess the SOH jointly with the model presented in III.A.

6.4 Resilience and Reliability Improvement

In this section, the methodology to evaluate the benefit of the BESS from improving the resilience and reliability is discussed. The uncertainty of the BESS is addressed and the equations for calcu-

lating the interruption cost are presented.

6.4.1 Value from Mitigating Outages

In recent times, severe weather and natural disasters have been the leading causes for several power outage events. For instance, hurricanes Sandy, Harvey and Irma have caused power outage events affecting millions of people [96]. In addition to these, numerous other factors may affect system reliability, such as failures of generating units, large variations in demand, and scheduled maintenance. All these factors may lead to loss of load. In such situations, a BESS can effectively support customer loads when partial or complete loss of power from the source utility takes place. Thus, grid resilience and reliability can be improved by utilizing energy storage systems.

A BESS can be installed at the transmission or distribution level, or directly at a customer location. It can contribute to the reliability improvement of an interconnected area by acting as a dispatchable resource, if it is owned by a utility with a large capacity. It can also serve the customer needs during an outage event, especially in some critical locations such as hospitals and correctional facilities, which can significantly benefit from using a BESS. For instance, the 2 MW, 3.9 MWh battery storage system at Sterling, MA, USA, supports critical infrastructure during grid outages. During a power outage, the BESS can provide up to 12 days of backup power to the police station and dispatch center with the support of existing solar generation [77].

For each power outage event, if the BESS can discharge $P^{\max}$ power to mitigate the outage, then the resilience value that a BESS can be calculated as follows.

$$R^{\mathrm{L}} \times \min(H^{\mathrm{L}}, H^{\mathrm{B}}) \times P^{\max} \tag{6.24}$$

where R^{L} is the interruption cost ($kWh), H^{L} is the outage duration of the contingency (hour), and H^{B} is the duration that a BESS can be deployed to mitigate the outage, which equals $SOC/P^{\max}$. The equation indicates that the resilience value of a BESS depends on the outage event duration and the availability of the battery.

6.4.2 Uncertainty of Battery Availability

Although the BESS is considered to be a controllable device, the availability of the BESS at an unpredictable outage event is unforeseeable since the BESS is participating in the energy market at normal operating states and thus the SOC of the BESS is always fluctuating. The integration of the BESS can be represented by a multi-state model which captures this stochastic nature. In this multi-state model, the SOC and its corresponding probability are calculated for all the N^{soc} states. The BESS resilience value can then be evaluated as follows.

$$R^{\mathrm{L}} P^{\max} \sum_{n=1}^{N^{\mathrm{soc}}} p_n^{\mathrm{soc}} \min(H^{\mathrm{L}}, \frac{SOC_n}{P^{\max}}) \tag{6.25}$$

where SOC_n and p_n^{soc} are the SOC value and the corresponding probability at the nth state, respectively.

Then the total resilience value of a BESS for a year with N^{evt} outage events can be calculated as follows.

$$\sum_{m=1}^{N^{\mathrm{evt}}} R_m^{\mathrm{L}} P^{\max} \Big(\sum_{n=1}^{N^{\mathrm{soc}}} p_n^{\mathrm{soc}} \min(H_m^{\mathrm{L}}, \frac{SOC_n}{P^{\max}}) \Big) \tag{6.26}$$

where R_m^{L} is the interruption cost of event m. H_m^{L} is the outage duration of event m (hour).

6.5 Case Studies and Results

In this section, several case studies are performed with different operating strategies, results are compared and findings are discussed.

Historical data from the PJM Interconnection is utilized for evaluating the revenue from participating in the energy markets [33, 34]. One year of real time energy prices, from January 1, 2017 to December 31, 2017, has been used for this study. Historical data has been used in this study as the focus of this work is not on price forecasting.

Lithium manganese oxide (LMO), a type of Li-ion battery, has been considered in this work.

Data related to the degradation of this type of battery can be found in [87]. The simulation is performed on a daily basis for one year. Some previous studies have performed the optimization for a longer periods of time, e.g. one month [21], to estimate the revenue from the energy market. This method can prove to be beneficial in the planning stage as it provides a larger estimate of the revenue that the BESS can generate. However, at the operation stage, it is not always possible to predict the energy prices one month in advance, and hence it is more practical to use day-ahead energy prices to optimize the operation. Thus, T is set as 24 and the optimization is performed for a 24-hour period.

The battery size is assumed to be 1 MW, 1 MWh with the calendar life as ten years. The charging and discharging efficiencies are assumed to be 95% for all the cases. The BESS parameters are shown in Table 6.1. Table 6.2 summarizes the operating range for all the cases. A total of 4×11 cases with different operating strategies are studied. The lower and upper bounds of the SOC are different for these cases, and the DCW varies from zero to one. Also, we assume that the BESS is a price-taker participant and the operator submits supply quantity bids in this study, i.e., $\mathbb{1}(R_t^{\mathrm{bd}} \leq R_{t,k}^{\mathrm{lmp}}) = 1$ and $\mathbb{1}(R_{t,k}^{\mathrm{lmp}} \leq R_t^{\mathrm{bc}}) = 1$ for all the cases.

Table 6.1: BESS Parameters

Parameter	Value
Battery Type	LMO
Power Capacity	1 MW
Energy Capacity	1 MWh
Calendar life	10 years
SOC^{c}	50%
γ_c	95%
γ_d	95%

Table 6.2: Operating Policies

	$\mathrm{SOC_{min}}$ (%)	$\mathrm{SOC_{max}}$ (%)
Case 1	20	80
Case 2	30	90
Case 3	10	90
Case 4	15	95

6.5.1 Solution Procedure

Results are obtained by following the four steps mentioned below for each case with different DCWs.

Step I

Solve the optimization problem given in (6.4)–(6.13). In this study, the optimization problem is solved by the General Algebraic Modeling System (GAMS) software. In this step, revenue from the energy market and the annual SOC of battery can be obtained.

Step II

Estimate the distribution of the annual SOC and develop the multi-state model for resilience and reliability analysis. Then evaluate the reduced interruption cost.

Step III

Investigate the battery cycling behavior with rainflow counting method and the degradation model to assess the SOH.

Step IV

Update the $SOC^{\max}$ in (6.9) as $SOC^{\max} = \min(SOC_{op}^{\max}, SOH)$ and go to Step I. Repeat until SOH $\leq 80\%$ or the simulation time reaches to the BESS calendar life.

Here the $SOC_{op}^{\max}$ is the maximum SOC value determined by the operator. For instance, in case 3, the operator has initially set the maximum SOC as 100%. However, after a period of time, the SOH of the battery decreases to 90%, so the maximum SOC also decreases to 90%.

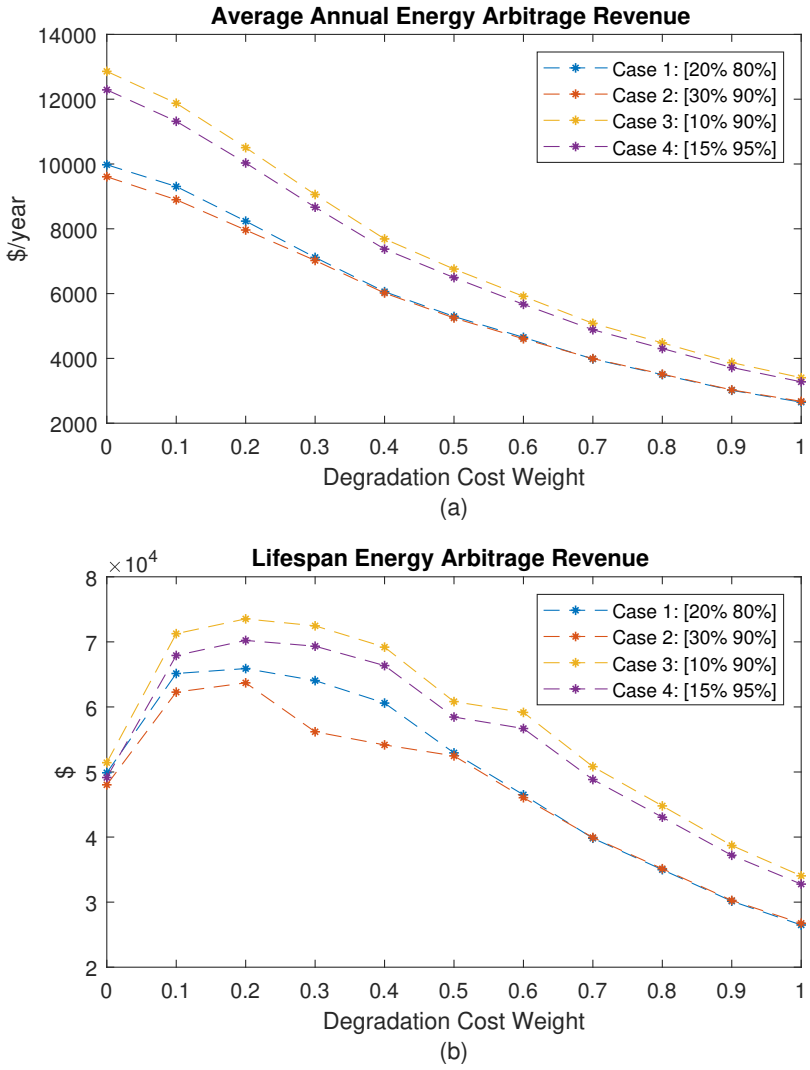

Figure 6.2: Revenue from the energy market

6.5.2 Results

Results from all the above cases, including the resilience value, battery life, profit from energy market, and stacked benefits are presented in this section and compared. The degradation weight is varied from zero to one for all cases.

6.5.2.1 Profit from the Energy Market

The revenue from the energy arbitrage application for different values of DCW are shown in figure 6.2. From these figures, it can be concluded that more revenue can be generated if the BESS is operated at a larger SOC range. Hence, the BESS generates more revenue for cases 3 and 4 than in cases 1 and 2. It is also evident that the revenue for a single year increases with decreasing DCW. However, the lifetime revenue does not follow this trend and the highest profit for most of the cases can be obtained when $\omega = 0.2$.

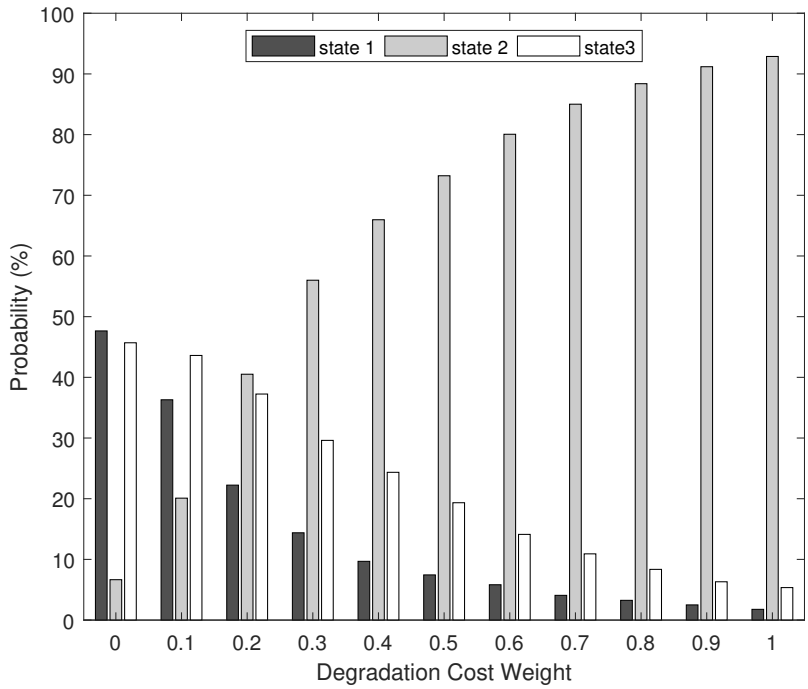

Figure 6.3: SOC states of Case 1 at year 1

6.5.2.2 SOC Multi-state

The multi-state model of battery based on the hourly SOC for each year, for different DCWs are evaluated for all cases. Figure 6.3 shows an example of the change in the multi-state model for case 1 at year one. There are three SOC states for case 1: 20% for state 1, 50% for state 2, and 80% for state 3. As the DCW increases, the probabilities of occurrence of state 1 and 3 decreases,

while that of state 2 increases. This implies that if degradation carries more penalty, then the BESS should decrease the number of cycles and idle at state 2 most of the time.

Table 6.3: Interruption Cost

Interruption Duration	Large and Medium C&I Customer ($/kWh)	Small C&I Customer ($/kWh)
30 minutes	37.3	474.1
1 Hour	21.8	295
4 Hours	12.1	214.3
8 Hours	12.9	267.3
16 Hours	12,7	258

6.5.2.3 Resilience Value

The value from outage mitigation is calculated based on existing survey results regarding interruption costs in the U.S. Two types of customer data are utilized in this study: the large and medium commercial and industrial (C&I) customer (Type 1) and the small C&I customer (type 2). The data is presented in Table 6.3 [97, 98].

Figures 6.4 and 6.5 show the value from outage mitigation for all the cases as ω is varied. From the figure, it can be concluded that the BESS has higher average annual resilience value when the minimum and maximum SOC are both higher. For instance, the value from outage mitigation is the highest for cases 2 and 4 as shown in figures 6.4 (a) and 6.5 (a). However, the total lifespan resilience value, as presented in figures 6.4 (b) and 6.5 (b), is the highest for case 1 and 2 when the ω is properly assigned.

6.5.2.4 Battery Life

Figures 6.7 and 6.8 illustrate the degradation process of the BESS for ten years of usage when the DCW is set as one and zero, respectively. When DCW equals one, the BESS can be utilized for ten years for all four operating ranges. However, when DCW equals zero, the life of the BESS is in the range of four to six years. Figure 6.6 illustrates the SOH of the BESS over ten years of usage with

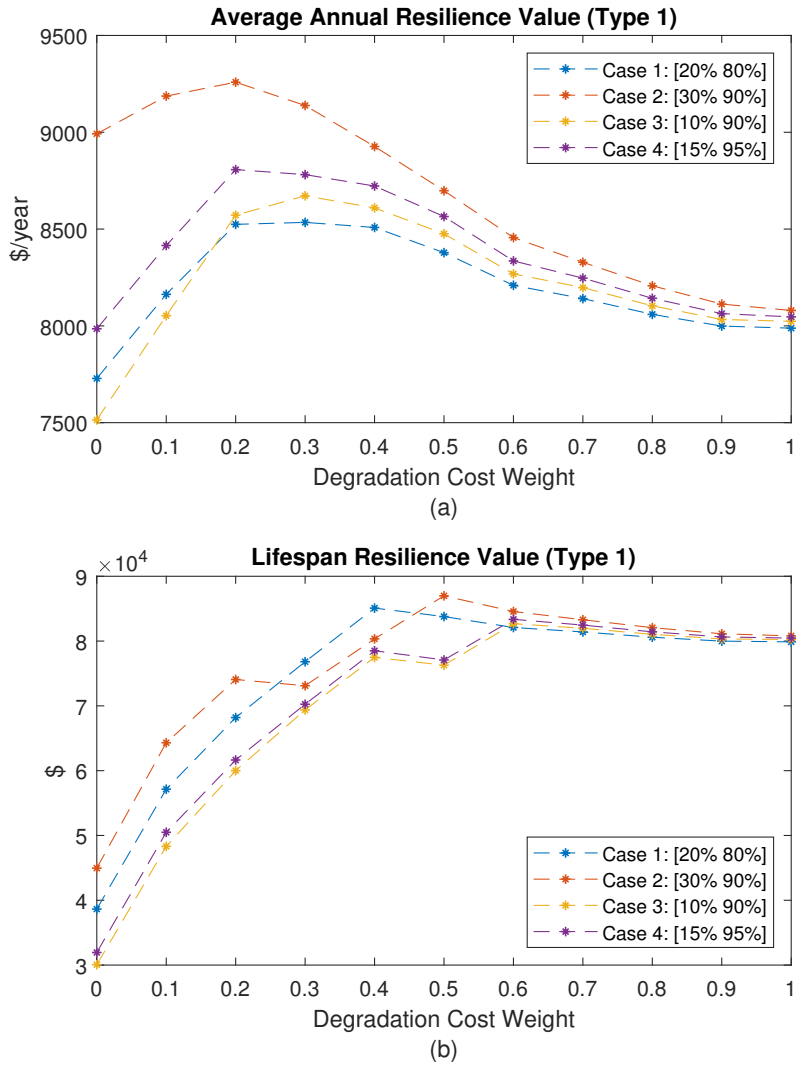

Figure 6.4: Resilience value for large and medium C&I customer

different DCWs for each case. The SOH of cases with $\omega > 0.6$ is not presented since the SOH for all the cases is higher than 80% at year ten. The results also show that if the DCW is less than 0.4, the BESS cannot last till the end of its calendar life, i.e., ten years, for any of the four cases.

6.5.2.5 Stacked Benefit

Figures 6.9 and 6.10 summarize the stacked value of the BESS from the energy market and outage mitigation before it reaches its EOL for the two types of customers. For large and medium C&I

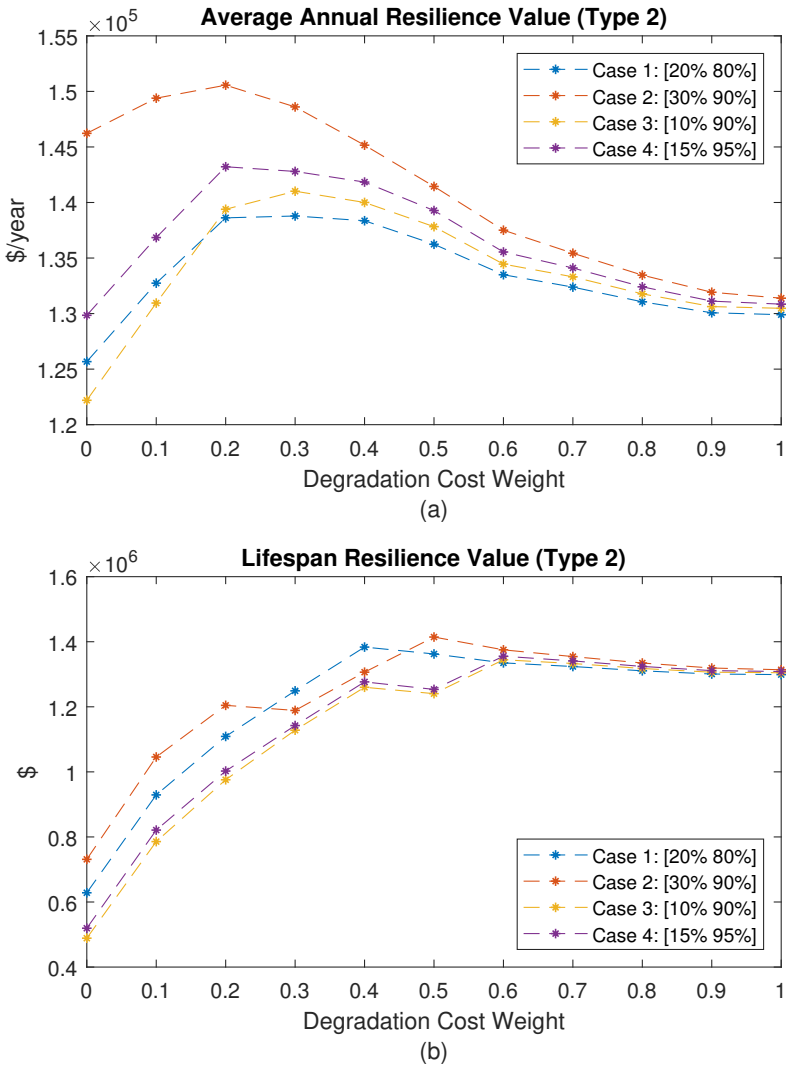

Figure 6.5: Resilience value for small C&I customer

customers, it can be observed that the BESS has the highest value when the DCW is set to 0.4 for all the four cases. This is more pronounced when the BESS operates between 10% and 90% SOC. For small C&I customers, the BESS has the highest value when operated between 30% and 90% SOC with the DCW being set to 0.5. The BESS also generates a relatively higher revenue when it is operated between 20% and 80% SOC and with the DCW being set as 0.4. Tables 6.4 and 6.5 present the highest values of BESS for the two types of customers.

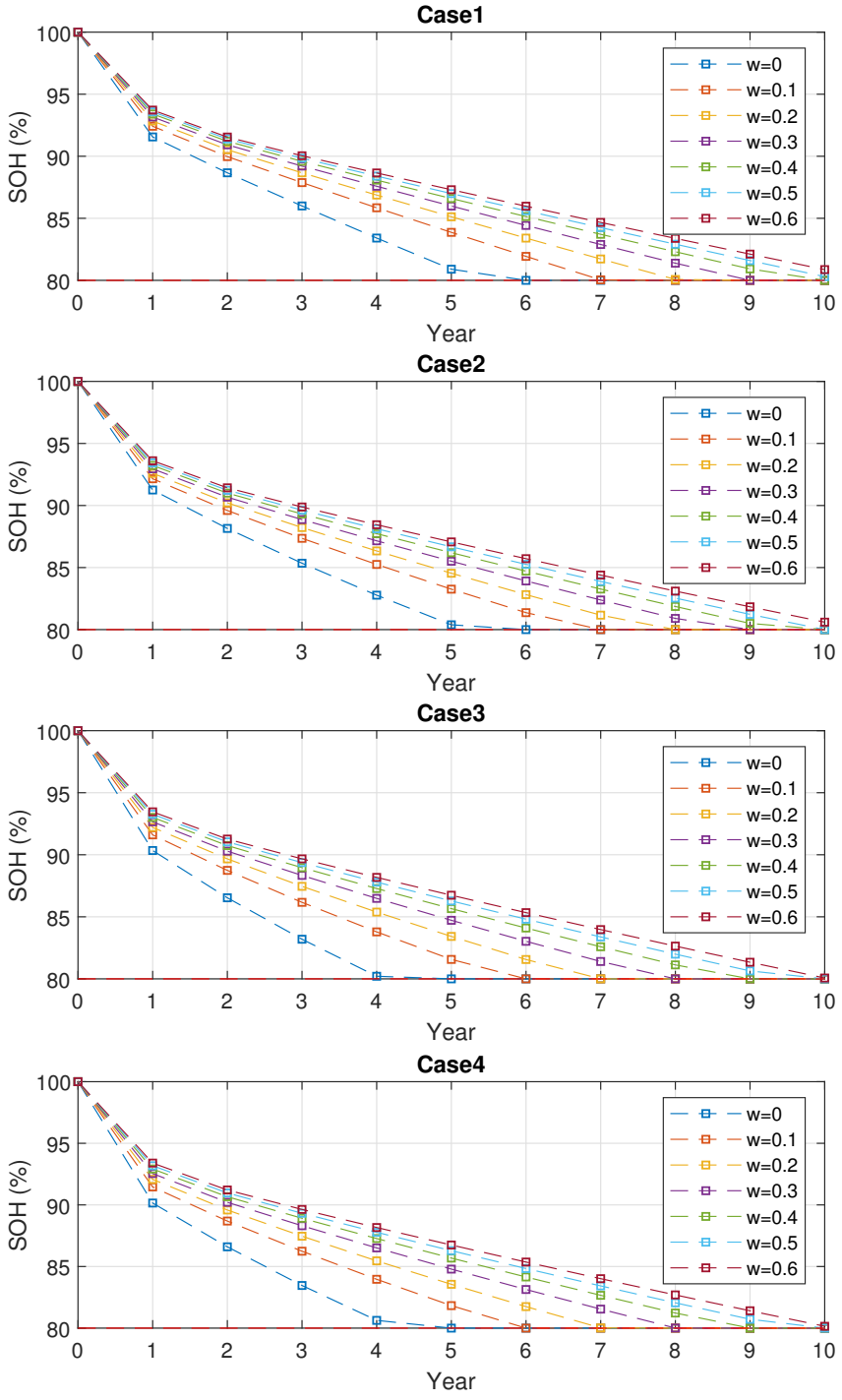

Figure 6.6: Degradation process with different ω

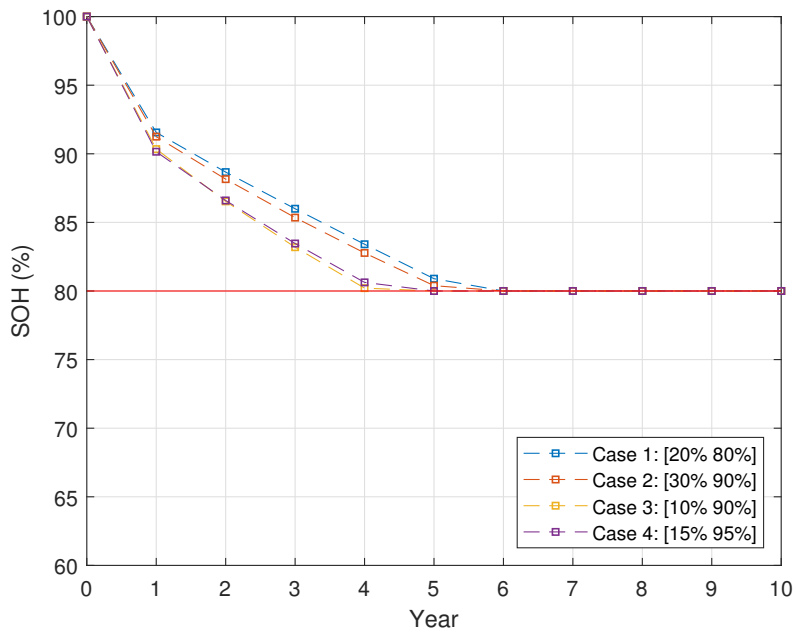

Figure 6.7: SOH with $\omega = 0$

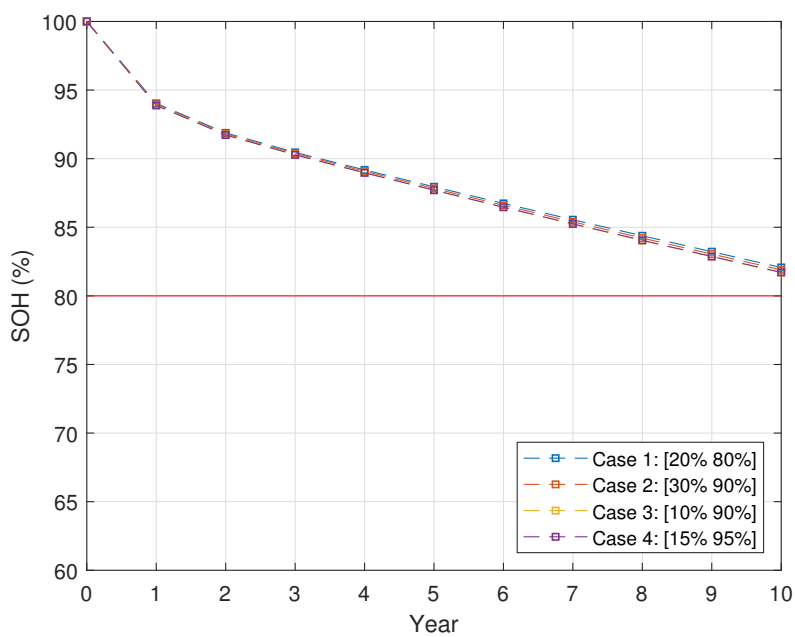

Figure 6.8: SOH with $\omega = 1$

6.5.3 Discussion

From the results of the case studies, it can be observed that,

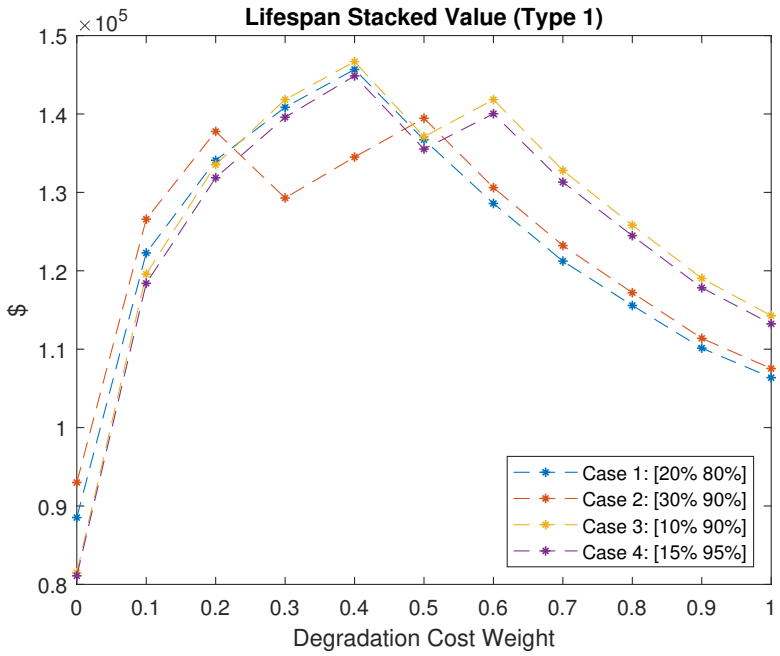

Figure 6.9: Stacked value for large and medium C&I

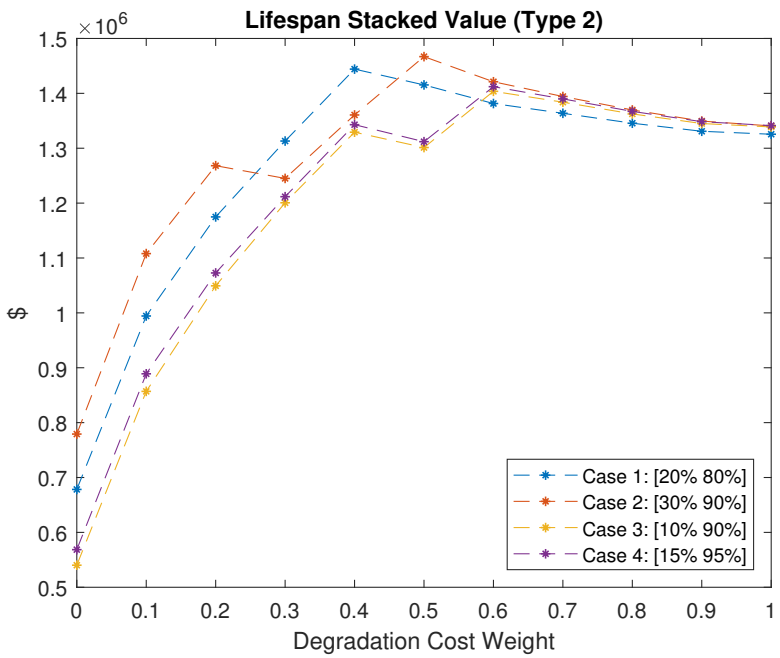

Figure 6.10: Stacked value for small C&I

1. The annual revenue from the energy market increases as ω decreases, i.e., as the importance on the degradation model decreases. The revenue is also higher for cases 3 and 4, where

Table 6.4: Stacked Value for Large and Medium C&I with $\omega = 0.4$: Case 3

Year	Energy Arbitrage	Resilience Value	Stacked Value
1	8079.18	8737.69	16816.87
2	8079.18	8737.69	16816.87
3	8079.18	8737.69	16816.87
4	7958.44	8698.16	16656.60
5	7762.54	8634.03	16396.57
6	7574.23	8572.37	16146.61
7	7392.60	8512.91	15905.51
8	7216.97	8455.41	15672.38
9	7046.98	8399.75	15446.74
10	0	0	0
Total	69189.3	77485.7	146675

Table 6.5: Stacked Value for Small C&I with $\omega = 0.5$: Case 2

Year	Energy Arbitrage	Resilience Value	Stacked Value
1	5583.12	143051.92	148635.03
2	5583.12	143051.92	148635.03
3	5583.12	143051.92	148635.03
4	5544.76	142868.23	148412.99
5	5390.54	142129.63	147520.17
6	5241.41	141415.42	146656.83
7	5096.27	140720.33	145816.60
8	4954.82	140042.91	144997.73
9	4816.88	139382.28	144199.16
10	4682.28	138737.67	143419.96
Total	52476.32	1414452.22	1466928.54

higher capacities of the BESS have been committed to the market and hence the results are quite obvious.

2. The BESS has higher resilience value for one year when the maximum and minimum SOC are both high. For instance, in figures 6.4 and 6.5, case 2 has the highest value from outage mitigation. Also, the BESS has higher lifespan resilience value when the DCW is between 0.4 and 0.5.

3. From Figure 6.6, it can be observed that when $\omega < 0.4$, the battery never lasts for ten years. If $0.4 \leq \omega \leq 0.6$, then for some cases it lasts for ten years, while if $\omega > 0.6$, the battery lasts for ten years for all the cases. This gives a lot of flexibility to the operators of the BESS who can choose ω according to their requirements.

It is worth mentioning that the optimal value of DCW depends on the planning horizon, the battery technology, and the BESS uses cases. As the battery cost is decreasing, operators may set different planning horizon based on their prediction of BESS replacement cost of their battery type. Also, the degradation process is different for different types of battery technologies. The BESS operators should apply the specified degradation model of their own to develop the degradation cost function. Moreover, the use cases of BESS also affect the choice of DCW. For instance, the BESS may experience deeper cycles when seeking for arbitrage opportunities than when it is providing frequency regulation service for most of the time.

6.6 Conclusion

In this chapter, an attempt has been made at optimizing the operating strategy of a BESS with the aim of maximizing its value by striking a balance between the revenue generated from its applications and the longevity of the battery. Several scenarios have been considered where the operating ranges of the BESS and the DCW have been varied to understand the merits of the BESS. The observations from the results underline the importance of the DCW metric, as the variation of DCW yields a significant effect on the value of the BESS. Extreme values of the DCW might not maximize the BESS value, and hence should be chosen wisely. It can also be observed from the results hat although the revenue from energy arbitrage is maximum when the degradation cost is not considered, the battery life is shortened and thus the overall value of the BESS is decreased. Also, the total stacked value is higher when the SOC is constrained properly with a wisely chosen DCW. The optimal operating strategy can be different for different types of customers. Therefore, it is necessary for the operators to conduct analyses based on their batteries and interruption costs. This

study framework and its results can be utilized by utilities and other BESS owners and operators for determining the capacity and operating strategy for their BESS, based on its applications. Future work involves the consideration of other applications of the BESS, including participation in the ancillary services market.

Chapter 7

Conclusion

In this dissertation, three aspects of studies are performed for grid-scale energy storage systems. A method for quantifying the benefits of stacking up the applications of an ESS is firstly presented. Three applications (outage mitigation, energy arbitrage, and frequency regulation) were considered. Several case studies were performed to evaluate the reliability indices and the cost benefits. Sequential MCS was used to track the charging and discharging performance of the ESS and also the outage events in the system while evaluating the reliability indices and interruption cost. The variable behavior of load demand and the forced outages of generators are also captured by the sequential MCS. A quadratically constrained linear programming model was established to estimate the potential revenue from arbitrage and regulation markets. It presents several benefits from installing an ESS and utilizing it for the applications stated above. The approach described in this part can be utilized by industries including utilities and manufacturers to build business cases when they want to install an ESS for their facilities.

Second, a methodology to evaluate the capacity value of the energy storage system when it is also participating in the energy market seeking arbitrage opportunities is proposed. The capacity value of ESSs with different energy capacity sizes are estimated. The results indicate that the longer the duration that an ESS can be used, the larger capacity contribution can be made. The results can provide the system planners estimations of the ESSs capacity value. More importantly,

the framework proposed here can be applied in the real world capacity planning process to evaluate the actual capacity contribution of energy storage systems when they are involved in multiple services. For planning purposes, this work has also introduced the use of sensitivity analysis and locational marginal price to determine the optimal placement of ESSs. The objective function used in the tested systems is the generation cost function. The best locations for different size ESSs are deployed according to the saving in generation production cost. The proposed algorithm is demonstrated on several test systems. For each case, economic dispatch and genetic algorithm are applied to search for the optimal solution. Also, the convergence performances to find the optimal solution with and without the proposed encoding strategy are compared. The results demonstrated that the computational efficiency and speed are improved by the sensitivity analysis-based encoding approach.

Finally, a battery ESS is considered to participate in the energy market for energy arbitrage, and also helps to improve system reliability and resilience. An optimal strategy is proposed for the operation of the BESS which aims at maximizing the value of the BESS by balancing the revenue from the applications and the longevity of the facility. The operation of the BESS is considered under several operating ranges with different degradation cost weights. The degradation cost weight is an important metric for the operation strategy. Very large or very small values of the weight might not maximize the value of a BESS, and hence should be chosen wisely based on the planning horizon, ESS applications and the battery technology. The results of case studies show that although the energy arbitrage revenue is maximum when the degradation cost is not considered, the battery life is shortened and thus the overall value of the BESS is decreased. The BESS has larger stacked value when a lower capacity of the battery is committed to the energy market with a reasonable degradation cost weight. This study framework and its results can be utilized by utilities and other BESS owners and operators for determining the capacity and operating strategy for their BESS, based on its applications.

The work developed in this dissertation presents studies on ESS cost-benefit analysis, capacity valuation, optimal siting, and operating strategy. For all the three aspects: benefits, planning, and

operation, it is necessary to consider the uncertainty of ESS availability as it is suitable to provide several services to the power grid, but with limited capability. This is because a quantity committed to one service may not be committed to another due to its energy-limited characteristic. Also, for some types of ESSs, i.e., battery ESSs, the degradation process needs to be included in the analysis as different applications have different levels of effect on the ESS longevity. The work presented in this dissertation could have potential improvements if more aspects are considered. For instance, other ESS applications can be incorporated into the cost-benefit framework. Also, different clustering methods can be investigated and compared for building the multi-state model of ESSs for different ESS applications. For instance, the SOC variation pattern of ESSs should be different when it is participating in the energy market and providing the frequency regulation service. Moreover, the degradation process for other types of batteries or ESSs could be investigated to present a more comprehensive study of ESS operating strategies.

BIBLIOGRAPHY

BIBLIOGRAPHY

[1] A. A. Akhil, G. Huff, A. B. Currier, B. C. Kaun, D. M. Rastler, S. B. Chen, A. L. Cotter, D. T. Bradshaw, and W. D. Gauntlett, *DOE/EPRI 2013 Electricity Storage Handbook in Collaboration with NRECA*. Sandia National Laboratories Albuquerque, NM, 2013.

[2] Department of Energy, "DOE Global Energy Storage Database," http://aiweb.techfak.uni-bielefeld.de/content/bworld-robot-control-software/, 2016, [Online; accessed 20-July-2016].

[3] J. Eyer and G. Corey, "Energy storage for the electricity grid: Benefits and market potential assessment guide," *Sandia National Laboratories*, vol. 20, no. 10, p. 5, 2010.

[4] Y. Tian, A. Bera, M. Benidris, and J. Mitra, "Stacked revenue and technical benefits of a grid-connected energy storage system," *IEEE Trans. Indus. App.*, vol. 54, no. 4, Jul-Aug 2018.

[5] V. Koritarov, T. D. Veselka, J. Gasper, B. M. Bethke, A. Botterud, J. Wang, M. Mahalik, Z. Zhou, C. Milostan, J. Feltes *et al.*, "Modeling and analysis of value of advanced pumped storage hydropower in the united states," *Argonne National Laboratory, Argonne, IL (United States)*, 2014.

[6] Apex. Bethel Energy Center. [Online]. Available: http://www.apexcaes.com/bethel-energy-center

[7] International Electrotechnical Commission, "Electrical energy storage white paper," *Geneva, Switzerland: International Electrotechnical Commission*, pp. 1–78, 2011.

[8] Á. Cunha, J. Martins, N. Rodrigues, and F. Brito, "Vanadium redox flow batteries: a technology review," *International Journal of Energy Research*, vol. 39, no. 7, pp. 889–918, 2015.

[9] Hornsdale Power Reserve, https://hornsdalepowerreserve.com.au/, 2017, [Online].

[10] F. Díaz-González, A. Sumper, O. Gomis-Bellmunt, and R. Villafáfila-Robles, "A review of energy storage technologies for wind power applications," *Renewable and sustainable energy reviews*, vol. 16, no. 4, pp. 2154–2171, 2012.

[11] A. Nourai, "Installation of the first distributed energy storage system (DESS) at American Electric Power (AEP)," *Sandia Report SAND2007-3580*, 2007.

[12] C. Horne, R. Mosso, T. Smith, and B. Adams, "Demonstration of enervault iron-chromium redox flow battery," *Energy Research and Development Division Final Project Report*, 2015.

[13] North American Electric Reliability Corporation, *Operating Practices, Procedures and Tools*. North American Electric Reliability Corporation, Princeton, NJ, Mar. 2011.

[14] J. Lin, B. Power, and X. Power, "Energy storage—a cheaper, faster, & cleaner alternative to conventional frequency regulation," *Prepared for the California Energy Storage Alliance, February*, vol. 16, 2011.

[15] M. Benidris, S. Elsaiah, and J. Mitra, "An emission-constrained approach to power system expansion planning," *International Journal of Electrical Power & Energy Systems*, vol. 81, p. 7886, Oct. 2016.

[16] Y. Tian, A. Bera, M. Benidris, and J. Mitra, "Reliability and environmental benefits of energy storage systems in firming up wind generation," in *North American Power Symposium (NAPS)*, Morgantown, WV, USA, Sept. 2017, pp. 1–6.

[17] R. Walawalkar, J. Apt, and R. Mancini, "Economics of electric energy storage for energy arbitrage and regulation in New York," *Energy Policy*, vol. 35, no. 4, pp. 2558–2568, April 2007.

[18] M. Benini, S. Canevese, D. Cirio, and A. Gatti, "Battery energy storage systems for the provision of primary and secondary frequency regulation in Italy," in *IEEE 16th International Conference on Environment and Electrical Engineering (EEEIC)*, Florence, Italy, June 2016, pp. 1–6.

[19] G. He, Q. Chen, C. Kang, Q. Xia, and K. Poolla, "Cooperation of wind power and battery storage to provide frequency regulation in power markets," *IEEE Trans. Power Syst.*, vol. 32, no. 5, pp. 3559–3568, Sept. 2017.

[20] R. H. Byrne and C. A. Silva-Monroy, "Estimating the maximum potential revenue for grid connected electricity storage: Arbitrage and regulation," *Sandia National Laboratories*, 2012.

[21] R. H. Byrne, R. J. Concepcion, and C. A. Silva-Monroy, "Estimating potential revenue from electrical energy storage in PJM," in *Power and Energy Society General Meeting (PESGM)*, Boston, MA, USA, July 2016, pp. 1–5.

[22] R. H. Byrne and C. A. Silva-Monroy, "Potential revenue from electrical energy storage in the electricity reliability council of texas (ERCOT)," in *Power and Energy Society General Meeting (PESGM)*, National Harbor, MD, USA, July 2014, pp. 1–5.

[23] J. Mitra, "Reliability-based sizing of backup storage," *IEEE Trans. Power Syst.*, vol. 25, no. 2, pp. 1198–1199, May 2010.

[24] J. Mitra and M. R. Vallem, "Determination of storage required to meet reliability guarantees on island-capable microgrids with intermittent sources," *IEEE Trans. Power Syst.*, vol. 27, no. 4, pp. 2360–2367, Nov. 2012.

[25] S. Sulaeman, Y. Tian, M. Benidris, and J. Mitra, "Quantification of storage necessary to firm up wind generation," *IEEE Trans. Indus. App.*, vol. 53, no. 4, pp. 3228–3236, July 2017.

[26] W. Li, *Risk Assessment of Power Systems: Models, Methods, and Applications*. John Wiley & Sons, 2005.

[27] C. Singh, P. Jirutitijaroen, and J. Mitra, *Electric Power Grid Reliability Evaluation: Models and Methods*. Wiley, 2019.

[28] R. N. Allan, *Reliability Evaluation of Power Systems*. Springer Science & Business Media, 2013.

[29] PJM, "Manual 28: Operating agreement accounting," 2014.

[30] H. Mohsenian-Rad, "Optimal bidding, scheduling, and deployment of battery systems in California day-ahead energy market," *IEEE Trans. Power Syst.*, vol. 31, no. 1, pp. 442–453, 2016.

[31] Reliability Test System Task Force of the Application of Probability Methods Subcommittee, "IEEE reliability test system," *IEEE Trans. Power Appar. Syst.*, vol. PAS-98, no. 6, pp. 2047–2054, Nov. 1979.

[32] R. F. Ghajar and R. Billinton, "Economic costs of power interruptions: a consistent model and methodology," *International Journal of Electrical Power & Energy Systems*, vol. 28, no. 1, pp. 29–35, Jan. 2006.

[33] PJM. PJM Data Miner. [Online]. Available: https://dataminer.pjm.com/dataminerui/pages/public/lmp.jsf

[34] PJM. PJM Data Miner2. [Online]. Available: http://www.pjm.com/markets-and-operations/etools/data-miner-2.aspx

[35] PJM. RTO Regulation Signal Data. [Online]. Available: http://www.pjm.com/markets-and-operations/ancillary-services.aspx

[36] P. Alotto, M. Guarnieri, and F. Moro, "Redox flow batteries for the storage of renewable energy: A review," *Renewable and Sustainable Energy Reviews*, vol. 29, pp. 325–335, 2014.

[37] M. Ulaganathan, V. Aravindan, Q. Yan, S. Madhavi, M. Skyllas-Kazacos, and T. M. Lim, "Recent advancements in all-vanadium redox flow batteries," *Advanced Materials Interfaces*, vol. 3, no. 1, 2016.

[38] P. Zou, Q. Chen, Q. Xia, G. He, and C. Kang, "Evaluating the contribution of energy storages to support large-scale renewable generation in joint energy and ancillary service markets," *IEEE Trans. Sustain. Energy*, vol. 7, no. 2, pp. 808–818, 2016.

[39] L. N. Kishore and E. Fernandez, "Reliability well-being assessment of pv-wind hybrid system using Monte Carlo simulation," in *Emerging Trends in Electrical and Computer Technology (ICETECT), 2011 International Conference on*. IEEE, 2011, pp. 63–68.

[40] R. M. Moharil and P. S. Kulkarni, "Reliability analysis of solar photovoltaic system using hourly mean solar radiation data," *Solar Energy*, vol. 84, no. 4, pp. 691–702, 2010.

[41] L. H. Stember, W. R. Huss, and M. S. Bridgman, "A methodology for photovoltaic system reliability & economic analysis," *IEEE Trans. Rel.*, vol. 31, no. 3, pp. 296–303, 1982.

[42] S. Sulaeman, M. Benidris, Y. Tian, and J. Mitra, "Modeling and evaluating the capacity credit of PVsolar systems using an analytical method," in *2016 IEEE/PES Transmission and Distribution Conference and Exposition (T&D)*, 2016, pp. 1–5.

[43] A. Keane, M. Milligan, C. J. Dent, B. Hasche, C. D'Annunzio, K. Dragoon, H. Holttinen, N. Samaan, L. Soder, and M. O'Malley, "Capacity value of wind power," *IEEE Trans. Power Syst.*, vol. 26, no. 2, pp. 564–572, 2011.

[44] B. Hasche, A. Keane, and M. O'Malley, "Capacity value of wind power, calculation, and data requirements: the Irish power system case," *IEEE Trans. Power Syst.*, vol. 26, no. 1, pp. 420–430, 2011.

[45] S. Sulaeman, M. Benidris, and J. Mitra, "Evaluation of wind power capacity value including effects of transmission system," in *North American Power Symposium (NAPS), 2015*. IEEE, 2015, pp. 1–6.

[46] R. Sioshansi, S. H. Madaeni, and P. Denholm, "A dynamic programming approach to estimate the capacity value of energy storage," *IEEE Trans. Power Syst.*, vol. 29, no. 1, pp. 395–403, 2014.

[47] Y. Zhou, P. Mancarella, and J. Mutale, "Framework for capacity credit assessment of electrical energy storage and demand response," *IET Gen., Trans. & Dist.*, vol. 10, no. 9, pp. 2267–2276, 2016.

[48] C. Singh and J. Mitra, "Monte Carlo simulation for reliability analysis of emergency and standby power systems," in *Industry Applications Conference, 1995. 13th IAS Annual Meeting*. IEEE, 1995, pp. 2290–2295.

[49] H. Lei and C. Singh, "Non-sequential Monte Carlo simulation for cyber-induced dependent failures in composite power system reliability evaluation," *IEEE Trans. Power Syst.*, vol. 32, no. 2, pp. 1064–1072, 2017.

[50] C. Singh and J. Mitra, "Monte Carlo simulation and intelligent search methods," *IEEE Tutorial on Electric Delivery System Reliability Evaluation*, pp. 23–38, 2005.

[51] Y. Tian, A. Bera, J. Mitra, B. Chalamala, and R. H. Byrne, "Effect of operating strategies on the longevity of lithium-ion battery energy storage systems," in *Industry Applications Society Annual Meeting*. IEEE, 2018, pp. 1–8.

[52] J. A. Hartigan and M. A. Wong, "Algorithm as 136: A k-means clustering algorithm," *Journal of the Royal Statistical Society. Series C (Applied Statistics)*, vol. 28, no. 1, pp. 100–108, 1979.

[53] J. Mitra, M. R. Vallem, and S. B. Patra, "A probabilistic search method for optimal resource deployment in a microgrid," in *Probabilistic Methods Applied to Power Systems, 2006. PMAPS 2006. International Conference on*. IEEE, 2006, pp. 1–6.

[54] M. R. Vallem, J. Mitra, and S. B. Patra, "Distributed generation placement for optimal microgrid architecture," in *Transmission and Distribution Conference and Exhibition, 2005/2006 IEEE PES*. IEEE, 2006, pp. 1191–1195.

[55] T. Sutthibun and P. Bhasaputra, "Multi-objective optimal distributed generation placement using simulated annealing," in *Electrical Engineering/Electronics Computer Telecommunications and Information Technology (ECTI-CON), 2010 International Conference on*. IEEE, 2010, pp. 810–813.

[56] J. Mitra, S. Patra, S. Ranade, and M. Vallem, "Reliability-specified generation and distribution expansion in microgrid architectures," *WSEAS Transactions on Power Systems*, vol. 1, no. 8, p. 1446, 2006.

[57] D. Sosic and I. Skokljev, "Optimal location and sizing of photovoltaic plant," in *Renewable Energy Research and Applications (ICRERA), 2013 International Conference on*. IEEE, 2013, pp. 121–126.

[58] X. Lili, Q. Xiaoyan, W. Xiwen, and L. Xingyuan, "Research of distribution generation planning in smart grid construction," in *Power and Energy Engineering Conference (APPEEC), 2010 Asia-Pacific*. IEEE, 2010, pp. 1–4.

[59] C. Wang, K. Chen, Y. Xie, and H. Zheng, "Siting and sizing of distributed generation in distribution network expansion planning," *Automation of Electric Power Systems*, vol. 3, pp. 38–43, 2006.

[60] M. Shaaban and E. El-Saadany, "Optimal allocation of renewable DG for reliability improvement and losses reduction," in *Power and Energy Society General Meeting (PESGM)*. IEEE, 2012, pp. 1–8.

[61] Y. Tian and J. Mitra, "A pareto-optimal approach to design of distribution system protection," in *North American Power Symposium (NAPS), 2015*. IEEE, 2015, pp. 1–5.

[62] Y. Tian, M. Benidris, S. Sulaeman, S. Elsaiah, and J. Mitra, "Optimal feeder reconfiguration and distributed generation placement for reliability improvement," in *Probabilistic Methods Applied to Power Systems (PMAPS), 2016 International Conference on*. IEEE, 2016, pp. 1–7.

[63] L. Guang, L. Chenching, and H. Salazar, "Forecasting transmission congestion using day–ahead shadow prices," in *IEEE PES Power Systems Conference and Exposition*. IEEE, Oct 2006, pp. 1705–1709.

[64] H. Zhao, P. You, and C. Li, "Study on the estimating model of shadow prices for national economy evaluation of construction projects," in *International Conference on Management and Service Science*, Sept 2009, pp. 1–4.

[65] M. Benidris, S. Elsaiah, and J. Mitra, "Sensitivity analysis in composite system reliability using weighted shadow prices," in *Power and Energy Society General Meeting (PESGM)*. IEEE, 2011, pp. 1–6.

[66] M. Benidris and J. Mitra, "Reliability and sensitivity analysis of composite power systems under emission constraints," *IEEE Trans. Power Syst.*, vol. 29, no. 1, pp. 404–412, 2014.

[67] Y. Tian, N. Cai, M. Benidris, A. Bera, J. Mitra, and C. Singh, "Sensitivity guided genetic algorithm for placement of distributed energy resources," in *Intelligent System Application to Power Systems (ISAP), 2017 19th International Conference on*. IEEE, 2017, pp. 1–5.

[68] J. H. Holland, *Adaptation in Natural and Artificial Systems: an Introductory Analysis with Applications to Biology, Control, and Artificial Intelligence*. MIT press, 1992.

[69] K. Deb, *Optimization for Engineering Design: Algorithms and Examples*. PHI Learning Pvt. Ltd., 2012.

[70] N. Cai, Y. Tian, and J. Mitra, "Optimal branch numbering for UPFC benefit study," in *North American Power Symposium (NAPS)*. IEEE, 2015, pp. 1–5.

[71] N. Cai, "Linearized and distributed methods for power flow analysis and control in smart grids and microgrids," Ph.D. dissertation, Michigan State University, 2014.

[72] R. D. Zimmerman, C. E. Murillo-Sánchez, and R. J. Thomas, "Matpower: Steady-state operations, planning, and analysis tools for power systems research and education," *IEEE Trans. Power Syst.*, vol. 26, no. 1, pp. 12–19, 2011.

[73] R. Christie, "Power systems test case archive," *Electrical Engineering dept., University of Washington*, 2000.

[74] M. Benidris, Y. Tian, S. Sulaeman, and J. Mitra, "Optimal location and size of distributed energy resources using sensitivity analysis-based approaches," in *North American Power Symposium (NAPS), 2016*. IEEE, 2016, pp. 1–5.

[75] K. Divya and J. Ostergaard, "Battery energy storage technology for power system–An overview," *Electric Power Systems Research*, vol. 79, no. 4, pp. 511 – 520, 2009. [Online]. Available: http://www.sciencedirect.com/science/article/pii/S0378779608002642

[76] A. Oudalov, T. Buehler, and D. Chartouni, "Utility scale applications of energy storage," in *2008 IEEE Energy 2030 Conference*, Nov 2008, pp. 1–7.

[77] Clean Energy Group, "Project Fact Sheet," https://www.cleanegroup.org/wp-content/uploads/Sterling-Overview.pdf, 2016, [Online].

[78] R. H. Byrne, S. Hamilton, D. R. Borneo, T. Olinsky-Paul, and I. Gyuk, "The value proposition for energy storage at the Sterling Municipal Light Department," in *Power and Energy Society General Meeting (PESGM)*, July 2017, pp. 1–5.

[79] R. H. Byrne, T. A. Nguyen, D. A. Copp, B. R. Chalamala, and I. Gyuk, "Energy management and optimization methods for grid energy storage systems," *IEEE Access*, vol. 6, pp. 13 231–13 260, 2018.

[80] Y. Shi, B. Xu, D. Wang, and B. Zhang, "Using battery storage for peak shaving and frequency regulation: Joint optimization for superlinear gains," *IEEE Trans. Power Syst.*, vol. 33, no. 3, pp. 2882–2894, 2018.

[81] M. Kazemi, H. Zareipour, N. Amjady, W. D. Rosehart, and M. Ehsan, "Operation scheduling of battery storage systems in joint energy and ancillary services markets," *IEEE Trans. Sustain. Energy*, vol. 8, no. 4, pp. 1726–1735, Oct 2017.

[82] D. I. Stroe, V. Knap, M. Swierczynski, A. I. Stroe, and R. Teodorescu, "Operation of a grid-connected lithium-ion battery energy storage system for primary frequency regulation: A battery lifetime perspective," *IEEE Trans. Ind. Appl.*, vol. 53, no. 1, pp. 430–438, Jan 2017.

[83] A. Oudalov, D. Chartouni, and C. Ohler, "Optimizing a battery energy storage system for primary frequency control," *IEEE Trans. Power Syst.*, vol. 22, no. 3, pp. 1259–1266, Aug 2007.

[84] N. Nguyen, A. Bera, and J. Mitra, "Energy storage to improve reliability of wind integrated systems under frequency security constraint," *IEEE Trans. Ind. Appl.*, vol. 54, no. 5, pp. 4039–4047, 2018.

[85] P. Hu, R. Karki, and R. Billinton, "Reliability evaluation of generating systems containing wind power and energy storage," *IET Gener. Transm. Distrib.*, vol. 3, no. 8, pp. 783–791, 2009.

[86] Y. Xu and C. Singh, "Power system reliability impact of energy storage integration with intelligent operation strategy," *IEEE Trans. Smart Grid*, vol. 5, no. 2, pp. 1129–1137, March 2014.

[87] B. Xu, A. Oudalov, A. Ulbig, G. Andersson, and D. Kirschen, "Modeling of lithium-ion battery degradation for cell life assessment," *IEEE Trans. Smart Grid*, vol. 9, no. 2, pp. 1131–1140, 2018.

[88] A. Perez, R. Moreno, R. Moreira, M. Orchard, and G. Strbac, "Effect of battery degradation on multi-service portfolios of energy storage," *IEEE Trans. Sustain. Energy*, vol. 7, no. 4, pp. 1718–1729, Oct 2016.

[89] P. Malysz, S. Sirouspour, and A. Emadi, "An optimal energy storage control strategy for grid-connected microgrids," *IEEE Trans. Smart Grid*, vol. 5, no. 4, pp. 1785–1796, July 2014.

[90] G. He, Q. Chen, C. Kang, P. Pinson, and Q. Xia, "Optimal bidding strategy of battery storage in power markets considering performance-based regulation and battery cycle life," *IEEE Trans. Smart Grid*, vol. 7, no. 5, pp. 2359–2367, Sept 2016.

[91] B. Xu, "Degradation-limiting optimization of battery energy storage systems operation," 2013.

[92] B. Xu, J. Zhao, T. Zheng, E. Litvinov, and D. S. Kirschen, "Factoring the cycle aging cost of batteries participating in electricity markets," *IEEE Trans. Power Syst.*, vol. 33, no. 2, pp. 2248–2259, 2018.

[93] M. Matsuishi and T. Endo, "Fatigue of metals subjected to varying stress," *Japan Society of Mechanical Engineers, Fukuoka, Japan*, vol. 68, no. 2, pp. 37–40, Jan. 1968.

[94] S. D. Downing and D. Socie, “Simple rainflow counting algorithms,” *International journal of fatigue*, vol. 4, no. 1, pp. 31–40, Jan. 1982.

[95] A. Niesłony, “Determination of fragments of multiaxial service loading strongly influencing the fatigue of machine components,” *Mechanical Systems and Signal Processing*, vol. 23, no. 8, pp. 2712–2721, Nov. 2009.

[96] C. Chen, J. Wang, F. Qiu, and D. Zhao, “Resilient distribution system by microgrids formation after natural disasters,” *IEEE Trans. Smart Grid*, vol. 7, no. 2, pp. 958–966, 2016.

[97] M. J. Sullivan, M. Mercurio, J. Schellenberg, and F. Sullivan, “Estimated value of service reliability for electric utility customers in the united states,” *LBNL Research Project Final Report*, 2009.

[98] M. J. Sullivan, J. Schellenberg, and M. Blundell, “Updated value of service reliability estimates for electric utility customers in the united states,” *Ernest Orlando Lawrence Berkeley Nat. Lab., Tech. Rep*, 2015.